

Spring 2015

# The role of death-associated protein kinase in endothelial apoptosis under fluid shear stress

Keith R. Rennie  
*Purdue University*

Follow this and additional works at: [https://docs.lib.purdue.edu/open\\_access\\_dissertations](https://docs.lib.purdue.edu/open_access_dissertations)



Part of the [Biomedical Engineering and Bioengineering Commons](#)

---

## Recommended Citation

Rennie, Keith R., "The role of death-associated protein kinase in endothelial apoptosis under fluid shear stress" (2015). *Open Access Dissertations*. 545.

[https://docs.lib.purdue.edu/open\\_access\\_dissertations/545](https://docs.lib.purdue.edu/open_access_dissertations/545)

This document has been made available through Purdue e-Pubs, a service of the Purdue University Libraries. Please contact [epubs@purdue.edu](mailto:epubs@purdue.edu) for additional information.

**PURDUE UNIVERSITY  
GRADUATE SCHOOL  
Thesis/Dissertation Acceptance**

This is to certify that the thesis/dissertation prepared

By Keith R. Rennier

Entitled

THE ROLE OF DEATH-ASSOCIATED PROTEIN KINASE IN ENDOTHELIAL APOPTOSIS UNDER FLUID SHEAR STRESS

For the degree of Doctor of Philosophy

Is approved by the final examining committee:

Julie Ji

Co-chair

Sherry Voytik-Harbin

Co-chair

Sungsoo Na

Patricia Gallagher

To the best of my knowledge and as understood by the student in the Thesis/Dissertation Agreement, Publication Delay, and Certification Disclaimer (Graduate School Form 32), this thesis/dissertation adheres to the provisions of Purdue University's "Policy of Integrity in Research" and the use of copyright material.

Approved by Major Professor(s): Julie Ji

Approved by: George R. Wodicka

Head of the Departmental Graduate Program

4/17/2015

Date



THE ROLE OF DEATH-ASSOCIATED PROTEIN KINASE IN ENDOTHELIAL  
APOPTOSIS UNDER FLUID SHEAR STRESS

A Dissertation

Submitted to the Faculty

of

Purdue University

by

Keith R. Rennie

In Partial Fulfillment of the  
Requirements for the Degree

of

Doctor of Philosophy

May 2015

Purdue University

West Lafayette, Indiana

## ACKNOWLEDGMENTS

I would like to gratefully thank and acknowledge my advisor, Dr. Julie Ying Hui Ji, for her mentoring and support along the way. I am appreciative of her giving me the chance to be a part of relevant research, sharing her expertise, and helping me develop the skills necessary to be successful moving forward.

I would like to thank my advisory committee members, Dr. Sherry Voytik-Harbin, Dr. Sungsoo Na, and Dr. Patricia Gallagher, for their time and support during the entire Ph.D. qualifying process.

I would also like to give a special thanks to all my family and friends for their endless support and understanding, especially my Mom, Dad, and fiancée Sarah Michelle.

Lastly, I offer my best regards and blessings to all of those who supported me in any respect during the completion of my dissertation project.

## TABLE OF CONTENTS

	Page
LIST OF TABLES .....	vi
LIST OF FIGURES .....	vii
ABSTRACT .....	x
1. INTRODUCTION .....	1
1.1 The Vasculature and Atherosclerosis .....	1
1.2 Endothelial Mechanotransduction .....	8
1.2.1 Shear stress: athero-prone vs. athero-protective profiles .....	8
1.2.2 Molecular pathways of endothelial mechanotransduction .....	11
1.3 Apoptosis .....	13
1.3.1 Signals and mechanisms of apoptosis .....	13
1.3.2 Shear stress and endothelial apoptosis .....	14
1.4 Death-Associated Protein Kinase .....	16
1.4.1 DAPK in apoptosis .....	16
1.4.2 DAPK in cancer .....	18
1.4.3 DAPK in endothelial apoptosis .....	19
2. EXPERIMENTAL METHODS .....	25
2.1 Cell Culture and Reagents .....	25
2.2 Parallel Plate Flow Chamber and Shear Stress .....	27
2.2.1 Fluid mechanics of the parallel plate flow model .....	27
2.2.2 Experimental shear stress setup .....	32
2.3 mRNA and Protein Analysis .....	36
2.3.1 Protein expression .....	36
2.3.2 Gel electrophoresis .....	37
2.3.3 Antibody labeling .....	38
2.3.4 Molecular imaging and protein quantification .....	39
2.3.5 RNA isolation .....	41

	Page
2.3.6 Reverse transcription .....	42
2.3.7 Primer development .....	44
2.3.8 Real-time RT-PCR.....	45
2.3.9 Quantifying RT-PCR results.....	47
2.4 Apoptosis and Necrosis Assay.....	49
2.4.1 Flow cytometry .....	50
2.4.2 Caspase assay.....	50
2.5 Gene Knockdown Techniques .....	51
2.5.1 DAPK RNA interference .....	51
2.5.2 Gene silencing with shRNA.....	52
2.6 Immunostaining .....	53
2.7 Statistics .....	54
3. SHEAR STRESS REGULATES EXPRESSION OF DAPK IN SUPPRESSING TNF $\alpha$ -INDUCED ENDOTHELIAL APOPTOSIS .....	55
3.1 Introduction.....	55
3.2 Results.....	58
3.2.1 Shear stress alone increases overall DAPK expression and mRNA level in endothelial cells .....	58
3.2.2 Shear stress alters phosphorylation of DAPK at serine 308 in a time dependent manner .....	60
3.2.3 Long term TNF $\alpha$ treatment affects phosphor-serine 308 DAPK, not overall DAPK expression .....	61
3.2.4 Shear stress significantly reduces endothelial apoptosis following TNF $\alpha$ activation.....	64
3.2.5 Shear stress reduces caspase-3 and -7 activity following TNF $\alpha$ activation .....	65
3.2.6 Apoptosis analysis in TNF $\alpha$ and shear treated adherent cells confirms results from flow cytometry.....	68
3.2.7 Necrosis is not altered in TNF $\alpha$ and shear activated endothelial cells ...	69
3.2.8 DAPK expression is decreased in TNF $\alpha$ and shear activated endothelial cells .....	71
3.2.9 Phosphorylated serine 308 DAPK is decreased in TNF $\alpha$ and shear activated endothelial cells .....	74
3.2.10 Transfection with siRNA against DAPK confirms its role in endothelial mechanotransduction .....	75
3.2.11 Cytoplasm localization of GFP-DAPK on the actin network in BAEC	78

	Page
3.2.12 Long term shear stress of up to 24 hours decreased overall DAPK expression and activation.....	80
3.3 Discussion.....	82
<b>4. SHEAR STRESS ATTENUATES APOPTOSIS DUE TO TNF<math>\alpha</math>, H<sub>2</sub>O<sub>2</sub>, AND SERUM DEPLETION VIA DAPK EXPRESSION .....</b>	<b>90</b>
4.1 Introduction.....	90
4.2 Results.....	92
4.2.1 DAPK expression is decreased in TNF $\alpha$ , H <sub>2</sub> O <sub>2</sub> treated, and serum depleted cells when exposed to shear stress before or after treatment ..	92
4.2.2 Phosphorylated serine 308 DAPK is decreased in TNF $\alpha$ , H <sub>2</sub> O <sub>2</sub> (0.5mM), serum depleted (0.5% FBS) and shear stress treated endothelial cells ...	97
4.2.3 Shear stress significantly reduced apoptosis following incubations with TNF $\alpha$ , H <sub>2</sub> O <sub>2</sub> , and low serum.....	99
4.2.4 Preconditioning cells before apoptosis induction reduced overall apoptosis and caspase activity .....	101
4.2.5 Subsequent shearing after apoptosis induction also showed a significant decrease in apoptosis.....	103
4.3 Discussion.....	104
<b>5. EFFECTS OF SHEAR STRESS AND SUBSTRATE ON ENDOTHELIAL DAPK EXPRESSION, CASPASE ACTIVITY, AND APOPTOSIS .....</b>	<b>110</b>
5.1 Introduction.....	110
5.2 Results.....	112
5.2.1 Shear stress significantly reduced apoptosis following TNF $\alpha$ activation on silicone substrate.....	112
5.2.2 Shear stress reduced DAPK expression following TNF $\alpha$ treatment on membrane substrates.....	114
5.2.3 Shear stress decreased phosphor-DAPK in TNF $\alpha$ treated cells on membrane substrates.....	116
5.2.4 Shear stress alone induced apoptosis in cells on both glass and membrane substrates.....	117
5.2.5 Shear-induced apoptosis correlated with caspase-3 and 7 activation ...	118
5.2.6 Shear stress increased overall DAPK expression in cells on both glass and membrane substrates.....	119
5.2.7 Shear stress decreased DAPK phosphorylation at serine 308 on glass and membrane substrates.....	122
5.3 Discussion.....	123



	Page
6. FLUID SHEAR INCREASES ENDOTHELIAL APOPTOSIS AND DAPK ACTIVITY IN LAMIN-DEFICIENT CELLS .....	128
6.1 Introduction.....	128
6.2 Results .....	133
6.2.1 DAPK expression and apoptosis in lamin-deficient cells under shear and TNF $\alpha$ .....	133
6.2.2 DAPK expression in lamin-deficient cells under shear stress and other environmental stimulus.....	141
6.2.3 Apoptosis in shRNA cells.....	146
6.3 Discussion .....	152
7. CONCLUSIONS AND RECOMMENDATIONS .....	155
7.1 Summary .....	155
7.2 Potential Limitations.....	160
7.3 Future Research Directions.....	161
7.3.1 Endothelial and smooth muscle cell mechanotransduction due to cyclic stretch.....	161
7.3.2 Shear impacts lamin expression in shRNA cells .....	162
REFERENCES .....	167
VITA .....	178

## LIST OF TABLES

Table		Page
Table 1.1	Cellular response to laminar vs. disturbed flow profile.....	4
Table 1.2	Pro- vs. anti-apoptotic factors and corresponding pathways in endothelial cells .....	15
Table 1.3	Specific DAPK phosphorylation sites .....	22
Table 2.1	Sample volume analysis report .....	40
Table 2.2	RNA isolation protocol .....	42
Table 2.3	Reverse transcription sample protocol (per sample).....	43
Table 2.4	Novel DAPK primes used for RT-PCR analysis .....	45
Table 2.5	Real-time RT-PCR solution protocol (per reaction).....	46
Table 2.6	Thermal cycling protocol for real time PCR.....	47

## LIST OF FIGURES

Figure		Page
Figure 1.1	Cumulative atherosclerosis progression .....	2
Figure 1.2	Directional fluid forces acting on the vessel wall .....	3
Figure 1.3	The role of DAPK in both atherosclerosis and cancer .....	7
Figure 1.4	Anatomy of the arterial wall .....	8
Figure 1.5	Fluid flow profiles elicit changes in endothelial expression.....	10
Figure 1.6	DAPK binding domains .....	17
Figure 1.7	A model of DAPK activity in endothelial mechanotransduction under fluid shear .....	21
Figure 1.8	DAPK signal transduction cascade in response to shear and apoptosis inducing agents .....	24
Figure 2.1	Fluid flow profile for the flow chamber .....	28
Figure 2.2	The three pieces of the flow chamber: top, middle, and bottom.....	32
Figure 2.3	Fully constructed parallel plate flow chamber.....	33
Figure 2.4	Housing environment for flow setup and temperature control .....	34
Figure 2.5	Sample calibration curve for quantifying protein concentration .....	37
Figure 2.6	Sample western blot image using Quantity One.....	40
Figure 2.7	Complementary primers binding to template cDNA .....	44

Figure	Page
Figure 2.8	Real-time RT-PCR mRNA amplification plot.....48
Figure 3.1	DAPK mRNA and protein analysis under shear.....60
Figure 3.2	Impact of TNF $\alpha$ on DAPK expression .....63
Figure 3.3	Experimental design quantifying apoptosis and caspase .....66
Figure 3.4	TUNEL using fluorescence microscopy .....67
Figure 3.5	Annexin V flow cytometry cell necrosis results .....70
Figure 3.6	Western analysis for DAPK expression due to shear and TNF $\alpha$ .....73
Figure 3.7	Endothelial apoptosis after DAPK siRNA knockdown .....76
Figure 3.8	Fluorescence microscopy images of BAEC immunostained for DAPK, actin, and nucleus.....79
Figure 3.9	Long-term shear effect of DAPK expression.....81
Figure 4.1	Experimental design to investigate DAPK expression due to shear and stimulants .....94
Figure 4.2	DAPK expression due to pre- and post-conditioning and apoptosis stimulants .....96
Figure 4.3	DAPKp308/DAPK expression due to shear and stimulants .....98
Figure 4.4	Quantifying TUNEL positive apoptosis using flow cytometry .....100
Figure 4.5	Quantifying caspase activity in stimulated BAECs .....102
Figure 5.1	Shear stress suppressed apoptosis subsequent to TNF $\alpha$ induction for cells plated on silicone membrane .....112
Figure 5.2	Western analysis of DAPK expression for BAECs on membranes.....115
Figure 5.3	Shear stress on membranes induced apoptosis similar to cells on glass..117
Figure 5.4	Overall DAPK activity in BAECs for both glass and membrane substrates.....121

Figure		Page
Figure 6.1	The various role of nuclear lamina in cells .....	129
Figure 6.2	Current understanding of apoptosis activation involving DAPK and lamin signaling.....	132
Figure 6.3	DAPK expression in MEFs under shear and TNF $\alpha$ exposure .....	134
Figure 6.4	Apoptosis results based on flow cytometry analysis of TUNEL in MEFs .....	136
Figure 6.5	Lamin A/C silencing in BAECs.....	137
Figure 6.6	DAPK western analysis in control and lamin shRNA BAECs.....	139
Figure 6.7	TUNEL positive apoptosis results using flow cytometry analysis in shRNA BAECs .....	140
Figure 6.8	DAPK activity in shRNA cells under shear and stimulants .....	143
Figure 6.9	DAPKp/DAPK activity in shRNA cells under shear and stimulants .....	145
Figure 6.10	Control shRNA representative 10X phase images.....	148
Figure 6.11	Lamin shRNA representative 10X phase images .....	149
Figure 6.12	Fold increase in apoptosis for control and lamin shRNA cells.....	151
Figure 7.1	Lamin expression in control shRNA cells .....	164
Figure 7.2	Lamin expression in lamin shRNA cells .....	165

## ABSTRACT

Rennier, Keith R. Ph.D. Purdue University, May 2015. The Role of Death-Associated Protein Kinase in Endothelial Apoptosis under Fluid Shear Stress. Major Advisor: Julie Ying Hui Ji.

Endothelial cells are the interface between hemodynamic fluid flow and vascular tissue contact. They actively translate physical and chemical stimuli into intracellular signaling cascades which in turn regulate cell function, and endothelial dysfunction leads to inflammation and diseased conditions. For example, atherosclerosis, a chronic vascular disease, favorably develops in regions of disturbed fluid flow and low shear stress. Apoptosis, or programmed cell death, must be properly regulated to maintain homeostasis in the vascular wall. The loss of apoptosis control, as seen in low shear stress regions, is implicated in various diseases such as atherosclerosis and cancer. Death-associated protein kinase, DAPK is a pro-apoptotic regulator for various cell types that is localized in the cell cytoskeleton and regulates changes in cytoplasm associated with apoptosis. Yet its role in endothelial cells remains unclear. DAPK is a positive regulator in tumor necrosis factor  $\alpha$  (TNF $\alpha$ ) induced apoptotic pathway, and DAPK expression is lost in cancer cells. In this project, we begin to assess the effect of shear stress on endothelial cell apoptosis and DAPK.

The potential role of DAPK and its corresponding signaling pathway in endothelial mechanotransduction and the role of nuclear lamina is further evaluated.

Using bovine aortic endothelial cells, we have shown that laminar shear stress modulates DAPK expression. Initially, our study examined the time-dependent effects of conditioning cells with shear stress on apoptosis triggered by TNF $\alpha$ , oxidative stress, and serum depletion; and the corresponding role of endothelial DAPK. Pre-conditioning cells with shear stress for 6 hours prior to apoptosis induction, decreased downstream caspase 3/7 activity, an apoptosis signaling constituent. Similarly, we also observed a corresponding decrease in DAPK in pre-sheared cells exposed to TNF $\alpha$ , H<sub>2</sub>O<sub>2</sub>, or serum starvation. Post-conditioning cells with 6 hours of shear after exposure to stimuli confirmed the protective effect of laminar shear stress in the presence of each apoptotic inducer. Our data suggest that shear stress and apoptosis agents may have competing effects on DAPK expression, and shear stress suppresses apoptosis by regulating DAPK in a time-dependent manner.

Additionally, we transitioned our study to endothelial cells on non-glass substrates, such as flexible silicone membrane normally used for cyclic strain studies. We have shown a link between shear stress and DAPK expression and apoptosis in cells on membrane. Along with biochemical and molecular signals, the hemodynamic forces that the cells experience are also important regulators of endothelial functions. We found that adding shear stress significantly suppressed TNF $\alpha$  induced apoptosis in cells; while shearing cells alone also increased apoptosis on either substrate. These data suggest that shear stress induced apoptosis in endothelial cells via increased DAPK expression and activation as well as caspase-3/7 activity. Most *in vitro* shear stress studies utilize the

conventional parallel plate flow chamber where cells are cultured on glass, which is much stiffer than what cells encounter *in vivo*. Other mechanotransduction studies have utilized the flexible silicone membrane as substrate, for example, in cyclic stretch studies. Thus, this study bridges the gap between shear stress studies on cells plated on glass to future studies on different stiffness of substrates or mechanical stimulation such as cyclic strain.

The nuclear lamina plays an important role in nuclear envelope structural support and connect to the cytoskeletal network through various co-localized proteins. Similarly, lamin is an integral part of the apoptosis process due to its direct linkage to the cytoskeleton and nuclear membrane. Conversely, lamin deficient cells lack nuclear structural integrity and the role of lamin in stress response is not completely understood. Mutations in lamin lead to changes in nuclear membrane mechanics eventually altering downstream signal response to stress. Therefore, we also looked at the impact of lamin deficiency in both MEF and BAEC cells on DAPK activity and apoptosis. We investigated the normally positive effects of shear on lamin deficient cells. The loss of lamin expression made cells more susceptible to shear stress and increased overall cell turnover compared to sheared control cells. Also, our results suggest the loss of lamin A/C expression mitigates TNF $\alpha$ -induced apoptosis and affects its associated signaling pathways.

In summary, the work presented in this dissertation has highlighted the role of DAPK in both mechanotransduction and endothelial apoptosis. Ultimately, this study demonstrates a key role lamin plays in mechanotransduction and apoptosis in response to both chemical and mechanical stimulation. By understanding how cells regulate



phenotypic and genotypic changes in response to stimulation, we can better address disease and develop effective therapeutics.

## 1. INTRODUCTION

This dissertation will provide background on the cardiovascular biology, key disease mechanisms, and endothelial cell mechanotransduction with relevant engineering principles, apoptosis and important DAPK signaling constituents. The specific experimental methods will be outlined, followed by the specific research objectives, results, and overall discussion. Finally, a summary of the project and future research directions will be discussed in detail.

### 1.1 The Vasculature and Atherosclerosis

Cardiovascular disease continues to be the leading cause of death in developed countries. Atherosclerosis, a chronic inflammatory cardiovascular disease, is characterized by the progressive buildup of oxidized low density lipoproteins in the arterial walls (4). In the development of atherosclerosis, local endothelial cell dysfunction leads to increased cell turnover and immune response recruitment to the site of vascular injury. Endothelium disruption causes increased inflammatory response and the infiltration of LDL, cholesterol, and fats into the sub-endothelial space (5). When LDLs become trapped in the wall, they become oxidized, and oxidized LDLs (ox-LDLs) lead to the recruitment of monocytes and other inflammatory response molecules to the entrapment site.

The ox-LDLs lose recognition of their receptors and bind to receptors non-specifically, resulting in a leaky vessel wall. Monocytes transition into macrophages that develop into foam cells with excessive lipid uptake. With the infiltration of smooth muscle cells (SMC), fibrous connective tissue form over the inflammation site. These arterial lesions develop into an atherosclerotic plaque that could result in an acute thrombotic event (Fig. 1.1) (6; 7).

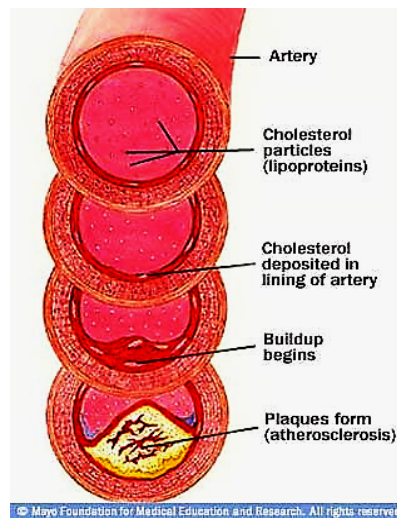


**Figure 1.1. Cumulative Atherosclerosis Progression (8).**

Proper endothelial functions are vital in maintaining vascular wall integrity and cellular homeostasis while endothelial dysfunction leads to pathological conditions, such as heart disease or cancer (9). The endothelial cells (EC) are constantly exposed to hemodynamic forces of the blood flow which exert both normal pressure and tangential shear stress on the endothelium. The hemodynamic forces within the vessel wall are shown in Figure 1.2 (10).

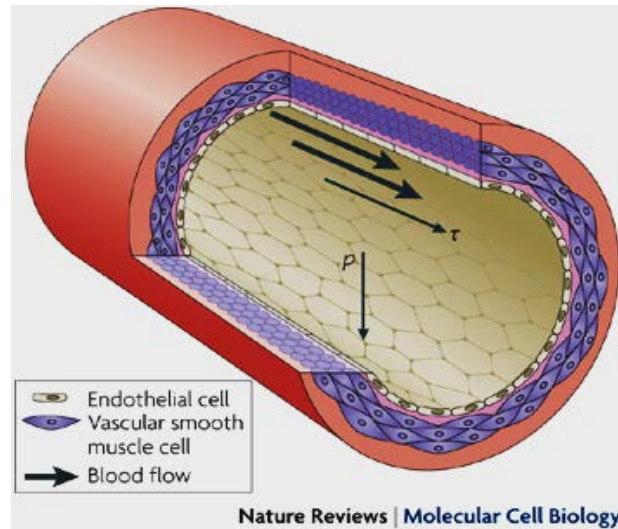


**Figure 1.2. Directional forces acting on the vessel wall (10).**

The ECs that line the arterial wall are exposed to the local environmental conditions and mechanical stimuli introduced by the blood. These stimulants in turn facilitate intercellular signaling response. For example, shear stress influences endothelial cell wall remodeling through modulation of growth-promoting and growth-inhibiting signaling pathways. Additionally, the endothelial cells control hemostasis and thrombosis by providing pro-coagulant, anti-coagulant, and fibrinolytic mediators. By releasing chemotactic and immune response surface molecules, the cells control inflammatory interactions that may occur within arterial system. Likewise, ECs release vasodilators and vasoconstrictors in order to regulate smooth muscle cell contraction (9). Collectively, ECs actively participate in all homeostatic activities of the vascular wall. Therefore, EC dysregulation leads to an increased susceptibility for atherogenic or thrombotic occurrences (11).

Interestingly, atherosclerotic plaque tends to occur near bifurcation sites with disturbed flow profiles where endothelial cells exhibit a pro-atherogenic phenotype.

On the other hand, straight artery sections with uniform, laminar flow profiles promote anti-inflammatory and athero-protective phenotypes, regardless of lifestyle choices (11; 12). The local hemodynamic profile is a key determinant of EC molecular expression, cell morphology, and overall function (13). ECs respond to both mechanical and biochemical stimuli in their environment via signaling transduction pathways that involve mitogen-activated protein kinases (MAPKs) and myriad of transcription factors (table 1.1).

**Table 1.1. Cellular response to laminar flow profile vs. disturbed flow profile.**

<b>Endothelial Cell Response</b>	<b>Key Signaling Constituents</b>	<b>Laminar Flow – Physiological Shear Stress (<math>\geq \sim 10</math> dyne/cm<sup>2</sup>)</b>	<b>Disturbed Flow – Low, Oscillatory Shear Stress (0 – 4 dyne/cm<sup>2</sup>)</b>
<b>Cell response compared to static state conditions (No fluid flow)</b>			
<b>Apoptosis</b>	Various activation pathways (14; 15)	Decreased	Increased
<b>Proliferation</b>	Cell division and vascular wall remodeling (16)	Decreased	Increased
<b>Adhesion</b>	Vascular Cell Adhesion Molecule 1 (VCAM-1) (17-19)	Decreased	Increased
<b>Vascular Constriction</b>	Endothelin 1 (ET-1) (20; 21)	Decreased	Increased

<b>Vascular Dilation</b>	Endothelial nitric oxide synthase (eNOS) (22-24)	Increased	Decreased
<b>Anti-Oxidative Response</b>	Cyclooxygenase 1 (COX-1) and Mn superoxide dismutase (Mn SOD) (25)	Increased	Decreased
<b>Inflammatory Response</b>	Monocyte chemotactic peptide 1 (MCP-1) (26)	Decreased	Increased
<b>Thrombosis Mediators</b>	Tissue plasminogen activator (TPA) (16; 27)	Increased	Decreased
<b>Growth Mediators</b>	Platelet Derived Growth Factor (PDGF) A or B (16; 19; 28)	Decreased	Increased
<b>Growth Mediators</b>	Growth inhibitor – Transforming growth factor $\beta$ 1 (TGF- $\beta$ 1) (29)	Increased	Decreased
<b>Alignment/Shape</b>	Cell motility and Focal adhesion kinase (FAK) (12; 30; 31)	Aligned w/ flow direction – elongated	No alignment – Random, polygon

Apoptosis is a highly regulated cell death process important in maintaining vascular wall integrity. The loss of apoptotic regulation is often associated with various disease mechanisms such as in cancer. Excessive cell turnover and endothelial apoptosis in athero-susceptible regions create leaky walls, disrupts the endothelium barrier and initiates inflammatory signals, allowing for ox-LDL accumulation. In fact, the lack of mechanical stimuli has been shown to trigger apoptosis in endothelial cells, highlighting the crucial role of hemodynamic forces in maintaining vascular wall integrity (14). Due to the important role of apoptosis in multiple cell processes, its dynamic regulation

mechanisms present an interesting avenue of research. Identifying key apoptosis regulators in response to shear stress will help delineate disease development and progression mechanisms.

Death-Associated Protein Kinase (DAPK), a known apoptosis activator, is up-regulated in atherosclerotic lesions (32). DAPK up-regulation leads to increased cell turnover and arterial wall instability, providing increased susceptibility to LDL absorption (33). DAPK activity is absent in some forms of cancer cells where DAPK gene promoter regions become hyper-methylated and influence downstream apoptosis regulation (34). The tumor suppression ability of DAPK has been demonstrated: both as inhibitor of metastasis *in vivo* and as an apoptotic promoter *in vitro* (35-38). Aside from its apoptosis activity, DAPK also attaches to and regulates actin in the cytoskeleton (39; 40). In endothelial cells, tropomyosin-1, another subject of DAPK phosphorylation, is important in maintaining cardiovascular homeostasis and its expression is lost in tumor cells (41). Thus, fluid shear stress may regulate DAPK activation and signaling for both pro- and anti-apoptotic processes. Understanding endothelial DAPK expression and function will help elucidate overlaps between the apoptotic and shear stress signaling pathways. This dissertation assesses the effect of shear stress on endothelial cell phenotype, apoptosis, and DAPK. The potential role of DAPK and its corresponding signaling pathway for endothelial mechanotransduction and endothelial apoptosis is further evaluated.

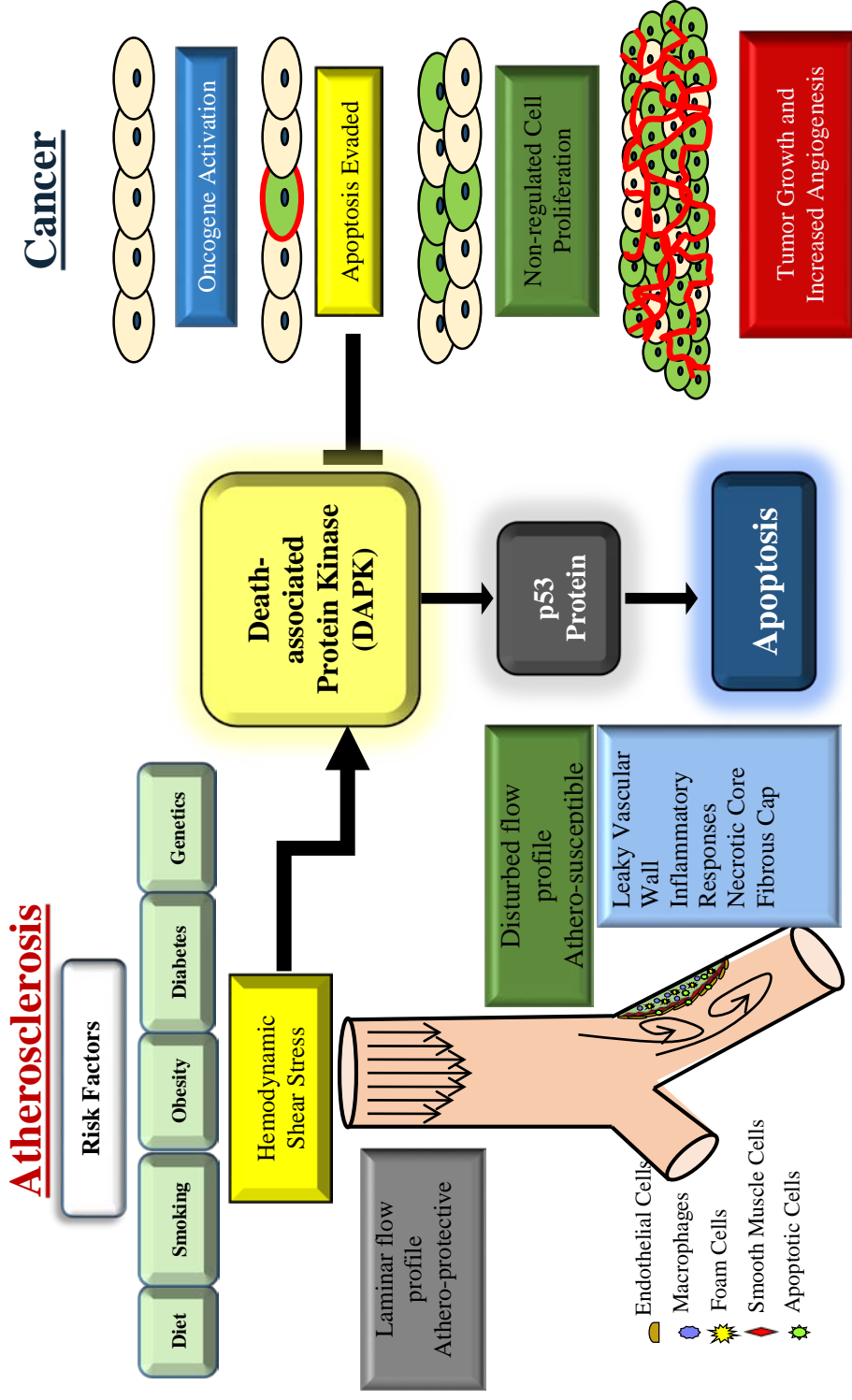


**Figure 1.3. The role of DAPK in both atherosclerosis and cancer (3).** In atherosclerosis, DAPK is upregulated resulting in an increase in vasculature cell turnover. In cancer, DAPK becomes hyper-methylated causing the highly regulated apoptosis process to be circumvented.



## 1.2 Endothelial Mechanotransduction

### 1.2.1 Shear stress: athero-prone vs. athero-protective profiles

The arterial vessel wall is composed of three different layers. The outermost layer, the adventitia, is made up of collection of connective tissue and interwoven thick collagen fibers, ultimately connecting blood vessels to external tissue networks. The central tissue layer, or media, contains smooth muscle cells within a network of collagen and externally protected by a layer of elastic tissue, also known as the external elastic lamina. Within the media layer, the smooth muscle cells and elastin fibers align circumferentially in order to provide structural integrity to the blood vessel wall. Lastly, the innermost layer, or intima, is composed of a layer of endothelial cells supported by a layer of elastic connective tissue, or internal elastic lamina. The intima layer is the tissue interface with blood flow within the vascular system (42). Figure 1.4 shows the three different blood vessel layers.

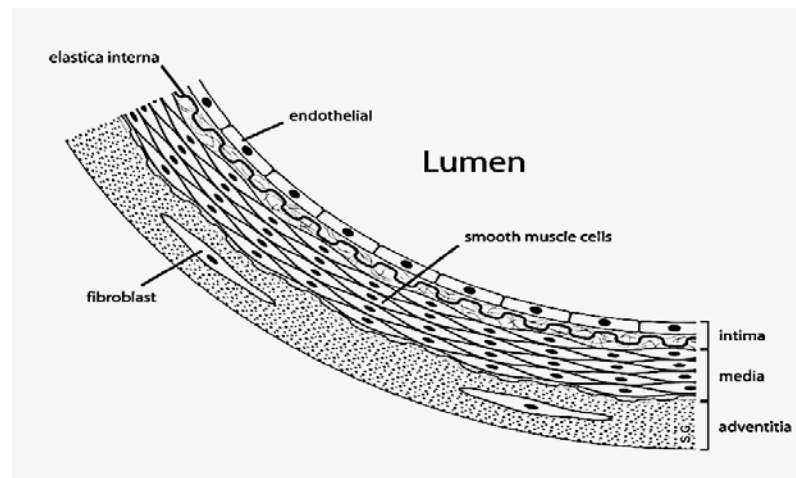


**Figure 1.4. Anatomy of the arterial wall (8; 42).**

The endothelial lining of the blood vessel wall plays a critical role in the initiation and progression of atherosclerotic lesions (43). In the vasculature, blood flow applies a frictional shear stress parallel to endothelial surface due to its viscosity and the velocity gradient. The complex geometry of the vasculature including disturbances, such as curves and bifurcations, gives rise to diverse flow dynamics, localized differences in magnitude and direction of shear stress (44). Endothelial cells are involved in mechanotransduction or the conversion of a mechanical force into biochemical signal response. Low shear or oscillatory flow promotes an atherogenic endothelial cell phenotype promoting increased endothelial turnover and proliferation (45; 46). Figure 1.5 gives a representative view of the difference in vascular fluid flow and specific genotypic changes for laminar and disturbed fluid flow regions.

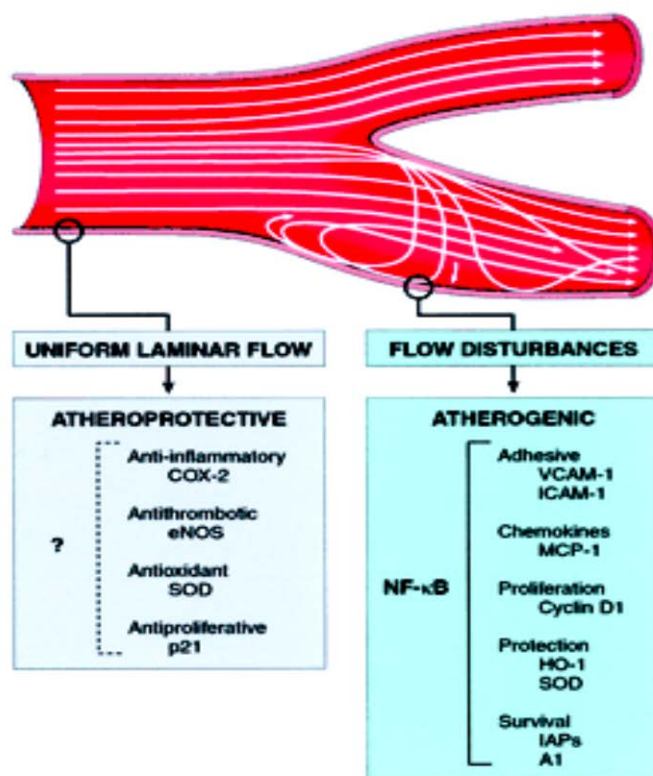


**Figure 1.5. Fluid flow profiles elicit changes in endothelial expression.**

Passerini *et al.* examined *in vivo* endothelial gene expression profiles in regions of both undeveloped or disturbed fluid flow and developed or laminar fluid flow.

Endothelial cells were isolated from different phenotypic regions including the inner curvature of the aortic arch (disturbed flow) and the descending thoracic aorta (laminar flow) of adult male pigs. Reverse transcription polymerase chain reaction (RT-PCR) was performed to amplify endothelial RNA samples followed by a nearly 2000 gene microarray analysis which identified specific gene expression profiles. Up-regulated

inflammatory cytokines were confirmed in the disturbed flow region, yet the particular pro-inflammatory pathways were shown to be inactive. Similarly, there was an enhanced anti-oxidative transcription profile present in the disturbed flow regions (47). Thus, the shear stress-endothelium interaction functions to maintain homeostasis in the vasculature, while also playing a large role in atherosclerosis pathology. Fluid shear stress affects endothelial function in both normal and diseased conditions.

### 1.2.2 Molecular pathways of endothelial mechanotransduction

Fluid shear stress influences endothelial cell phenotype and directly impacts cell functions. Laminar flow (high shear stress) and disturbed, oscillatory flow (low shear stress) affect key differences in endothelial cell phenotype, some of which are outlined in table 1.1. Shear stress of 10 to 70 dynes/cm<sup>2</sup> is observed in normal arteries, and in *in vitro* studies, shear stress between 10 to 25 dynes/cm<sup>2</sup> is commonly used. Endothelial responses to shear stress can be categorized as immediate (rapid release of nitric oxide, NO (48), short-term (up-regulation of tissue plasminogen activator (tPA) gene (27)) and long-term sustained exposure to shear stress leads to endothelial cell re-alignment in the direction of flow and changes in structural organization, mechanical properties, and nuclear activities (30). Endothelial mechanotransduction involves a variety of signaling molecules such as heat shock proteins, transcription factors, mitogen-activated protein kinases (MAPKs) and phosphoinositide 3 (PI3) kinase (20). Ongoing research is mapping out the pathways involved in shear induced endothelial responses and their interplay with apoptosis pathways.

Inflammatory, thrombotic, and proliferative modalities are expressed in arterial regions susceptible to atherosclerotic lesions (44). Low shear stress in these regions affects endothelial expression and results in increased cell turnover. Increased apoptosis disrupts the local endothelial layer and exposes the underlying layers to lipid accumulation and inflammation (45; 46). Studies have identified various key signaling molecules that respond to endothelial shear, although their specific role in apoptosis and atherosclerosis remain ambiguous (49); (14); (47). One key mechanotransduction element, MAPK is also transiently activated in immune response cascades by inflammatory cytokines such as those found in regions of low shear stress (19). Tissue necrosis factor  $\alpha$  (TNF $\alpha$ ) and interleukin (IL) 1 $\beta$  are inflammatory cytokines that regulate endothelial responses. Cytokine induction of endothelial cells stimulates MAPKs such as c-Jun N-terminal kinase (JNK), extracellular signal-regulated kinase (ERK), and p38 proteins that play a significant role in mediating inflammatory responses including apoptosis.

Alternatively, high laminar shear stress was shown to inhibit cytokine activation of key MAPK signaling constituents. For example, shear stress phosphorylates MAPK which results in the activation of (ERK). Surapisitchat et al. confirmed that laminar shear stress inhibits downstream inflammatory signaling in endothelial cells (50). For each experiment, laminar shear stress (12 dynes/cm<sup>2</sup>) was applied for 10 minutes followed by a 15 minute cytokine, TNF $\alpha$  (10 ng/mL), incubation of sheared human umbilical vein endothelial cells (HUVECs). Shear stress alone was shown to stimulate ERK and p38 activity while JNK expression was decreased compared to non-sheared controls. Furthermore, the exposure of shear stress decreased JNK expression by nearly 46%,

while ERK and p38 activation under cytokine induction was not significantly affected by shear (50). This study highlights a key role of laminar shear stress in mitigating downstream inflammatory response stimulated by cytokine exposure. Mitogen activated protein kinase phosphatase 1 (MKP-1) is a negative mediator of inflammatory signals and dephosphorylates both p38 and JNK. Laminar shear increased MKP-1 expression and down-regulated vascular cell adhesion molecule 1 (VCAM-1) expression in HUVECs. These findings suggest that laminar shear stress induced MKP-1 expression to suppress JNK and p38 MAPK expression, both of which were stimulated by inflammatory cytokines. These studies emphasize the importance of laminar shear stress in suppressing inflammatory responses, which also overlaps with endothelial apoptosis signaling cascades.

## **1.3 Apoptosis**

### **1.3.1 Signals and mechanisms of apoptosis**

Apoptosis is a highly regulated cell death pathway triggered by external stimuli or internal cell stressors. In apoptosis, as the nuclear chromatin begins to condense and the cell starts to shrink, the cell membrane stays intact but begins to deform in a process also known as blebbing. Eventually chromosomal DNA begins to fragment, and the cytoplasm and nucleus fragments form into apoptotic bodies. At the same time, surface receptors are exposed to the environment, signaling for macrophages and phagocytes to engulf the apoptotic bodies (51). Cellular apoptosis is mediated through various external and internal signals. External stimuli that directly bind to or infiltrate the cell membrane

to initiate apoptosis include: inflammatory cytokines, growth factors, hormones, and cytotoxic molecules (52). Binding to their respective cell surface receptors triggers receptor mediated extrinsic pathways in cells and apoptotic agents are released subsequently. The extrinsic apoptosis pathway is utilized in inflammatory responses associated with pathological conditions such as atherosclerosis (53). Other apoptotic triggers that induce apoptosis include cell stressors such as internal DNA damage, oxidative stress, nutrient and serum deprivation, hypoxia, heat, and radiation (54). As a result, cells have increased intracellular calcium, hydrogen peroxide, glucocorticoids, or other intra-molecular imbalances. Intrinsic apoptosis initiated in cells under stress occurs through mitochondria-mediated intrinsic pathways. Cell stressors change the mitochondria membrane permeability which results in the release of apoptosis-inducing proteins such as Cytochrome C (55). Continued stress leads to the activation of caspases, DNA fragmentation, and eventually cell death (56).

### 1.3.2 Shear stress and endothelial apoptosis

A functional balance between cell death and cell proliferation in the endothelium helps regulate vascular wall homeostasis. While endothelial apoptosis is a critical regulatory cell process that helps maintain tissue homeostasis, it also has key implications in various pathologies. Misdirected apoptotic signaling is involved in diseases such as cancer and vascular diseases such as atherosclerosis (57; 58). As previously described, the local hemodynamic profile of the endothelium also dictates endothelial cell functions. Cell organization, migration, and structural changes are tightly coordinated in vascular wall remodeling and adaptation under various flow conditions. For example, in regions of

disturbed, oscillatory flow with low shear stress, excess cell turnover generates spatial differences in the apoptosis in the endothelium (57; 59). Thus, the relationship between shear stress and endothelial apoptosis presents an important area of research with significant implication in vascular diseases.

Excess endothelial apoptosis *in vivo* are recognized in various human and animal disease models (60-62). In the endothelium, increased apoptosis disrupt the cell lining and potentially expose vessels to accumulation of oxidized lipoprotein and macrophages in the sub-endothelium, as during the disease progression of atherosclerosis. External biochemical and mechanical triggers such as shear stress induce a variety of signal transduction pathways including mediators of apoptosis. However, endothelial apoptosis under fluid shear stress is not fully understood. Table 1.2 summarizes current findings on endothelial apoptosis.

**Table 1.2. Pro- vs. anti-apoptotic factors and corresponding pathways in endothelial cells.**

<b>Interaction</b>	<b>Key Signaling Components</b>	<b>Cell Response</b>	<b>Apoptosis Effect</b>
<b>Extracellular matrix interactions</b>	$\beta$ 1 integrins - signal FAK, activates MAPK and phosphoinositide 3-kinase (PI3-K) (63)	Promotes cell survival through PI3K/Akt survival pathway	Anti-apoptotic
	Integrin antagonist ( $\alpha$ 2 $\beta$ 1, $\alpha$ v $\beta$ 3, $\alpha$ v $\beta$ 5) (64)	Disrupts integrin signaling leading to cell death process	Pro-apoptotic
<b>Growth factors</b>	Vascular endothelial growth factor (VEGF), Fibroblast growth factor (FGF), Insulin, Angiopoietin-1 (65; 66)	Inactivates pro-apoptotic molecules (i.e. caspase-9) Promotes cell survival through PI3K/Akt path	Anti-apoptotic
<b>Nuclear factor kappa B (NF-<math>\kappa</math>B)</b>	Activated via TNF $\alpha$ , integrin antagonist, hypoxia (67; 68)	Increases anti-apoptotic gene expression	Anti-apoptotic



<b>Shear Stress</b>	Laminar Shear – physiological shear stress	Atheroprotective cell phenotype; See table 1.1	Anti-apoptotic
	Disturbed Shear – low shear stress	Atherogenic cell phenotype; See table 1.1	Pro-apoptotic

While several *in vitro* studies have investigated pro- and anti-apoptotic factors and signaling pathways in endothelial cells, those studies were not carried out in the presence of shear stress (62; 63; 69). On the other hand, most shear stress studies in endothelial cells have focused more on understanding inflammatory responses (70-73). Future apoptosis studies in the presence of fluid shear stress can help clarify important mechanotransduction mechanisms under both physiological and pathological conditions.

## 1.4 Death-Associated Protein Kinase

### 1.4.1 DAPK in apoptosis

The apoptotic process is tightly regulated by environmental stimuli including biochemical signals and physiological injuries. Death-associated protein kinase (DAPK) functions primarily as a mediator of programmed cell death whose expression is lost in cancerous cells (34). Loss of DAPK expression in human carcinoma cell lines and its ubiquitous presence in many cell and tissues types emphasize its importance in regulating apoptosis. DAPK was discovered in HeLa cells transfected with antisense cDNA libraries that inactivated growth-resistance genes under interferon-gamma (IFN- $\gamma$ ) incubation. IFN- $\gamma$  is an immune response cytokine protein with anti-tumor properties.

The subsequent cDNA fragments from the transfected cells were studied, and genes involved in the suppression of IFN- $\gamma$ -induced apoptosis were identified (74; 75).

DAPK is a 160 kD, calcium/calmodulin ( $\text{Ca}^{2+}/\text{CaM}$ ) regulated serine/threonine protein kinase that includes a regulatory calmodulin binding domain, a cytoskeleton binding domain, two P-loop nuclear binding domains, a stretch of 8 ankyrin repeat domains, and an independent death domain required for initiating cell death processes (74). DAPK is activated when calcium-modulated  $\text{Ca}^{2+}/\text{CaM}$  complex binds to the CaM domain of DAPK, which causes a conformational change and a release of DAPK auto-inhibition. In the absence of  $\text{Ca}^{2+}/\text{CaM}$  binding, DAPK is auto-phosphorylated at serine 308 in the CaM domain. Following apoptotic signals, the dephosphorylation of serine 308 and  $\text{Ca}^{2+}/\text{CaM}$  binding are necessary to fully activate the catalytic apoptotic activities of DAPK (40). The DAPK protein structure is shown in Figure 1.6, including its various binding sites and domains.

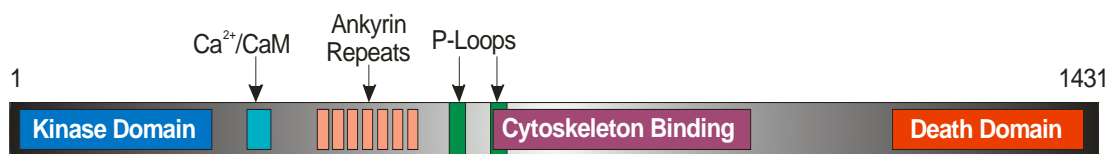


**Figure 1.6. DAPK binding domains.**

DAPK is activated following a variety of stimuli including and tumor necrosis factor ( $\text{TNF}\alpha$ ), ceramide, interferon (IFN- $\gamma$ , and oncogenes such as p53 (76-79). DAPK also promotes apoptosis triggered by other factors including: transforming growth factor (TGF- $\beta$ ), anti-Fas, ceramide, oxidative stress, and serum starvation of cells (75; 78; 80; 81). Serving as a converging point for apoptotic signaling, DAPK is upstream of

caspsases, except caspase 8, and induces other caspase-independent cell death or autophagy (82).

DAPK promotes TNF $\alpha$  and Fas-induced apoptosis in HeLa cells. TNF $\alpha$  and Fas cytokine incubation did not affect cell death populations after antisense cDNA silenced DAPK expression in epithelial cells. However, over-expression of DAPK significantly increased cell death under the same cytokine induction (78). Similarly, Raveh *et al.* showed that DAPK was up-regulated in the presence of oncogenes such as c-Myc protein, activated via the MAPK/ERK mitogenic pathway (36). Further DAPK studies are needed to clarify the oncogene pathway and its association with apoptosis, and to examine the effect of cytokine induction on DAPK in apoptosis.

#### 1.4.2 DAPK in cancer

Most recent DAPK research focuses on apoptosis in cancer cells as well as HeLa cells, fibroblasts, and neurons. Decreased DAPK expression results in a loss of apoptosis regulation and diminished cell turnover (34; 35). A lack of controlled apoptosis can lead to tumorigenesis and subsequent metastasis in surrounding tissue. DAPK expression is silenced by DNA hyper-methylation in some types of cancer pathologies. Endogenous DAPK expression can be restored by removing methyl groups from DAPK nucleotides in various types of carcinoma cell lines, and certain cancer cells can evade p-53 dependent apoptosis through DAPK gene methylation and inactivation (83). The resulting recovery of apoptosis shows DAPK as an important positive modulator of cell death.

DAPK activity is also inhibited by upregulated expression of cellular Src kinase. Src kinase is a non-receptor tyrosine kinase, whose over-expression is implicated in the

development in colon cancers (84). Wang et al. showed that epidermal growth factor (EGF) stimulated an increase in Src kinase activation, resulting in DAPK inhibition. DAPK activates some apoptotic activities following the dephosphorylation at Y491/Y492 in the ankyrin domain (85). Therefore, an increase in Src kinase activity suggests that DAPK expression may be detected but inactive in certain cancer cells, due to a competing tyrosine phosphorylation modality. This study highlights an importance in also understanding post-translation DAPK regulation and its role in cancer pathology. Alternatively, DAPK expression may have a role in cell survival. In cancer cells where DAPK remains functional, studies have shown that silencing normal DAPK expression can trigger caspase-dependent apoptosis in the absence of other apoptotic stimuli (86). Therefore, DAPK expression plays a crucial role in overall apoptosis regulation and remains a relevant target for potential anti-cancer therapies.

#### 1.4.3 DAPK in endothelial apoptosis

Loss of apoptosis regulation can facilitate atherosclerotic disease progression. In the vasculature, there is an increase of endothelial cell turnover in regions of low shear stress and disturbed flow condition. Laminar shear stress inhibits apoptosis activated by cytokines, oxidative stress, and serum starvation of cells (87). At the onset of shear, endothelial responses include: increase of intracellular calcium, nitric oxide, and rapid and transient activation of MAPKs that could also interact with and regulate DAPK activity. Three major families of MAPKs (ERK, JNK and p38) have been identified to both play a role in endothelial mechanotransduction and interact with DAPK in its apoptotic activities. Under shear stress, ERK activation is maximal between 5 to 10 min,

5 to 30 min for JNK and p38; with all 3 returning to basal level after 1 hr (88; 89).

Interestingly, ERK phosphorylates DAPK at serine 735 which inhibits the ERK-C/EBP-beta pathway and up-regulates apoptosis activation (90). TNF $\alpha$  and IL-1 $\beta$  incubation alone stimulated JNK expression, while laminar shear at 12 dynes/cm<sup>2</sup> inhibited JNK activation under the same conditions. Pre-exposure of endothelial cells to shear stress prevents TNF- $\alpha$  activation of JNK, but not ERK or p38 (50). DAPK phosphorylates protein kinase D (PKD) which in turn stimulates JNK expression in response to oxidative stress (91). Eisenberg-Lerner et al. revealed an interesting oxidative stress activation pathway, although the full effects of oxidative stress on cell apoptosis are not fully understood.

Figure 1.7 outlines some of the molecular signaling pathways that cross-talk with DAPK, following various extracellular triggers, leading to apoptosis or other cellular responses. Mechanical stimulation, shear stress, leads to focal adhesion kinase activation and cytoskeletal response mechanisms. The resultant signals are transduced to the nuclear membrane eventually leading to changes in gene expression. These upstream cell signals lead to changes in cell activity to counteract the external forces and maintain homeostasis.

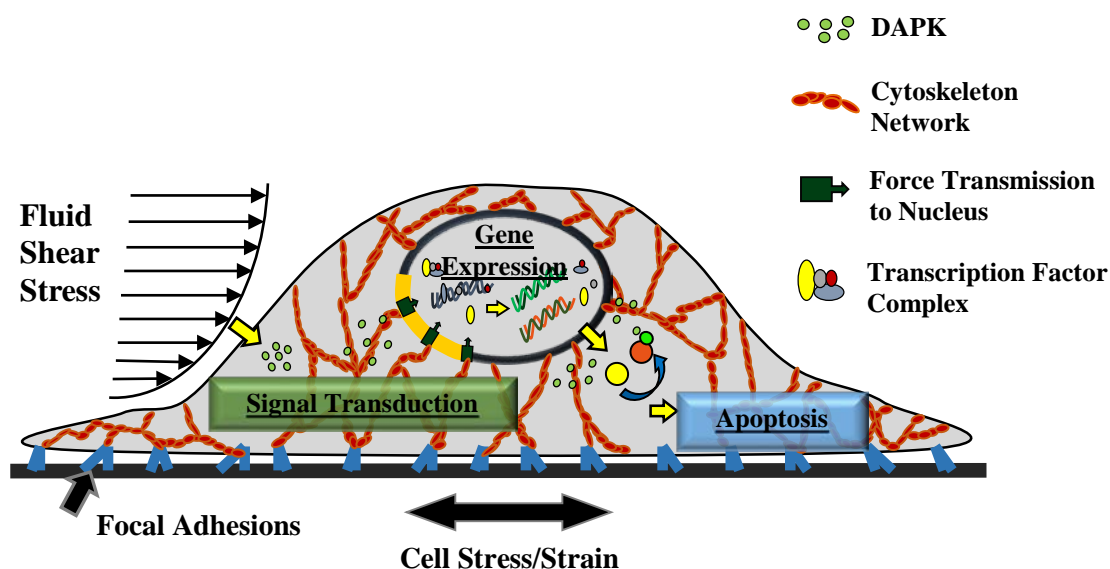


**Figure 1.7. A model of DAPK activity in endothelial mechanotransduction under shear stress** (highlighted by arrows in yellow). Shear stress triggers signal transduction through the cytoskeletal network to the nucleus and modulates changes in cell phenotype, proliferation, motility, and apoptosis. The expression and activity of DAPK, which resides in the actin network, is susceptible to shear stress. Endothelial DAPK could participate in either signal transduction related to cytoskeleton changes or regulation of cell apoptosis.

Specifically, the  $\text{Ca}^{2+}$ /Calmodulin and the kinase domains are responsible regulating catalytic activities and recognizing specificities of substrate interaction. The rest of the molecular components of DAPK (P-loops, ankyrin repeats, and cytoskeleton and death domains) are involved in sub-cellular localization and protein interactions (78).

Table 1.3 describes multiple phosphorylation sites that control DAPK activity, along with the specific domain binding locations. Different phosphate binding sites lead to overall DAPK activation and modulate various cell signaling mechanisms such as apoptosis or cytoskeletal network changes.

**Table 1.3. Specific DAPK phosphorylation sites.**

<b>Phosphorylation Site</b>	<b>Location of Phosphorylation</b>	<b>Mechanism of Action</b>
Phosphorylation due to p90 ribosomal S6 kinases (RSK) at Serine 239	Ca <sup>2+</sup> /Calmodulin domain	Triggers suppression of pro-apoptotic function (92)
Auto-phosphorylation at Serine 308	Ca <sup>2+</sup> /Calmodulin domain	Influences cytokine apoptotic pathway; p53 dependent pathway (93)
Extracellular Signal-Regulated Kinase (ERK) phosphorylation at Serine 735	In between Ankyrin repeats and the P-loop	Switches off the ERK-C/EBP-beta pathway, Up-regulating the cell turnover processes (90)
Phosphorylation by SRC at Tyrosine 491/492	Within the 8 Ankyrin repeats	Stimulates intra-molecular interaction and inactivation (85)
Dephosphorylated due to leukocyte common antigen-related (LAR) tyrosine phosphatase at Tyrosine pY491/492	Within the 8 Ankyrin repeats	Induces the catalytic activity of DAPK, reducing cell adhesion and motility (85)

The auto-phosphorylation site at Serine 308 is involved in overall DAPK kinase activation. After binding Ca/Calmodulin, DAPK must be dephosphorylated at serine 308 to be proceed in other cell activities. By studying both overall and phosphorylated DAPK, the kinase activation profile and connection between applied shear and apoptosis can be better understood.

Aside from its role in apoptosis, DAPK also regulates actin cytoskeleton and contributes to cytoplasmic changes associated with apoptosis such as stress fibers and membrane blebbing (94). While DAPK is a positive mediator for apoptosis, it is localized to the actin network, and phosphorylates myosin regulatory light chain (MLC) at Ser19 both *in vivo* and *in vitro* (39; 95). As a result, DAPK promotes acto-myosin contractility and stabilizes stress fibers in serum starved fibroblasts, and mediates serum-induced stress fiber formation. Interestingly, in endothelial cells DAPK phosphorylates

tropomyosin-1 (TM-1) at Ser283 in response to ERK activation under oxidative stress, and this phosphorylation in turn, is required for formation of stress fibers (96). Therefore, DAPK localization and interaction with the cytoskeleton influences cell motility, cytoplasmic changes, and focal adhesion coordination. The cytoskeleton effect of DAPK occurs before onset of apoptosis, and it is independent of the DAPK death domain. The role of DAPK in apoptosis and its association with the actin cytoskeleton suggest it as a potential regulator of endothelial responses in mechanotransduction. Mechanisms of DAPK regulation and function in endothelial cells are largely unknown, and are currently being analyzed (Fig. 1.8). DAPK studies has mainly focused on select types of cancer cells (97), the potential interaction between shear stress and DAPK activity warrants further studies in both apoptotic and non-apoptotic actions of DAPK in endothelial cells.





## 2. EXPERIMENTAL MATERIALS AND METHODS

### 2.1 Cell Culture and Reagents

Bovine aortic endothelial cells (BAEC; Lonza) were cultured using Dulbecco's Modified Eagle Medium (DMEM) with 10 % fetal bovine serum (JR Scientific), 1 % L-glutamine, and 2% penicillin/streptomycin (Sigma), in tissue culture flasks at 37°C with 5% CO<sub>2</sub>. Cell media was changed on a regular basis to supply nutrients and control the pH environment for the BAECs. The cell cultures were grown to 95% - 100% confluency before passage and plating. To pass, cells were washed with Phosphate Buffered Saline (PBS; SIGMA) and incubated with Trypsin (SIGMA) for approximately 3 - 5 minutes at 37°C. After trypsin, DMEM was added to re-suspend the BAECs. The cell solution was collected in a 15mL tube and centrifuged at 2100 rpm for 5 minutes to pellet the cells. Next, the cells were re-suspended in new DMEM and plated on sterile glass or silicone membrane slides for mechanotransduction experiments.

BAEC at passage number 4 to 10 were passed and plated on 38x75x1 mm glass slides at approximately 600,000 cells per slide (for shear stress experiments) and cultured for 24 hours to confluency before experiments.

For silicone membrane studies, silicone sheets were obtained from Specialty Manufacturing. MTS testing done on the material in our laboratory obtained elastic modulus 1.2 to 1.5 MPa. The silicone membrane was cut to similar size as glass slides (38×75 mm), and placed in 10 cm petri dishes to be cleaned with ethanol, followed by sterilization under UV light. Both silicone and glass substrates were coated with 1.5 µg/ml fibronectin for at least 4 hours on an orbital shaker and stored at 4°C. BAEC at passage number 4 to 10 were passed and plated on 38x75x1 mm silicone membranes with approximately 700,000 cells/membrane.

Human TNF $\alpha$  (Sigma) was reconstituted in water to a stock concentration of 10 µg/ml and added to static or shearing media for final working concentration of 10 or 25 ng/ml. Hydrogen peroxide (H<sub>2</sub>O<sub>2</sub>, Sigma) was diluted to a 750 mM stock concentration and added to static or shearing media for a final working concentration of 0.3-0.5 mM. For serum depletion, cell media for static and shearing conditions was the same components as previously described except decreasing the FBS from 10% down to 0.5% to initiate apoptosis. The peGFP human DAPK wildtype plasmid was constructed based on the Clontech peGFP plasmid, using the original promoter (a gift from Dr. Patricia Gallagher). After plasmid amplification and purification, transfection into BAEC plated on glass slide was done using Metafectene (Biontex USA) for 4 hours at a ratio of 5 µg DNA to 15 µl Metafectene. Transfection was done in serum free DMEM, and cells recovered in incubator overnight before experiments.

## 2.2 Parallel Plate Flow Chamber and Shear Stress

### 2.2.1 Fluid mechanics of the parallel plate flow model

For the shear stress experiments, a parallel plate flow chamber was used to simulate fluid shear on bovine aortic endothelial cells (BAEC). A parallel plate flow chamber is a rectangle-shaped chamber with multiple components (95). The flow chamber has a bottom section to house the glass slides containing the cells. There are rubber gaskets to aid in sealing in between the sections. Also, the top section has an inlet and outlet for the circulating media to flow through the chamber. There is a small gap height between the frame pieces to allow for fluid to flow across the cells (Fig. 2.1). The controlled simulated shear was used to induce mechanical stimulate the endothelial cells, mimicking the physiological hemodynamics in the vasculature.

Blood flow in the arteries can be rather difficult to mimic, therefore some fluid mechanics simplifications had to be applied for the experimental flow setup. The Navier-Stokes equation, describing differential fluid flow movement for a relative system, was deduced from a possible three dimensional to a one dimensional flow system considering horizontal flow across an assumed infinite parallel plate. This assumption is valid due to a small height to width ratio within our flow chamber. Equation 2.1 describes the 1-D Navier-Stokes equations used for our infinite parallel plate flow system.

$$\rho * \left( \frac{\partial u}{\partial t} + u \frac{\partial u}{\partial x} + v \frac{\partial u}{\partial y} + w \frac{\partial u}{\partial z} \right) = - \frac{\partial p}{\partial x} + \mu \left( \frac{\partial^2 u}{\partial x^2} + \frac{\partial^2 u}{\partial y^2} + \frac{\partial^2 u}{\partial z^2} \right) + \rho g_x \quad \text{Eq. 2.1}$$

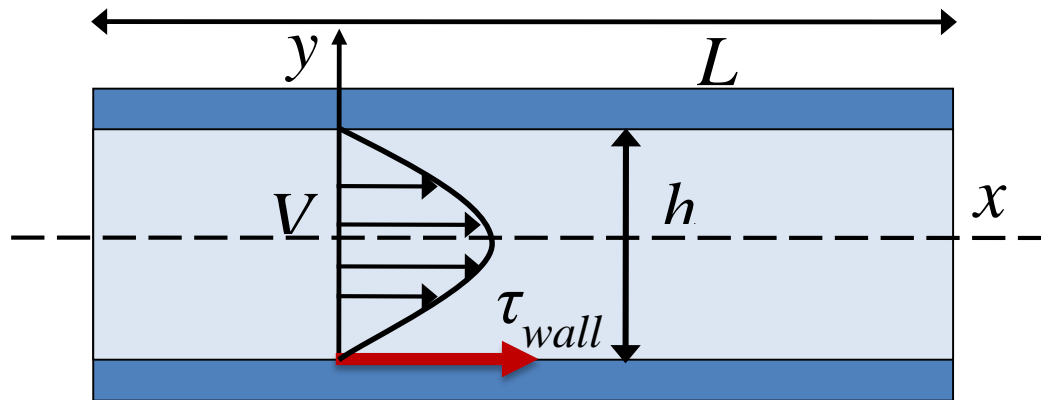


**Figure 2.1. Fluid flow profile for the flow chamber.**

Additionally, the assumption of laminar flow is accepted based on low velocity flow, which in turn yields a low Reynolds number, the ratio between inertial forces and viscous forces in the fluid. The entrance length of the flow chamber is neglected due to a smaller entrance length compared to the entrance length of the chamber, where fully developed velocity profiles are validated. The fluid is characterized as a fully developed parabolic flow assuming flow symmetry occurring uniformly across the samples.

Steady state flow conditions were used to negate any time-dependent calculations for the flow system, assuming the flow would be stable within a short period of time after initial exposure of flow. Lastly, the flow was considered incompressible, due to very little to no pressure applied to the fluid within the system. Collectively, the simplifications helped to define the Navier-Stokes equation for fluid movement and shear applied within the flow system.

Assuming uniform flow in 1-D, fully developed parabolic, steady state, laminar, and incompressible flow, the Navier-Stokes equations becomes only dependent upon pressure and shear forces applied to the system as seen in Eq. 2.2.

$$0 = -\frac{\partial p}{\partial x} + \mu \left( \frac{\partial^2 u}{\partial y^2} \right) \quad \text{Eq. 2.2}$$

Where  $p$  is the pressure,  $\mu$  is the viscosity of the flow medium, and  $u$  is the x- direction velocity of the flow in the system.

Two specific boundary conditions are applied to further simplify the equations and to define the flow within the chamber. Boundary condition 1 will imply a no slip condition at the wall-fluid interface showing that the flow velocity will be zero at this interface. For boundary condition 2, the flow is considered to be fully developed, implying that there is no change in the velocity at the center of the flow profile. At the center of the flow, the velocity is at the maximum.

$$y = 0, h \rightarrow u = 0 \quad \text{[Boundary Condition 1]}$$

$$y = h/2 \rightarrow \frac{du}{dy} = 0 \quad \text{[Boundary Condition 2]}$$

Where  $h$  is the height of the flow chamber along the y-axis and the flow is along the x-axis.

$$\text{Equation 2.2: } \frac{d^2 u}{dy^2} = \frac{1}{\mu} \frac{dp}{dx}$$

$$1^{\text{st}} \text{ Integration: } \frac{du}{dy} = \frac{y}{\mu} \frac{dp}{dx} + C_1 \quad \text{Eq. 2.3}$$

$$2^{\text{nd}} \text{ Integration: } u = \frac{y^2}{2\mu} \frac{dp}{dx} + yC_1 + C_2 \quad \text{Eq. 2.4}$$

$$\text{Applying both boundary conditions: } C_1 = -\frac{h}{2\mu} \frac{dp}{dx} ; C_2 = 0$$

$$\frac{du}{dy} = \frac{y}{\mu} \frac{dp}{dx} - \frac{h}{2\mu} \frac{dp}{dx} \rightarrow \frac{du}{dy} = \frac{1}{\mu} \frac{dp}{dx} \left( y - \frac{h}{2} \right) \quad \text{Eq. 2.5}$$

$$\text{Definition of Shear Stress: } \tau = \mu \left( \frac{\partial u}{\partial y} + \frac{\partial v}{\partial x} \right); \text{ with } \frac{\partial v}{\partial x} = 0 \text{ in 1 - D.} \quad \text{Eq. 2.6}$$

$$\text{Substituting Eq. 2.5: } \tau = \frac{dp}{dx} \left( y - \frac{h}{2} \right) \quad \text{Eq. 2.7}$$

$$\text{Volumetric Flow Rate} \rightarrow Q = \int_A \bar{V} * d\bar{A} = \int_0^h u * w dy = -\frac{1}{12} \frac{dp}{dx} * h^3 \quad \text{Eq. 2.8}$$

With  $\bar{V}$  representing the average flow velocity integrated over the entire flow area, and  $w$  is the width of the flow chamber which is a constant value. In result,  $\frac{dp}{dx}$  has to be less than 0 in order to have flow across the chamber. The average flow velocity is defined as the volumetric flow rate per unit depth, as seen in Equation 2.9.

$$\text{Average Flow Velocity} \rightarrow \bar{V} = Q/A = \frac{\frac{-1}{12\mu dx} * h^3}{h * w} = -\frac{1}{12\mu} \frac{dp}{dx} * h^2 \quad \text{Eq. 2.9}$$

Next, the maximum flow velocity is derived to relate to the average flow velocity.

$$\begin{aligned} \text{After integrating: } \frac{du}{dy} &= 0 = \frac{1}{\mu} \frac{dp}{dx} \left( y - \frac{h}{2} \right) \\ u_{\max} = u\left(\frac{h}{2}\right) &= \frac{1}{\mu} \frac{dp}{dx} \left( y^2 - \frac{yh}{2} \right); \text{ where } y = h/2 \\ u_{\max} &= -\frac{1}{8\mu} \frac{dp}{dx} * h^2 \end{aligned} \quad \text{Eq. 2.10}$$

After finding the average and maximum flow velocities, we can find a relation between the two, in order to manipulate the shear stress equation into variables that are known.

$$\frac{u_{\max}}{\bar{V}} = \frac{\frac{-1}{8\mu dx} * h^2}{-\frac{1}{12\mu dx} * h^2} = 3/2; \quad u_{\max} = \frac{3}{2} \bar{V} \quad \text{Eq. 2.11}$$

Using the definition for the mass flow rate,  $\dot{m} = \rho \bar{V} A$ , Eq. 2.12, we can express the average velocity as:  $\bar{V} = \frac{\dot{m}}{\rho A}$ , Eq. 2.13. Next, we further simplify Equation 2.10 using our new variable relationships from Equation 2.13 to define the new pressure gradient relationship, as seen in Equation 2.14.

$$\frac{dp}{dx} = -\frac{8\mu}{h^2} u_{\max} = -\frac{8\mu}{h^2} \left(\frac{3}{2} \bar{V}\right) = -\frac{8\mu}{h^2} \left(\frac{3}{2}\right) \left(\frac{\dot{m}}{\rho A}\right) \quad \text{Eq. 2.14}$$

Now that the pressure gradient is defined, we can rewrite the shear stress equation that was previously defined in equation 2.7.

$$\tau = \frac{dp}{dx} \left(y - \frac{h}{2}\right) = -\frac{8\mu}{h^2} \left(\frac{3}{2}\right) \left(\frac{\dot{m}}{\rho A}\right) \left(y - \frac{h}{2}\right) = -\frac{12\mu\dot{m}}{h^2\rho A} \left(y - \frac{h}{2}\right) \quad \text{Eq. 2.15}$$

Using the volumetric flow rate and mass flow rate, Equations 2.8 and 2.12, we already have defined  $Q = \bar{V}A$  and  $\bar{V} = \frac{\dot{m}}{\rho A}$ . Therefore  $Q = \frac{\dot{m}}{\rho}$ ; which can be inserted into the shear stress relationship.

When the shear stress equation is evaluated at  $y = 0, h$ ; at the chamber walls, shear stress becomes:

$$\tau = -\frac{12\mu\dot{Q}}{h^2\rho} \left(y - \frac{h}{2}\right) \rightarrow \tau(0) = \frac{6\mu\dot{Q}}{hA} \text{ and } \tau(h) = -\frac{6\mu\dot{Q}}{hA} \quad \text{Eq. 2.16}$$

Ultimately, the final form of the shear stress applied at the surface from the flow is dependent on the viscosity of the media, volumetric flow rate, height of the chamber, and the total flow area.

$$\tau = \frac{6\mu\dot{Q}}{hA} \quad \text{Eq. 2.17}$$

Equation 2.17 displays all known variables to express the shear stress of the flow. This calculation will show what shear is applied to the cells, and just how we can vary the amount of shear applied by our system, specifically through varying the volumetric flow rate,  $Q$ .



### 2.2.2 Experimental shear stress setup

Cells were grown on glass slides to approximately 100% confluency. Cell slides were placed in a flow chamber and hooked up to a flow loop placed in an environment chamber, to mimic physiological conditions. Figures 2.2 and 2.3 show the flow chamber setup that houses the sheared cells.

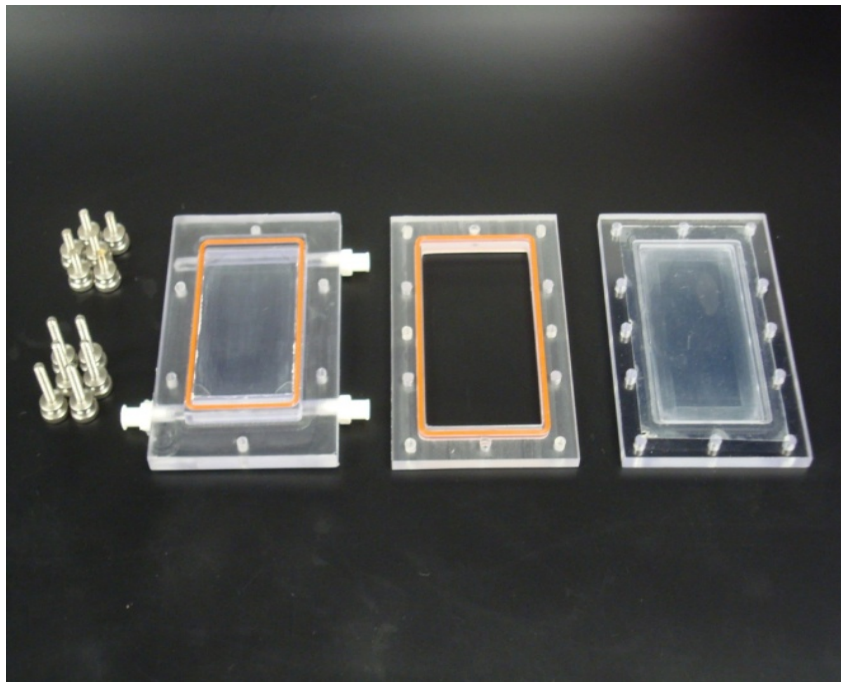


**Figure 2.2. The three pieces of the flow chamber: top, middle, and bottom.**

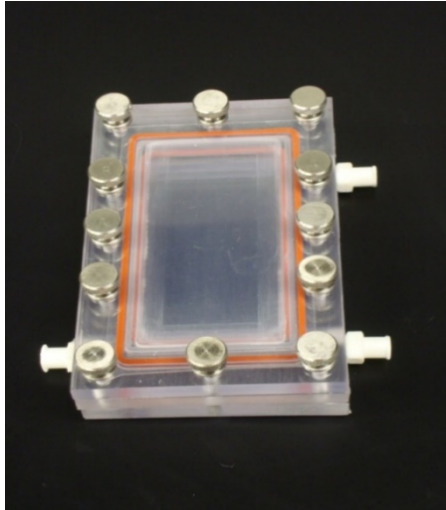


**Figure 2.3. Fully constructed parallel plate flow chamber.**

The middle and bottom pieces of the chamber are held together by stainless steel screws to house the glass slide containing cells. Media flowing in and out of the top piece horizontally shears the cells. All three pieces are tightened together with screws and setup in the Plexiglas housing (Fig. 2.4).

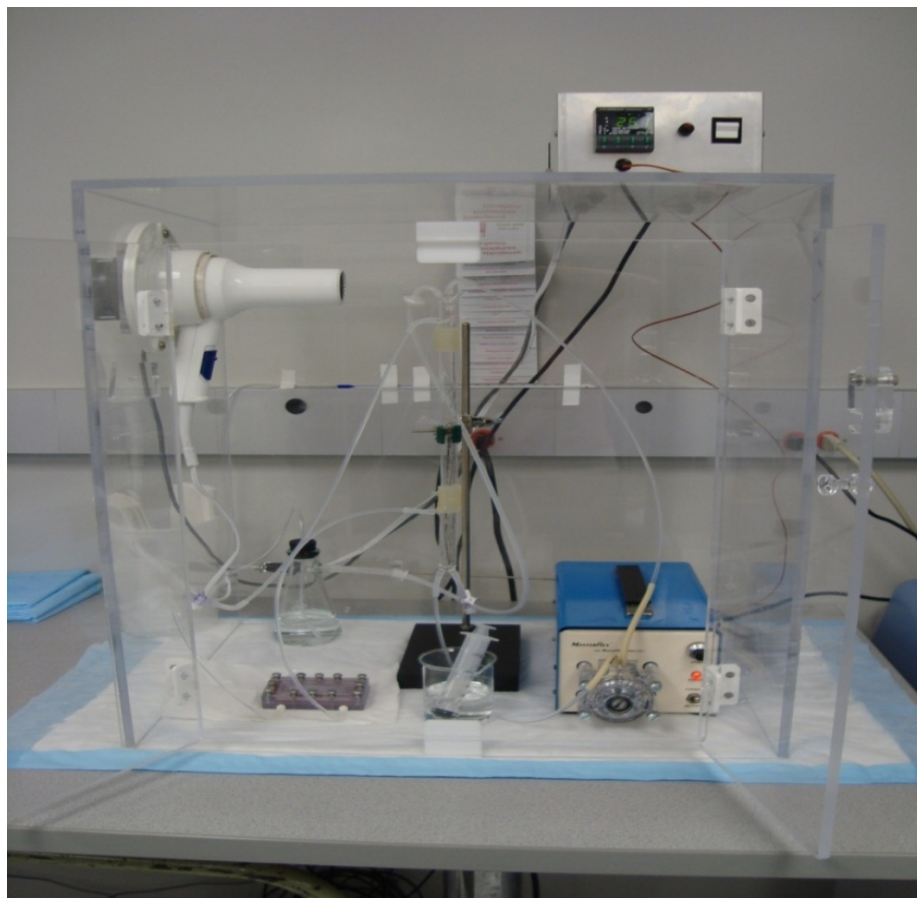


**Figure 2.4. Housing environment for flow setup and temperature control.**

The housing environment consists of multiple components for the flow experiments. There is a power supply unit and digital thermometer calibrated to keep the temperature inside the Plexiglas chamber at 37° C. A Masterflex rotating pump cycles media throughout the flow system. A modified hair dryer heats the chamber during experiments, controlled internally by a heat sensor probe and externally by the digital thermometer (Fig. 2.4). The hair dryer will turn on when the temperature falls below the preset value until the preset temperature has been restored.

The glass tube reservoir system consists of three different sections connected with silicone and Teflon tubing: a top glass tube with three inlets and one outlet, a straight

section glass tube, and a bottom glass reservoir with one inlet and two outlets. There are inlets for CO<sub>2</sub>, flow media, and an air release in the top tube. The first outlet is for distributing media to the flow chamber. The bottom section of tubing contains an inlet that receives media flow from the attached flow chamber that returns to the bottom glass tube into the reservoir. The other inlet is plugged with a three-way stopper allowing for adding or subtracting media to the reservoir. From the reservoir, there is an outlet where the media is cycle back to the pump, eventually recycled to the top glass tube.

For running the shear experiment, the housing environment was brought to the temperature set at 37° C and 5% CO<sub>2</sub> air being pumped into the setup for cell viability and physiological pH control. The confluent cells on glass slides are placed in the flow chamber setup. The flow chamber is hooked up to tubing and a peristaltic pump that continuously circulates media. After all the tubes are connected, 20mL of media is added to a three-way connector to fill the reservoir and to clear any air bubbles in the system. After all portions are filled, the clamp to the inlet of the flow chamber can be removed. All air bubbles must be cleared from the flow chamber and any sections of the tubing to ensure constant steady state flow to the cells. Specifically, the shear stress is based on the constant fluid flow rate and the flow area of the system in the flow chamber. The straight section of glass can be varied changing the overall flow rate of the media and the applied shear stress.

For shear experiments, cells on slides were placed in the parallel plate flow chamber attached to a sterile, laminar flow system as previously described (98; 99), in an environmental chamber kept at 37°C with 5% CO<sub>2</sub>. The magnitude of shear stress ( $\tau$ ) on the cell monolayer is calculated based on the Navier-Stokes equation for a Newtonian

fluid in a parallel plate geometry. The equation for wall shear stress simplifies to:  $\tau = \frac{6\mu Q}{bh^2}$ , where  $\mu$  is the viscosity of the media (0.01 dynes-sec/cm<sup>2</sup>),  $Q$  is the volumetric flow rate (~0.5 ml/s),  $b$  is the width of the flow chamber (2.5 cm), and  $h$  is the height distance between the chamber and the glass slide (0.027 cm). Using this system, cells were exposed to 12 dynes/cm<sup>2</sup> laminar wall shear stress. Flow experiments were done using regular growth media (including 10% fetal bovine serum). Each inducing agent could be added to flow system without interruption. For some experiments, cells were sheared in regular media without phenol red, to reduce background fluorescence. For static control, cells on slides were kept in incubator in regular media.

## 2.3 mRNA and Protein Analysis

### 2.3.1 Protein Expression

After experiments, the cells were lysed with RIPA buffer and scraped from the glass slide, in order to isolate and collect cellular protein. The RIPA lysis buffer with 50mM NaF to maintain DAPK phosphorylation was combined with PMSF and a protease inhibitor (Sigma P-2714) to release protein and prevent protein degradation (100). Next, the protein is isolated from cell fragments leaving the respective sample to be further analyzed.

Protein concentration for each sample was determined using a Bradford colorimetric protein assay. The assay displays protein concentrations based on specific absorbance values read using a spectrophotometer. In order to find the sample concentrations, an absorbance calibration curve was created using Bovine Serum Albumin (BSA) protein standard and specific dilutions with known concentrations. The protein concentration of each of the samples was calculated based on the calibration equation and where they fell relative to the known protein concentrations (Fig. 2.5).

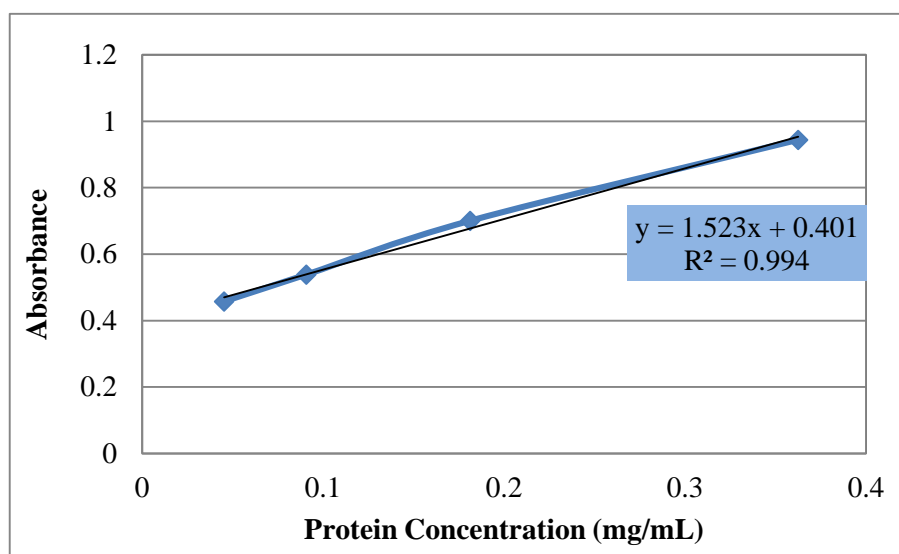


**Figure 2.5. Sample calibration curve for quantifying protein concentration.**

### 2.3.2 Gel Electrophoresis

Using the protein concentrations, an equal amount of sample protein, protein dye, and sample buffer were loaded into the top of each well in a 10-well, pre-cast, polyacrylamide gel. The loaded gel was run in MOPS running buffer at 180V for approximately an hour, or until the dye begins to run out of the bottom of the gel.

During electrophoresis, the denatured proteins within each sample would run vertically down the gel, aligning based on the molecular weight (size) of each protein in the sample solutions.

### 2.3.3 Antibody Labeling

After electrophoresis, the gel was placed on a nitrocellulose transfer membrane and run at 25V for 45 minutes to transfer the protein to the membrane surface. Next, the membrane was blocked in a blotto solution (5% non-fat milk powder in PBS + 1% Tween). The transfer membrane was blocked for 1 hour on a shaker at room temperature. After blocking, the membrane was then incubated in a primary DAPK antibody (DAPK55 antibody, overall DAPK protein, or DAPKPS308, phosphorylated DAPK) blotto solution at a 1:1000 dilution, approximately 5 $\mu$ L of antibody to 5mL of blotto. The membrane was placed on a shaker and allowed to incubate overnight.

After the primary antibody incubation, the membrane was washed 3 times with PBS-T. Next, the protein membrane was incubated with a secondary antibody (Horse Radish Peroxidase, HRP) in blotto solution in a 1:5000 ratio dilution for 2 hours, approximately 1 $\mu$ L of antibody to 5mL of solution. After 3 washes with PBS-T, the membrane was put into a chemiluminescence reagent; contain equal parts of enhanced luminal and oxidizing agents (101). The chemiluminescence reagent will fluorescently label the secondary HRP antibody that is conjugated to all primary DAPK antibody molecules that have attached to the DAPK proteins in each sample.

#### 2.3.4 Molecular Imaging and Protein Quantification

Lastly, the membranes were imaged in a molecular imager (ChemiDoc XRS+; Bio-Rad Laboratories). To quantify protein expression, blot images were analyzed using Quantity One 1-D analysis software. Western blots were imaged and uploaded into the analysis program. Rectangular volume boxes were placed on the each target protein expression, such as overall DAPK, phosphorylated DAPK, and actin. Each protein box is drawn to the same sizes, and one box is drawn as a background to represent the color of the surrounding plot with no protein expression, subtracted as a baseline. Figure 2.6 illustrates a Quantity One volume analysis example of the protein expression process.



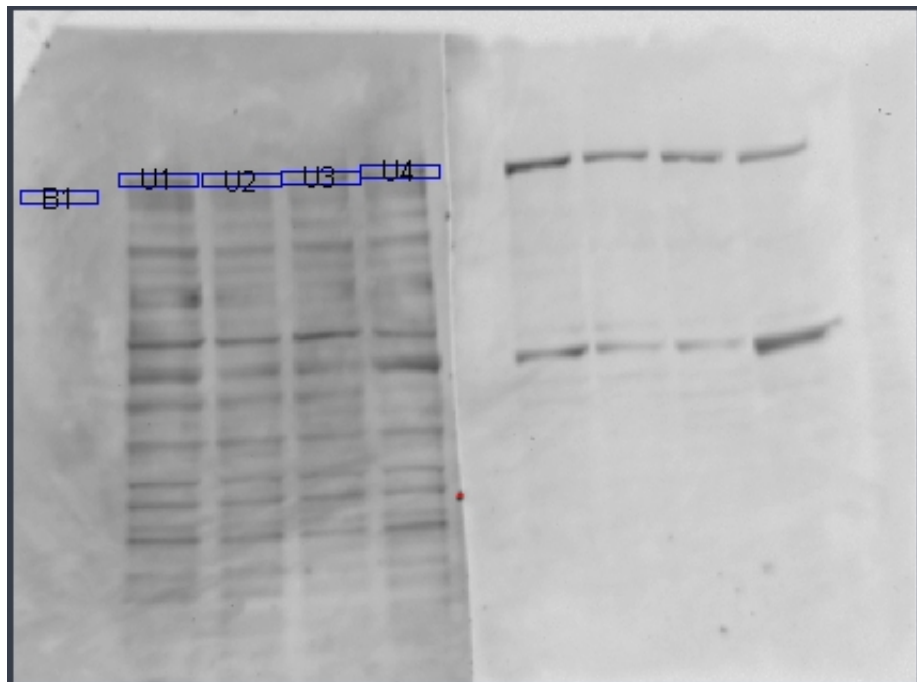


**Figure 2.6. Sample western blot image using Quantity One software.**

After capturing the protein expression, volume analysis reads the amount of target protein in each sample, minus the background read from box B1. Each sample is labeled with a different number and expressed in a volume analysis report, describing each of the volumes of protein expressed (table 2.1). The relative protein expression was calculated with respect to actin for each experimental sample, a loading control.

**Table 2.1. Sample volume analysis report.**

<b>Index</b>	<b>Name</b>	<b>Volume (INT*mm<sup>2</sup>)</b>	<b>Adj. Vol. (INT*mm<sup>2</sup>)</b>	<b>% Adj. Vol.</b>	<b>Mean Value(INT)</b>
1	U1	318814.9533	<b>168013.2975</b>	33.45618766	13283.955
2	U2	210627.3472	<b>109825.6915</b>	19.62351747	10859.47167
3	U3	276170.6288	<b>121368.9731</b>	24.77060383	12507.10833
4	U4	275005.5087	<b>124203.853</b>	23.54969104	11458.56167
5	B1	150801.6557	<b>0</b>	0	6283.401667

### 2.3.5 RNA Isolation

Cells were collected to isolate purified total RNA, and successfully removing genomic DNA using the Qiagen RNeasy Plus Mini Kit (102). To start, cells were trypsinized to detach and collect them from the glass slides. From there, cells were disrupted by adding approximately 350  $\mu$ L of Buffer RLT Plus, which contains  $\beta$ -mercaptoethanol. Cells were homogenized by pipetting and transferred to a gDNA eliminator spin column. The spin column was placed in a 2 mL collection tube and centrifuged at 10,000 rpm for 30 seconds, in order to separate the genomic DNA from the solution. Next, 350  $\mu$ L of molecular biology grade 70% ethanol was mixed with the flow through solution collected from the spin column.

The solution was next pipetted into an RNeasy spin column, which contained a 2mL flow collection tube. The lysate was centrifuged in the RNeasy spin column at 10,000 rpm for 15 seconds. Then, 700  $\mu$ L of Buffer RW1 was added to the RNeasy spin column and spun at 10,000 rpm for 15 seconds. After centrifugation, the next two steps involve adding 500 $\mu$ L of Buffer RPE to the spin column, which is again spun at 10,000 rpm. The first addition of Buffer RPE initially calls for 15 seconds centrifugation. After adding another 500 $\mu$ L of Buffer RPE, the column is spun for 2 minutes, effectively drying the spin column of any leftover ethanol. Lastly, 55  $\mu$ L of RNase-free water is added to the RNeasy spin column and centrifuged for 1 minute, which will elute the purified RNA. After isolating the RNA, each sample was stored in RNase-free water at 20° C, prior to performing any reverse transcription procedures (table 2.2).

**Table 2.2. RNA isolation protocol.**

Step	Action	Solution	Volume (μL)	Spin at 10,000 rpm
1	Trypsinize			
2	Homogenize	RLT (lysis buffer)	350	
		transfer to		
3	gDNA eliminator			2 min.
4	Add to Flow Through	70% ethanol		
		transfer to		
5	RNeasy spin Column			15 sec.
6	Add/Spin	Buffer RW1	700	15 sec.
7	Add/Spin	Buffer RPE	500	15 sec.
8	Add/Spin	Buffer RPE	500	2 min. (dry)
9	Elute RNA	water	55	1 min. (collection)

### 2.3.6 Reverse Transcription

Following RNA isolation, the next step was to perform reverse transcription on the RNA molecules, in order to create cDNA of the RNA expressed by each sample. The RNA goes through reverse transcription to become a copy of DNA that transcribes that specific RNA molecule. The RNA has to be reversed into cDNA to subsequently quantify overall mRNA expression, using a real-time polymerase chain reaction protocol.

Using the High Capacity cDNA Reverse Transcription Kit (Applied Biosystems), the single-stranded collection of sample RNA was converted in to cDNA. Initially, 10x RT buffer was added to RNase-free water in the sample tube, to help present the optimal physiological conditions for the reverse transcription to occur. Additionally, 10x random primers were added to the solution in order to present templates for transcription back

into cDNA. To generate the cDNA, Deoxynucleoside triphosphates (dNTP) were added to the mix solution, aiding the primers in the conversion process. MultiScribe™ MuLV reverse transcriptase, the enzyme that catalyzes the conversion of RNA into cDNA, is added to the mix before adding the sample RNA solution to be transformed back into DNA.

After adding specific quantities of each reverse transcription component, each respective sample solution was placed in a thermal cycler. Initially, the samples are incubated at 25°C for 10 minutes, before being ramped up to 37 °C for 2 hours. After synthesizing cDNA from the thermal cycling, the samples are then held at 4 °C to stop synthesis and preserve the cDNA sample. Now, the sample can be further processed using real-time PCR to amplify target DNA and quantify overall mRNA expression results. Table 2.3 gives a reverse transcription protocol for one tube of sample RNA, and the cycling procedure used for the samples.

**Table 2.3. Reverse transcription sample protocol (per sample).**

<b>Solution</b>	<b>1 tube</b>	<b>Thermal cycler</b>	
		<b>Temp.</b>	<b>Time</b>
Water	9.2 µL		
10x RT Buffer	2 µL		
10x Random Primer	2µL	25°C	10 minutes
25x dNTP's	0.8 µL	37°C	2 hours
MultiScribe™ Reverse Transcriptase	1 µL	4°C	Hold
Sample RNA	5 µL		

### 2.3.7 Primer Development

After reverse transcription, the resulting cDNA sample could be cycled using polymerase chain reaction mechanisms (PCR). PCR is used to amplify small amounts of DNA, by several orders of magnitude, to be able to quantify overall target DNA amounts, compared to the expression of a reference gene.

Before PCR sampling, a specific primer template for DAPK and GAPDH, reference gene, had to be developed for DNA amplification. Primers, short DNA strands, are composed of specific complementary sequences for the target gene. The primers are very specific sequences to replicate only that certain target gene (103).

As PCR cycles temperatures, the primer DNA is used as the template, binding to target DNA and replicating several times over, exponentially increasing the amount of target DNA (Fig. 2.7).

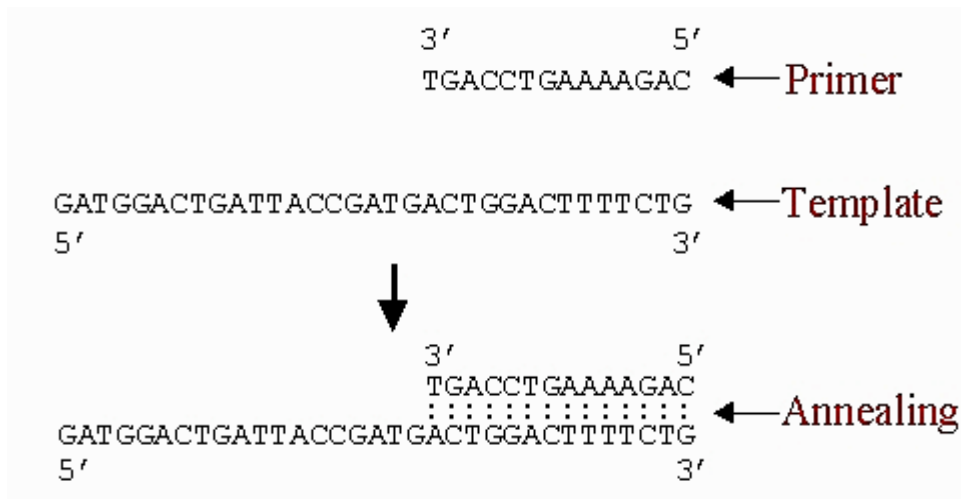


**Figure 2.7. Complementary primers binding to template cDNA.**

To create highly specific primers, NCBI Primer-BLAST tools were used to choose potential primer pairs based on mRNA sequences of bovine DAPK and GAPDH (reference gene) (104). The actual mRNA sequence for each target gene expression were

input into the Primer-BLAST program, specifying bovine and product lengths less than 150 base pairs. Primer pairs had to have a product length of 150 or less for optimal real-time PCR results. Once potential primer pairs were found for each gene, the primer pairs were then input into the NCBI Nucleotide BLAST program make sure the primers were highly specific to each target gene, and no other genes would be amplified by mistake. From the possible primer selections, a successful primer pair for each gene was identified to use for real-time PCR expression (table 2.4).

**Table 2.4. Novel DAPK primers used for RT-PCR analysis.**

<b>Gene</b>	<b>Forward Primer (5'-3')</b>	<b>Reverse Primer (5'-3')</b>
DAPK	CAAGCCGGCAGTGTCCGTGA	CAGTGCGGATGGTGGGACGG
GAPDH	CATTGACCTTCACTACATGGT	ACCCTTCAAGTGAGCCCCAG

Both primer strands are needed due to the sequence reading activity of the enzymes, and the way the DNA is setup in an anti-parallel arrangement. Both primers anneal to the target DNA, extending one direction from the 5' to 3' end (forward) and extending in the opposite direction from 3' to 5' (reverse).

### 2.3.8 Real Time RT-PCR

As previously mentioned, real-time polymerase chain reaction is a process that exponentially amplifies small amounts of target DNA, while detecting the fluorescence of the sample quantifying specific gene expression quantities as PCR is cycled. To run the PCR experiment, the Applied Biosystems 7500 Fast Real-Time PCR System was used for each of the samplings.

First, SYBR Green PCR Master mix (Applied Biosystems) was combined with RNase-free water, in each tube depending on the number of desired PCR reactions. Next, each target gene forward and reverse primers are added (DAPK or GAPDH), as shown in table 2.4. Lastly, each cDNA template is distributed to their own PCR tube, mixed with one reaction aliquot of the SYBR-Primer solution. Table 2.5 displays the specific distribution of each of the PCR components, per reaction.

**Table 2.5. Real time RT-PCR solution protocol (per reaction).**

<b>Solution</b>	<b>Amount</b>
Water	5.6 $\mu$ L
SYBR Green	10 $\mu$ L
Forward Primer (10 $\mu$ M)	1.2 $\mu$ L
Reverse Primer (10 $\mu$ M)	1.2 $\mu$ L
cDNA template	2 $\mu$ L

Once each reaction solution is mixed, the samples are placed in the Real-Time PCR System to begin amplifying the target DNA. Using PCR software, all of the specific parameters for the relative quantification (ddCT) plate study were input, along with the cycling times and temperatures for each amplification step, as shown in table 2.6. As the temperature is cycled, the cDNA is denatured at 95°C allowing for the temperature stable polymerase to extend new DNA from the primers. Next, the temperature is cooled to 60°C to allow for the primers to bind the template DNA. Subsequently, the temperature is ramped back up to 95°C for the polymerase to amplify template DNA, all while fluorescently labeling target DNA with SYBR green for real time quantification of gene expression (105).

**Table 2.6. Thermal cycler protocol for the real time PCR.**

<b>Thermal Cycler Profile</b>			
<b>Stage</b>	<b>Repetitions</b>	<b>Temperature</b>	<b>Time Held</b>
1	1	50.0 °C	2:00 minutes
2	1	95.0 °C	10:00 minutes
3	40	95.0 °C	0:15 seconds
		60.0 °C	1:00 minute

### 2.3.9 Quantifying RT-PCR Results

Cells were collected to isolate total RNA and remove genomic DNA using RNeasy Plus Mini Kit (Qiagen) per manufacturer's instruction, in a sterile, RNase-free environment. The kit utilizes a spin column isolation technique, and purified RNA was stored in  $-20^{\circ}\text{C}$ . Reverse transcription was done using the High Capacity cDNA Reverse Transcription Kit (Applied Biosystems), cycled at  $25^{\circ}\text{C}$  to  $37^{\circ}\text{C}$  for 2 hours and held at  $4^{\circ}\text{C}$ . Using primer3/BLAST tools, we designed primer pairs based on mRNA sequences of bovine DAPK and GAPDH as control. Possible primer pairs, with product length of 150 base-pairs or less, were compared to all bovine mRNA sequences using BLAST to select for high specificity. We chose only primers with more than 85% specificity to evaluate, and the successful primer pair sequences for DAPK:

*CAAGCCGGCAGTGTCCGTGA* (forward) and *CAGTGCGGATGGTGGGACGG*

(reverse) and GAPDH: *CATTGACCTTCACTACATGGT* (forward) and

*ACCTTCAAGTGAGCCCCAG* (reverse). Real time quantitative RT-PCR was

performed in an Applied Biosystems 7500 Fast Real-Time PCR System using the SYBR Green PCR Master mix reagent system (Applied Biosystems). Fold increase of mRNA



levels was calculated based on critical threshold cycle values. The  $2^{\Delta\Delta C_t}$  method was used to calculate the fold increase in DAPK mRNA expression. We calculated amplification efficiency for both DAPK and GAPDH based on standard curves of a series of 10-fold dilution, and confirmed that they are similar (93.97% for DAPK and 94.43% for GAPDH). The  $\Delta C_t$  of the control and experimental samples was calculated from the difference between the threshold cycle of the target gene (DAPK) and the threshold cycle of the reference gene (GAPDH). The fold increase of each sample was calculated, after PCR cycles, using the below equation:

$$(1 + \text{DAPK Primer Efficiency})^{\text{DAPK}_{\Delta C_t}} - (1 + \text{GAPDH Primer Efficiency})^{\text{GAPDH}_{\Delta C_t}}$$

Figure 2.8 is a representative real-time RT-PCR plot showing the fluorescence mRNA amplification activity plotted against the PCR cycle number. An appropriate cycle threshold is set at the mid-line slope. From these  $C_T$  values, a representative fold expression increase is calculated between the specific samples.

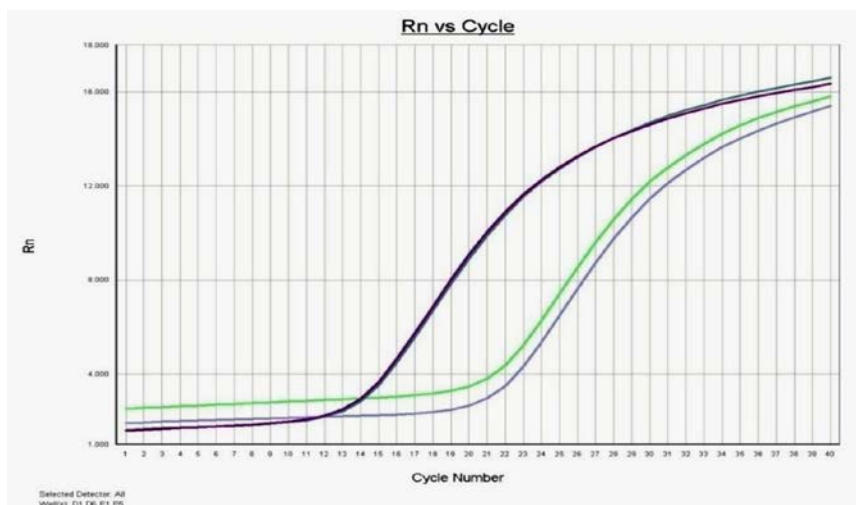


**Figure 2.8. Real-time RT-PCR mRNA amplification plot.**

## 2.4 Apoptosis and Necrosis Assay

Apoptosis was evaluated via TUNEL staining both as adherent cells on glass slide and via cell suspension with flow cytometry using the In Situ Cell Death Detection Kit, Fluorescein (Roche) per manufacturer's instruction. After experiments, cells were fixed with 4% paraformaldehyde, permeabilized with 0.2% Triton X-100. Cells were then incubated with a TUNEL reaction mixture that includes terminal deoxynucleotidyl transferase enzyme (TdT) which labels DNA strands broken or cleaved during apoptosis with fluorescein labeled dUTP, for 60 minutes at 37°C. Cells were also stained using Hoechst Blue nucleus staining solution at 1:1000 dilution in PBS solution. Cell images were captured using a Leica DMI600 B inverted fluorescence microscope system. Leica Application Suite program was used for image acquisition. Quantitative analysis was done using ImagePro Analyzer 6.2 software, to determine TUNEL positive cells based on fluorescein (green) and total number of cells based on Hoechst stain (106). Images were digitally filtered based on fluorescence thresholds, and the numbers of positive cells were counted. For each sample, 10–12 images were acquired at various locations on the slide and analyzed by a blinded observer. Cell necrosis was analyzed using a FITC-Annexin V Detection Kit (BD Pharmingen) per manufacturer's instruction. Since Annexin is a membrane stain, cells were not fixed or permeabilized. Instead, cells were washed with cold PBS and incubated with FITC-Annexin V, propidium iodide (PI) in binding buffer for 15 minutes at room temperature. Cells were co-stained with PI to distinguish between apoptotic cells and necrotic cells within each sample group.

#### 2.4.1 Flow Cytometry

TUNEL, Annexin V, and PI stained cells were all quantified using flow cytometry on suspended cells. After experiments, adherent cells on slides were detached gently using non-enzymatic Cell Stripper (Cellgro Mediatech) and fixed with 1% paraformaldehyde and permeabilized with 0.2% Triton X-100 before TUNEL staining using In Situ Cell Death Detection Kit, or Annexin V Detection Kit (see previous section). RNase A (Roche) and Propidium Iodide (Roche) were used to stain the nucleic acids of the cells. DNase I (Roche) was used to initiate DNA strand breaks and simulate apoptosis for a positive control sample to set the flow cytometry quadrants. The FACScan flow cytometer (BD Biosciences) was used to categorize cells based on fluorescence characteristics, and CellQuest Pro software (BD Biosciences) was used for data analysis.

#### 2.4.2 Caspase Assay

Cells were plated on glass slides at approximately 500,000 cells per slide 1 day prior to experiments. Afterwards, cells were trypsinated and counted for each sample set, and adjusted to 15,000 cells per 50  $\mu$ l of culture media. Caspase assay was carried out as per manufacturer's protocol. Briefly, equal volumes (50  $\mu$ l) of Caspase Glo<sup>®</sup> 3/7 Reagent (Promega) and cell suspension were combined at a 1:1 ratio, mixed gently, and added to white-walled 96-well plates. Blank wells containing media only were used as negative controls against control BAEC and treated cells (Static + inducer, 6hr shear + inducer, and 6hr shear only). After incubation for 1 hour at room temperature, luminescence of each well was read using a luminometer (PerkinElmer).

Each sample was done in triplicates, and averaged values were corrected for background readings from wells with media only, and normalized to control samples.

## **2.5 Gene Knockdown Techniques**

### **2.5.1 DAPK RNA Interference**

Cells were plated on glass slides at approximately 400,000 cells per slide, and grown to 60-80% confluency overnight. DAPK siRNA (sc-38976) and Control siRNA-B (sc-44230), as well as siRNA Transfection Reagent System (sc-45064) are from Santa Cruz Biotechnology (SCBT). Our optimized transfection protocol for siRNA uses a ratio of 5  $\mu$ l of siRNA duplex to 6  $\mu$ l of Transfection Reagent for each sample. Both siRNA and Transfection Reagent were diluted in 100  $\mu$ l of Transfection Medium, which were then combined and incubated for 30 minutes at room temperature. This was followed by the addition of 800  $\mu$ l of Transfection Medium. Cells were rinsed with Transfection Medium, and the transfection mixture was pipetted on to the cells. Cells were incubated with the transfection mixture for 8 hours in incubator, after which 2X growth medium (twice the fetal bovine serum, penicillin/streptomycin, and L-glutamine of regular cell media) was added to each cell sample, and cells were placed back into the incubator for 20-24 hours to recover. Afterwards, medium was replaced with 1X regular growth medium, and cells were then ready for further experiments and treatments.

### 2.5.2 Gene Silencing with shRNA

Lamin A/C silencing was carried out using short-hairpin RNA (shRNA) in stable transfections with lentivirals. A sufficient lamin shRNA Bacterial Glycerol Stock (Sigma SCHLNG NM-170707) was used after confirming the sequence conservation to the bovine lamin A/C gene and stored at -80°C. The Non-Target shRNA Control Plasmid (Sigma SHC002) was chosen as a control and stored at -20°C. Lentiviral particles were developed using the MISSION Lentiviral Packaging Mix (Sigma SHP001) and extracted via manufacturer's protocol. After creating and confirming lentiviral concentration, BAECs were grown out to 70% confluency and treated with the lentiviral particles at a multiplicity of infection, either 1 or 5, in regular growth media with 8 ug/ml hexadimethrine bromide for improved lentiviral uptake. Puromycin (2ug/ml) was used to select for positive shRNA BAECs, and grown out to confluency (1). For mouse embryonic fibroblast (MEF) studies, wild-type and lamin-deficient (Lmn A<sup>-/-</sup>) MEFs were provided by Jan Lammerding from Cornell University. MEF cells were cultured in regular cell media conditions and plated/treated at the same specifications as the BAECs.

## 2.6 Immunostaining

After experiments, cells were washed twice with PBS, before fixation with 4% paraformaldehyde and permeabilized with 0.2% Triton X-100 for 15 min and blocked with 1% bovine serum albumin (BSA) in PBS solution for 1 hour (Sigma) on a shaker.

Staining for DAPK was done as follows: slides were incubated with goat anti-DAPK primary antibody (sc-8163) for 1 hour at 1:250 dilution in 1% BSA-PBS (or 12  $\mu$ l in 3 ml of 1% BSA-PBS). Afterward, samples were washed 3 times with PBS for 5 minutes each. Next, samples were incubated with secondary chicken anti-goat IgG-FITC (sc-2988) for 1 hour, at a dilution of 1:200 in 1% BSA solution (or 15  $\mu$ l in 3 ml of 1% BSA PBS), followed by washing 3 times in PBS for 5 minutes each. This was followed by 1 hour incubation in chicken anti-goat IgG-FITC conjugate secondary antibody (sc-2988) at 1:200 dilution in 1% BSA solution. To stain actin, cells were incubated with Atto 660 Phalloidin F-actin conjugate probe (Sigma 49409) for 1 hour at a dilution of 1:250 in 1% BSA solution (or 12  $\mu$ l in 3 ml 1% BSA PBS). This was again followed by washing 3 times in PBS, 5 minutes each. Finally, cell nuclei were stained using Hoechst at 1:1000 dilution (or 5  $\mu$ l in 5 ml PBS) in PBS for 15 minutes followed by washing 3 times in PBS. Slides were stored in PBS at 4°C. Images were taken at 10X and 40X using Leica DMI6000 fluorescence microscope.

## 2.7 Statistics

All experiments were carried out for a minimum of three times, and each time samples were prepared and analyzed independently. Standard error of each group was calculated to verify the statistical significance of the results. For protein and mRNA analysis, each sample was normalized to a control standard which serves as a baseline. Quantification of digital band images was done to incorporate repeated blotting results and generate statistical analysis. Each Western band is corrected for background and the loading control on the same blot. Student *t*-test was used to compare one condition between two sample sets. *P* values less than 0.05 was considered sufficient for statistical significance.

### 3. SHEAR STRESS REGULATES EXPRESSION OF DAPK IN SUPPRESSING TNF $\alpha$ -INDUCED ENDOTHELIAL APOPTOSIS

#### 3.1 Introduction

Mechanotransduction in endothelial cells involves a variety of pathways and signaling molecules that collectively bring about changes in cellular functions such as proliferation, apoptosis, migration and structural alignment (107). While endothelial dysfunction can lead to diseased conditions such as atherosclerosis (4), maintaining homeostatic processes like apoptosis and angiogenesis ensures blood supply to tissues. The apoptotic process is tightly regulated by environmental stimuli including biochemical signals as well as non-physiological injuries to cells. Recent studies have revealed that the pro-apoptotic death-associated protein kinase (DAPK) functions primarily as a mediator of programmed cell death (34). DAPK is a 160 kDa, serine/threonine protein kinase that contains a calmodulin (CaM) binding domain, a kinase binding domain, eight ankyrin repeats, two P-loops (putative nuclear binding domain), a cytoskeleton binding plus an independent death domain necessary for promoting apoptosis (95). Loss of DAPK expression in human carcinoma cell lines and its ubiquitous presence in many cell and tissues types suggest its importance in regulating apoptosis (108).



A  $\text{Ca}^{2+}$ /CaM dependent kinase, DAPK is activated following a variety of stimuli including tumor necrosis factor ( $\text{TNF}\alpha$ ), ceramide, interferon ( $\text{IFN-}\gamma$ ), and oncogenes such as p53 (76; 78; 79; 109), serving as a converging point for apoptotic signaling. DAPK is upstream of caspases, except caspase 8, and induces other caspase-independent cell death or autophagy (82).

In the vasculature, misdirected control of apoptosis in endothelial cells can lead to pathological conditions such as inflammation, clotting, and smooth muscle cells recruitment (51). Increased cell turnover rate exists at sites prone to lesion development – areas of disturbed flow and low levels of shear stress (110; 111). On the other hand, laminar shear stress inhibits apoptosis induced by serum depletion, oxidative stress, and  $\text{TNF}\alpha$  (87; 112; 113). At the onset of shear, endothelial responses include increase in intracellular calcium, nitric oxide (NO), and rapid and transient activation of MAPK's that also interact with and regulate DAPK. ERK phosphorylates DAPK at serine735 and enhances its apoptotic activity, and DAPK binds to phospho-p38 in  $\text{TNF}\alpha$ -induced apoptosis (90; 114). Interestingly, DAPK activates and phosphorylates protein kinase D (PKD) which in turn activates JNK (91), while pre-exposure of endothelial cells to shear stress prevents  $\text{TNF}\alpha$  activation of JNK, but not ERK or p38 (50).

Aside from its role in apoptosis, DAPK also binds to and regulates actin cytoskeleton and contributes to cytoplasmic changes associated with apoptosis, such as stress fibers formation and membrane blebbing (94). DAPK is localized to the actin microfilament, and phosphorylates myosin regulatory light chain (MLC) at Ser19, both *in vivo* and *in vitro* (39; 95). DAPK promotes actomyosin contractility and stabilizes stress fibers in serum starved fibroblasts, and mediates the induced stress fiber formation (39).

Interestingly, in endothelial cells, DAPK phosphorylates tropomyosin-1 at Ser283 in response to ERK activation under oxidative stress; and this phosphorylation in turn is required for the formation of stress fibers (96). With extended shearing (hours), endothelial cells undergo morphological changes: stress fiber formation, focal adhesion reorganization, elongation and eventual re-alignment of cytoskeleton in the direction of flow (115). DAPK is potentially utilized by endothelial cells to affect morphological changes in response to shear stress. The cytoskeleton effect of DAPK occurs before onset of apoptosis, and is independent of DAPK death domain.

Due to its regulatory role in programmed cell death and its presence in numerous cell types, tight control of DAPK activation is necessary to ensure normal cellular functions as well as rapid activation of apoptosis when triggered. Aside from calcium activated calmodulin binding, which frees DAPK catalytic activity from an auto-inhibitory state; auto-phosphorylation of DAPK at Ser 308 is another important inhibitory regulatory checkpoint (40). Serine 308 is in the  $\text{Ca}^{2+}$ /CaM binding and regulatory domain of DAPK, and is phosphorylated in growing cells. Phosphorylation at serine 308 serves as a further restriction on CaM binding, as well as another checkpoint in DAPK activation. Apoptotic signals trigger dephosphorylation of serine 308, which along with CaM binding are required for full activation of DAPK catalytic activities.

Precise mechanisms of DAPK regulation in apoptosis or cytoskeleton changes are currently being analyzed, and its function in endothelial cell is largely unknown. Due to its location on the cytoskeleton, DAPK expression and activity are potentially susceptible to mechanical and structural stresses. In this study, we begin to investigate the interactions between shear stress and DAPK in endothelial cells. We found increased DAPK protein

and mRNA levels in cells exposed to laminar fluid shear stress at 12 dynes/cm<sup>2</sup> for up to 8 hours. Shear stress also decreased phosphorylated DAPK at serine 308 in a time dependent manner. Additionally, we observed suppression of apoptosis by applied shear stress subsequent to long term TNF $\alpha$  activation. Under the same conditions, DAPK expression decreased as well, compared to static + TNF $\alpha$  treated cells. Overall, our data suggest an important role for DAPK in the suppression of TNF $\alpha$  induced apoptosis by shear stress in endothelial cells. Understanding fully how cells respond to not only their biochemical but also mechanical microenvironments, will allow us to better manipulate and mimic the desired cellular responses for therapeutic purposes.

Research Objective 1: **Does fluid shear stress regulate DAPK expression?**

Research Objective 2: **Will fluid shear stress attenuate TNF $\alpha$  endothelial apoptosis via DAPK activity?**

## 3.2 Results

### 3.2.1 Shear stress alone increases overall DAPK expression and mRNA level in endothelial cells

First, we explored expression of overall DAPK in static and BAEC exposed to 12 dynes/cm<sup>2</sup> for 3, 6, and 8 hours. Western analysis showed an increase in total DAPK expression directly related to the length of shearing (Figure 3.1A top). Blots were digitally quantified as relative intensity compared to the loading control, actin. Samples from at least three different experiments were analyzed separately. Following quantitative analysis of Western results, we consistently observed a 2.35 fold increase in overall DAPK expression in cells sheared for 6 and 8 hours ( $P < 0.05$ ), compared to static cells

(Figure 3.1A bottom). Our data suggest that expression of DAPK is at least in part modulated by elevated shear stress in a time-dependent manner.

To further confirm increased DAPK expression under shear stress is due to increased transcription, we examined DAPK mRNA expression level using quantitative real-time PCR technology. We found a significant increase in DAPK mRNA level in cells exposed to shear stress for 2, 4, and 6 hours ( $P < 0.001$ ) compared to static cells. BAEC sheared for 4 hours showed a 1.85 fold increase in DAPK mRNA level compared to static BAEC (Fig. 3.1B). After 8 hours of shear stress, however, DAPK mRNA level dropped to close to static level. This early increase in DAPK mRNA agrees with the increase in DAPK protein expression later at 6 and 8 hour time points (Fig. 3.1A). DAPK mRNA level decreased after 4 hours of shearing, down to static level by 8 hours, suggesting that the increase in DAPK expression could be temporary. Furthermore, this data suggests that the up regulation of DAPK protein with shear stress can be attributed to increased transcription of DAPK gene, and not post-translational adjustments such as changes in protein degradation. DAPK expression may be under a mechano-sensitive promoter and regulatory mechanism.

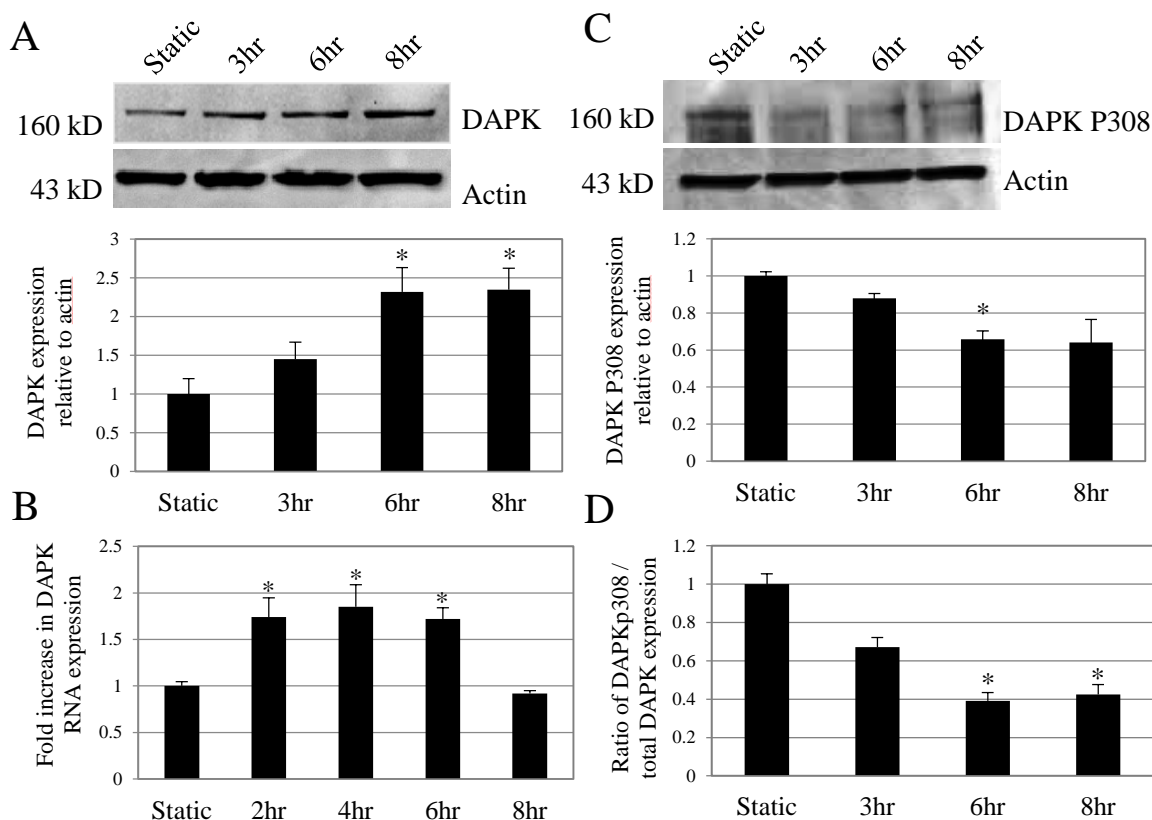


**Figure 3.1. DAPK mRNA and protein analysis under shear.** (A) Western blot of overall DAPK expression in control and sheared cells (3, 6, 8 hours). (B) Fold increase in DAPK mRNA levels for static and sheared cells at 2, 4, 6, and 8 hours based on real time quantitative RT-PCR. (C) Western blot of phosphorylated DAPK at serine 308, for static and sheared cells (3, 6, 8 hours). (D). Fraction of phosphorylated DAPK decreased to a minimum at 6 hours of shear stress. All data represent average  $\pm$  standard error ( $n = 3$ ). \*  $P < 0.05$  compared to static BAEC.

### 3.2.2 Shear stress alters phosphorylation of DAPK at serine 308 in a time-dependent manner

Auto-phosphorylation of DAPK at serine 308 is an inhibitory regulatory checkpoint, and dephosphorylation of DAPK at serine 308, along with CaM binding, are needed for full activation of its kinase activities. We found in Western blot protein analysis that the expression of phosphorylated serine 308 DAPK gradually decreased with 3, 6, and 8 hours of shearing (Figure 3.1C top). Quantitative analysis of Western

blots confirmed significant dephosphorylation of serine 308 DAPK after 6 hours of shearing ( $P < 0.05$ ) compared to control cells (Figure 3.1C bottom). Since quiescent DAPK is phosphorylated at serine 308, this suggests that shear stress dephosphorylates or activates DAPK within 3 hours of shear stress, reaching maximum after 6 hours. Because total DAPK protein also changed with shearing based on Western analysis, we correlated phospho-DAPK with total DAPK changes (Figure 3.1D). The fraction of phosphorylated DAPK at serine 308 decreased with shearing, down to a minimum of 39% at 6 hours, followed by a slight increase at 8 hours to 42%. Since DAPK in its basal state is phosphorylated at serine 308, the increase in total DAPK that we observed at 6 to 8 hours of shearing may account for the leveling off of decrease in phospho-DAPK between 6 and 8 hours.

### 3.2.3 Long term TNF $\alpha$ treatment affects phospho-serine 308 DAPK, not overall DAPK expression

To investigate DAPK expression and activity under apoptotic conditions in endothelial cells, we examined DAPK expression in BAEC incubated with TNF $\alpha$  (10 ng/ml) and collected protein for analysis at 6, 24, and 48 hours. We found that while overall DAPK expression remained the same (Figure 3.2A left), phospho-serine 308 DAPK increased after 6 hours of TNF $\alpha$  treatment (Figure 3.2B left). Based on quantitative analysis of repeated Western results, we saw no significant changes in overall DAPK expression with long term TNF $\alpha$  treatment or up to 48 hours (Figure 3.2A right). However, at 6, 24, and 48 hours of TNF $\alpha$  treatment, we saw a significant increase in phospho-serine 308 DAPK ( $P < 0.05$ ) compared to non-treated BAEC (Figure 3.2B

right). Figure 3.2C shows the ratio of phospho-DAPK to total DAPK changes, and the fraction of phosphorylated DAPK at serine 308 follows the same trend. This increase in phosphorylated DAPK is consistent with other studies on tumor cells (114). Our data suggest that DAPK phosphorylation at serine 308 is sensitive to TNF $\alpha$  treatment since long term treatment with TNF $\alpha$  (24 hours) increased phosphorylated DAPK.

Furthermore, shear stress, increases overall DAPK expression, while both shear stress and TNF $\alpha$  affect DAPK phosphorylation at serine 308 in a time-dependent manner.

DAPK expression may be sensitive to mechanical stress but not as sensitive to TNF $\alpha$ ; while its activation, through serine 308 dephosphorylation, on the other hand may be regulated by both.

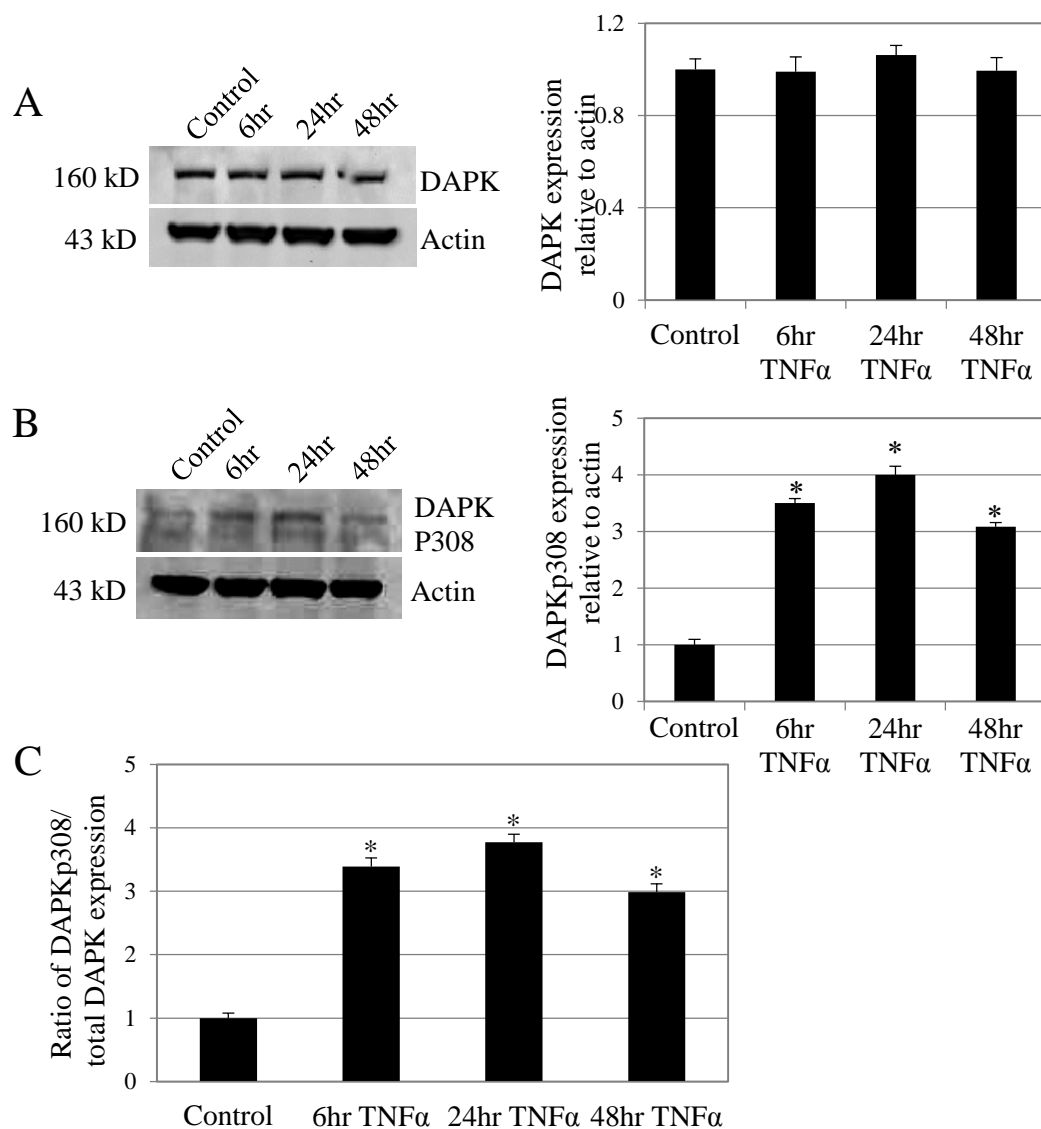


**Figure 3.2. Impact of TNF $\alpha$  on DAPK expression.** (A left) Western analysis of overall DAPK expression. (A right) Quantitative analysis of bands as fold increase compared to control, showing that the bands are not significantly different. (B left) Western analysis of phosphorylated serine 308 DAPK expression. (B right) Quantitative analysis of phosphoserine DAPK bands as fold increase compared to control. (C). Fraction of phosphoserine 308 DAPK increased with time of treatment with TNF $\alpha$ .



### 3.2.4 Shear stress significantly reduces endothelial apoptosis following TNF $\alpha$ activation

Shear stress has been shown to attenuate apoptosis in endothelial cells induced by TNF $\alpha$  (112). Since our data demonstrate that shear stress increases DAPK overall expression after 6 hours and TNF $\alpha$  activates DAPK in long term treatment of 24 hours, we examined the corresponding time-dependent effects of shear stress on TNF $\alpha$  induced apoptosis. Cells were either incubated with TNF $\alpha$  (25 ng/ml) for a 24-hour period to fully induce apoptosis (Static + TNF $\alpha$ ) or treated with TNF $\alpha$  for 18 hours followed by shearing cells in media containing TNF $\alpha$  for another 6 hours (6 hr Shear + TNF $\alpha$ ). Control groups included static (Control BAEC) and cells sheared for 6 hours alone (6 hr Shear) as outlined in Figure 3.3A.

Apoptosis in endothelial cells was assessed by TUNEL staining with fluorescein label. After TNF $\alpha$  and shear stimulation in flow chambers, cells on slides were stained and quantified using flow cytometry. TNF $\alpha$  alone induced a significant two-fold increase in apoptotic cells over control BAEC (Figure 3.3B). We found that applying 6 hours of shear stress to cells already activated by TNF $\alpha$  for 18 hours, significantly decreased the fraction of apoptotic cells ( $P < 0.05$ ), compared to TNF $\alpha$  treatment under static condition. At the same time, we also saw a significant increase of apoptosis in control BAEC with 6 hours of shear stress alone; however, the result was still significantly less than that of TNF $\alpha$  treated static cells. The increase in apoptosis after 6 hours of shear stress, without TNF $\alpha$ , could be due to the increased expression of DAPK, as supported by our earlier data.

This data suggests that while shear stress alone induces apoptosis, it also represses apoptosis subsequent to TNF $\alpha$  induction. As a result, sheared BAEC, either with or without TNF $\alpha$  pretreatment, demonstrated similar levels of apoptosis that is significantly different from both static control and TNF $\alpha$  induction alone.

### 3.2.5 Shear stress reduces caspase-3 and -7 activity following TNF $\alpha$ activation

Further quantitative analysis of cellular apoptosis based on caspase-3 and -7 activities supported TUNEL staining results in the same experimental groups. Caspases are downstream of p53, which is activated by DAPK in the apoptotic pathways (36). Luminescence measured is directly related to activities of caspase-3 and -7 (Figure 3.3C), and the results indicate that caspase activity follows closely the same trend as cellular apoptosis. We again saw a significant increase in caspase activation with TNF $\alpha$  treatment alone for 24 hours ( $P < 0.01$ ), correlating with the increase in apoptosis we saw in Figure 3.3B. Adding shear stress to TNF $\alpha$  treated cells significantly reduced caspase activity ( $P < 0.01$ ), as well as apoptosis (Figure 3.3C). Shearing cells for 6 hours alone promotes caspase activity, which is also reflected in the increase in apoptosis from Figure 3.3B. Thus caspase-3 and -7 activation reflect the apoptosis results observed subsequent to TNF $\alpha$  and shear stimulation. This result further supports the potential role for DAPK in regulating the apoptosis pathway since they are down stream of DAPK activation of p53.

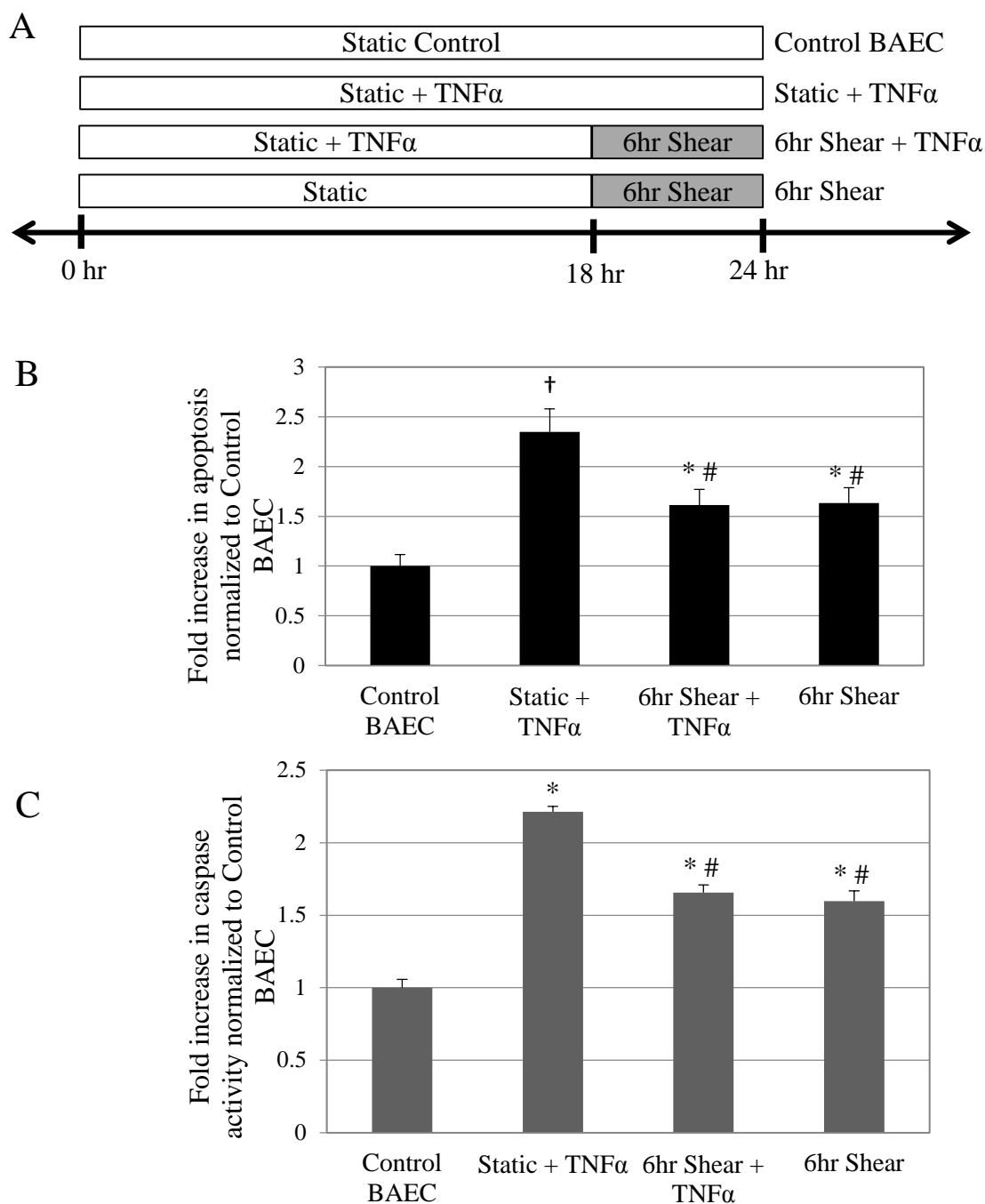


**Figure 3.3. Experimental design quantifying apoptosis and caspase activation.** (A) Experimental setup for analysis of the effects of simultaneous shear stress and TNF $\alpha$  induction on endothelial apoptosis. (B) Apoptosis data is presented as fold increase over control BAEC. (C) To further quantify apoptosis for experimental groups, caspase-3 and -7 activities were measured using Caspase-Glo 3/7 Assay.

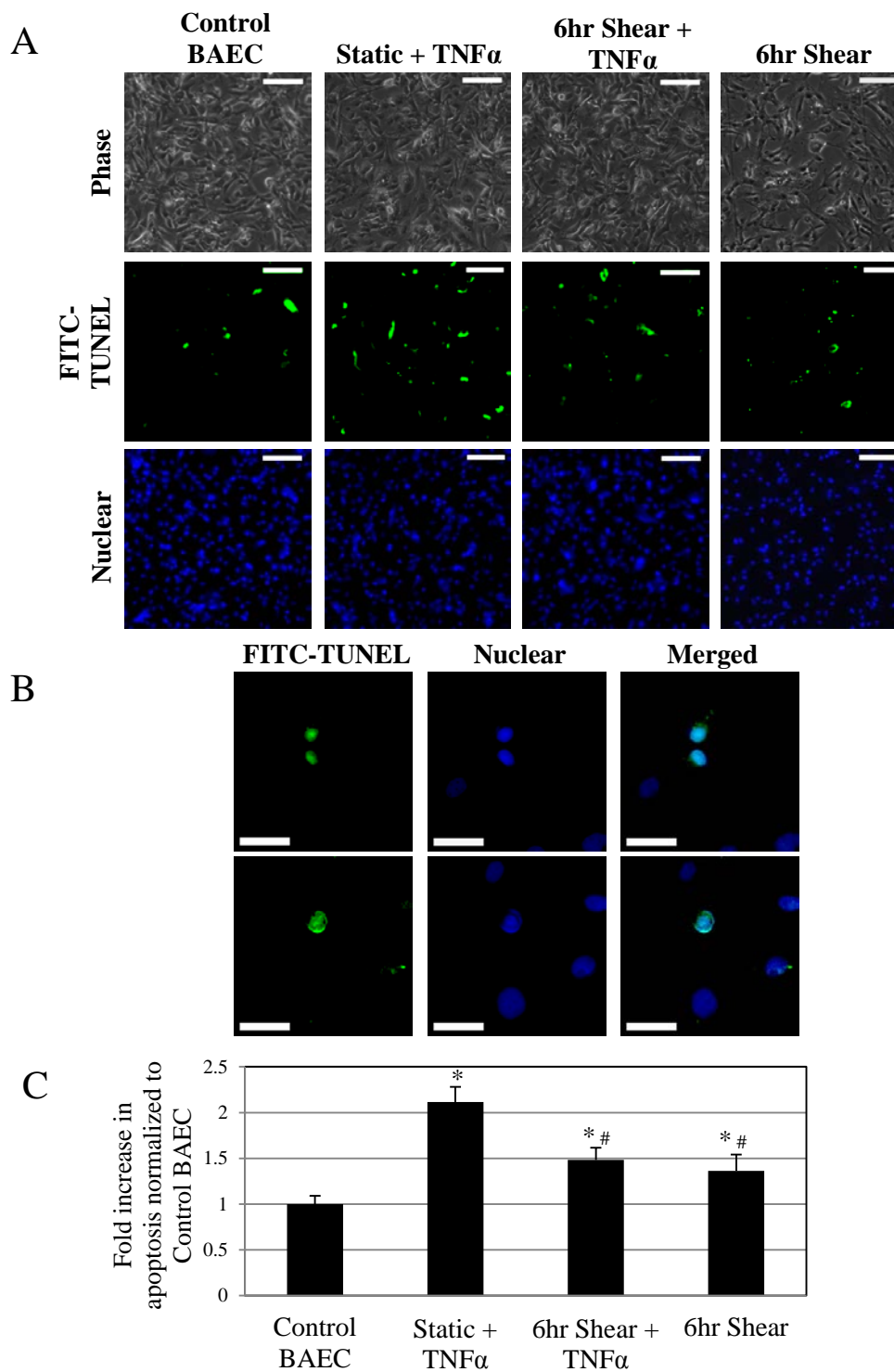


**Figure 3.4. TUNEL using Fluorescence microscopy.** (A) Fluorescence microscopy images of adherent sheared cells after TUNEL staining at 10X. (B) Close up images of representative apoptotic cell nuclei at 40X magnification. (C) Quantitative analysis of TUNEL stain was carried out based on fluorescence images.

### 3.2.6 Apoptosis analysis in TNF $\alpha$ and shear treated adherent cells confirms results from flow cytometry

TUNEL stained adherent cells were also nuclear stained with Hoechst, imaged, and quantified using ImagePro software. Figure 3.4A demonstrates representative images of control, TNF $\alpha$  treated static and sheared cells, as well as cells sheared alone. Images are in phase contrast, FITC (green), and Hoechst (106) fluorescence, top to bottom. As expected, FITC staining is more evident in TNF $\alpha$  treated static cells compared to control or TNF $\alpha$  plus sheared BAEC. Shear stress alone also induced apoptosis in cells. Figure 3.4B shows a close up image of TUNEL positive apoptotic cell at 40X magnification. There is clear overlap of blue nuclear stain and green FITC label, indicating apoptotic DNA fragmentation in the nucleus. Experiments are carried out at least 3 times, and 5-10 images from each are analyzed. TUNEL positive cells were quantified by thresholding FITC fluorescence and normalizing to total cell count quantified based on nuclear staining. Results are presented as fold increase over control (Figure 3.4C). We again saw a significant two-fold increase in apoptosis in TNF $\alpha$  treated cells under static condition. If these cells were exposed to shear stress for 6 hours at the end of 18-hour TNF $\alpha$  induction, there was a significant decrease in apoptosis ( $P < 0.05$ ). Furthermore, shearing stress alone also induced a marked increase in cell apoptosis compared to control, though still significant less than TNF $\alpha$  induction alone ( $P < 0.05$ ). Image analysis results are consistent with flow cytometry TUNEL results of Figure 3.3B, as well as caspase results of Figure 3.3C. Two methods of TUNEL analysis were used to ensure that possible disruption of cell membrane during detachment of cells did not influence our results.

### 3.2.7 Necrosis is not altered in TNF $\alpha$ and shear stress activated endothelial cells

For the same experimental groups, we also examined necrosis using Annexin V FITC detection assay. Cells were co-stained with propidium iodide (PI) to distinguish between apoptotic and necrotic cells, and flow cytometry scatter plots of non-stained and stained control cells are presented in Figure 3.5, A to C. After running apoptotic (Annexin V) and necrotic (PI) controls, we counted cells in the necrotic only as well as the overlapping necrotic and apoptotic (late stage apoptosis) quadrants to be included in our necrosis count. Purely Annexin V positive, or early stage apoptotic cells were not counted as necrotic. Figure 3.5D shows the scatter plot for three experimental groups, and quantitative results are summarized in Figure 3.5E. We found that necrosis was not affected by TNF $\alpha$  treatment with or without shear stress. Flow cytometry results following Annexin V staining assay indicated no significant difference in the number of necrotic cells between static control, TNF $\alpha$  treated, and TNF $\alpha$  treated plus sheared cells.

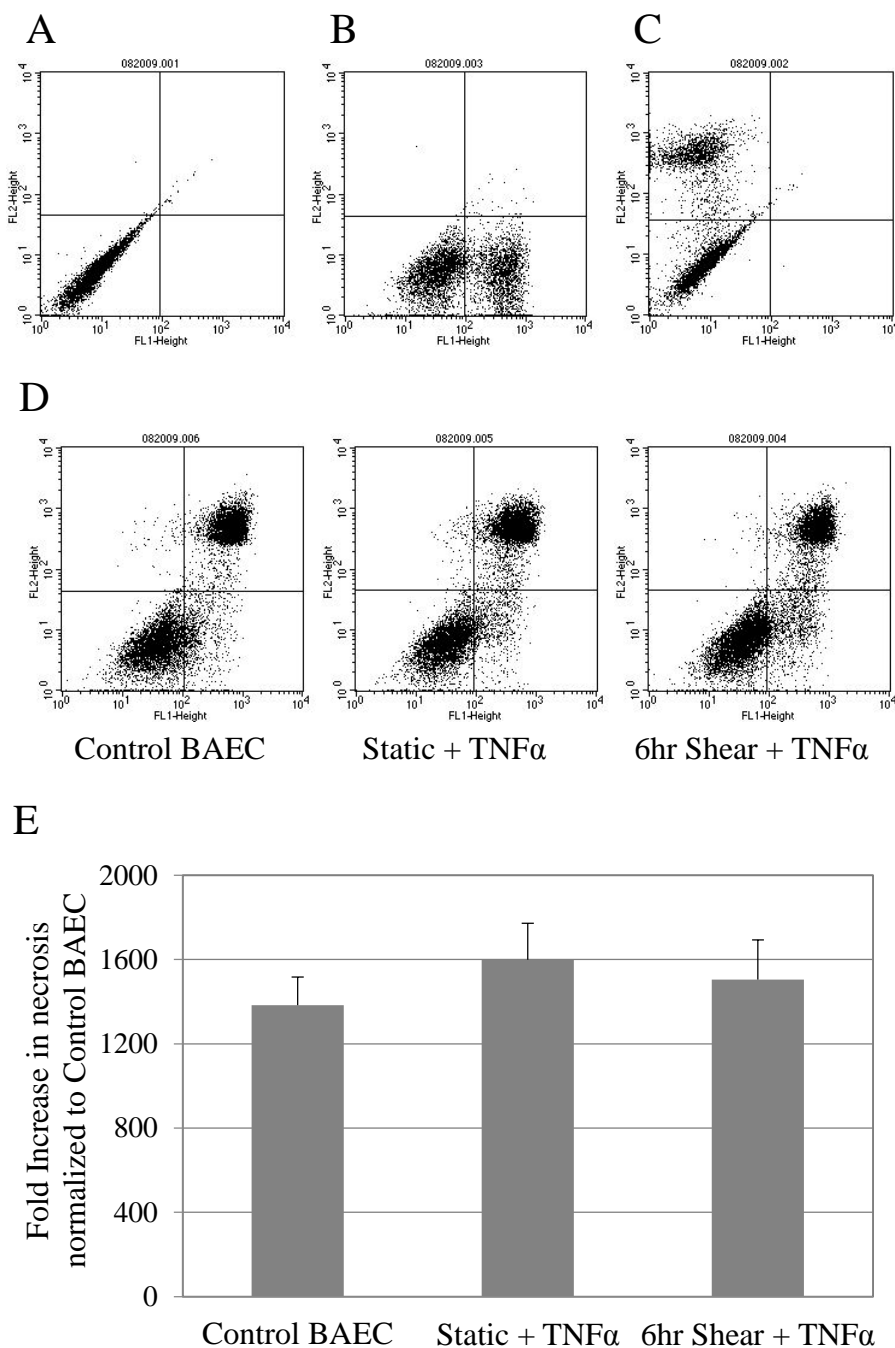


**Figure 3.5. Annexin V flow cytometry cell necrosis results.** Scatter plots of non-stained BAEC control (A); Annexin V stained apoptotic control (B), and (C) propidium iodide (PI) stained necrotic cells. Based on flow cytometry results of cells co-stained with Annexin V and PI after experiments (D), both purely necrotic and last stage apoptotic cells were quantified (E). Cellular necrosis as well as late stage apoptosis, but not purely apoptotic, cells were considered to be necrotic.

This data, which includes both necrotic as well as late stage apoptotic cells, suggests that shear stress does not suppress TNF $\alpha$  activated necrosis. After TNF $\alpha$  activation, cellular apoptosis and necrosis may be modulated differently by DAPK in sheared endothelial cells. DAPK has been identified as a key player in apoptosis pathways; however, this data suggests an independent role for DAPK in necrosis. Furthermore, results for late stage apoptosis alone also demonstrated a similar, though not statistically significant, trend compared to what we observed with TUNEL staining: elevated apoptosis with TNF $\alpha$  induction in static state, and decrease in apoptosis with the addition of applied shear stress.

### 3.2.8 DAPK expression is decreased in TNF $\alpha$ and shear stress activated endothelial cells

Interestingly, when we analyzed the DAPK expression for cells under control, TNF $\alpha$  treated, TNF $\alpha$  plus shear, and shear alone conditions, we observed that TNF $\alpha$  treatment alone (25 ng/ml) induced an increase in DAPK expression, which would be consistent with its role in promoting apoptosis. Protein analysis also showed that DAPK expression significantly decreased in TNF $\alpha$ -treated then sheared cells compared to TNF $\alpha$  alone (Figure 3.6A top). Quantitative analysis of relative band intensity revealed that the decrease in DAPK for TNF $\alpha$  treated then sheared cells was significant ( $P < 0.01$ ) (Figure 3.6A bottom). This decrease in DAPK expression correlates well with the drop in apoptosis as well as caspase activity (Figures 3.3B, 3.3C, 3.4B). TNF $\alpha$  treatment alone significantly increased apoptosis in endothelial cells, and a corresponding increase in DAPK expression was also observed.



Applying shear stress for 6 hours following TNF $\alpha$  induction of 18 hours resulted in a significant decline in apoptotic cells, as well as a significant drop in DAPK. We had previously observed a two-fold increase in DAPK by 6 hours of shearing alone (Figure 3.1A), and again the same is observed here. Combining 6 hours of shear stress following an 18-hour TNF $\alpha$  induction, however, resulted in a slight drop in DAPK expression compared to TNF $\alpha$  induction alone. This data indicates that shear stress in the presence of TNF $\alpha$  induction, attenuates DAPK expression instead, and suggests a functional role for DAPK in shear induced reduction of cytokine activated apoptosis. Shear stress could modulate DAPK expression as part of the overall endothelial mechanotransduction pathways in exerting its athero-protective functions.

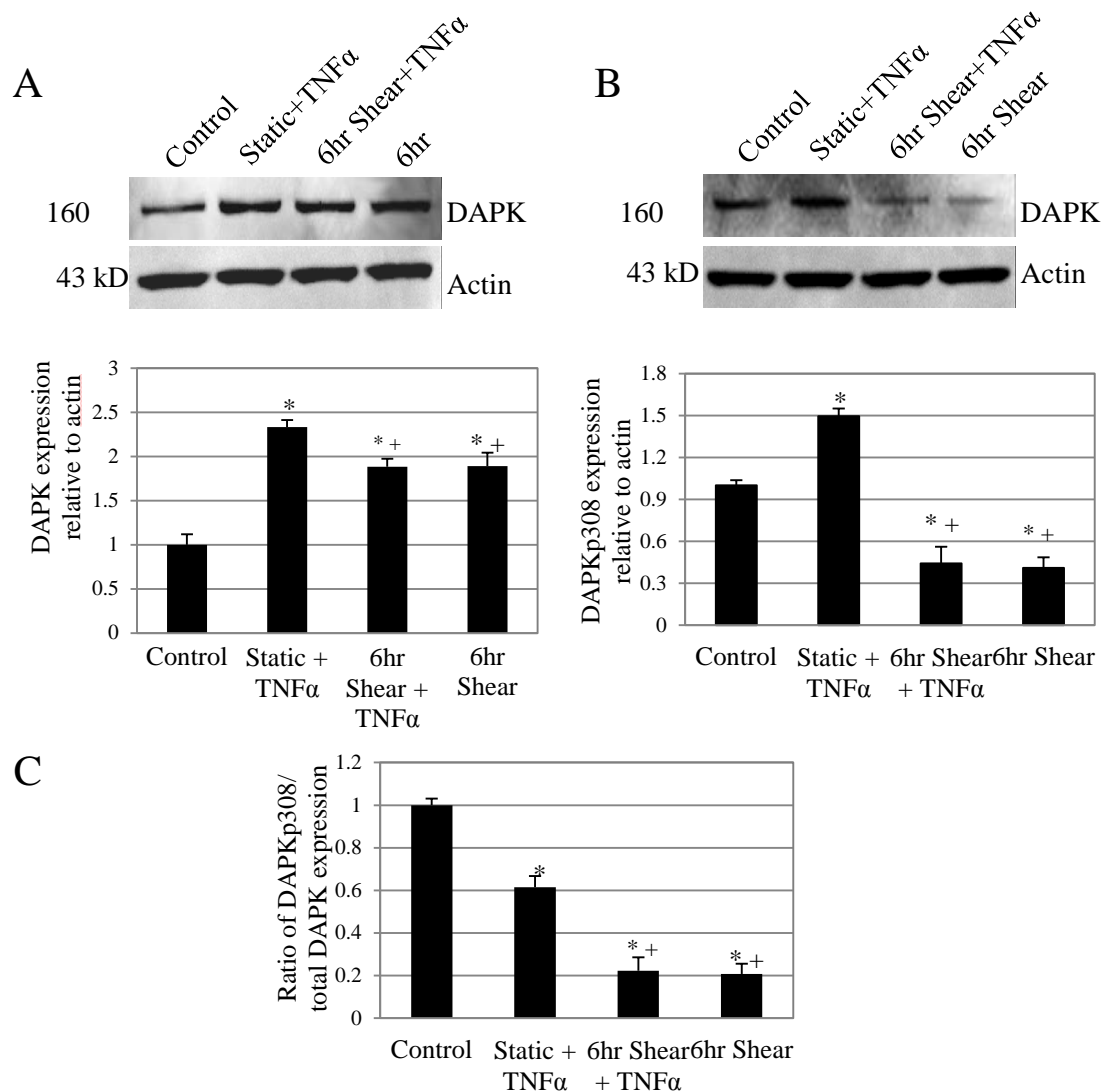


**Figure 3.6. Western analysis for DAPK expression due to shear and TNF $\alpha$ .** Total DAPK expression (A top) as well as phosphorylated serine 308 DAPK (B top) in control, static TNF $\alpha$ , and TNF $\alpha$  plus sheared, as well as sheared cells. Loading control bands are probed with anti-actin antibody on the same blot. Relative band intensity was quantified and analyzed based on results from 3 independent experiments, and presented as fold increase over control BAEC for overall DAPK (A bottom) and phospho-serine 308 DAPK (B bottom). (C). Phosphorylated DAPK as a fraction of total DAPK expression was calculated for each sample group based Western blots.

### 3.2.9 Phosphorylated serine 308 DAPK is decreased in TNF $\alpha$ and shear stress treated endothelial cells

Similarly, we examined the expression of phospho-serine 308 DAPK in cells under control, TNF $\alpha$ -treated, TNF $\alpha$  plus shear, and shear alone conditions. We found that phospho-serine 308 DAPK increased after 24-hour TNF $\alpha$  treatment in static condition (Figure 3.6B), which is consistent with our previous data (Figure 3.2B). Quantitative analysis based on Western blots also showed significant increase in phospho-308 DAPK in TNF $\alpha$  treated cells compared to control ( $P < 0.01$ ). However, with the addition of 6-hour shear following 18-hour TNF $\alpha$  induction, we observed a significant decrease in phospho-serine 308 DAPK compared to TNF $\alpha$  treatment alone ( $P < 0.01$ ), suggesting that shear stress dephosphorylates DAPK subsequent to and in the presence of TNF $\alpha$  induction. Similarly, we again observed a significant decrease in phospho-DAPK by 6 hours of shearing alone (see Figure 3.1B).

For sheared cells, either with or without TNF $\alpha$  treatment, we observed a more significant decrease in phosphorylated DAPK than overall DAPK. As a result, the ratio of phosphorylated to total DAPK changes is significantly decreased (Figure 3.6C). Static cells treated with TNF $\alpha$  alone experienced a reduction in fraction of phosph-DAPK, down to 61.5%; and the fraction of phosphorylated DAPK decreased further in TNF $\alpha$  treated and sheared cells (22.3%) or sheared cells (20.6%). Dephosphorylation of DAPK suggests activated kinase activity. It is expected then that TNF $\alpha$  treatment alone resulted in significantly less phospho-DAPK. Adding 6 hours of shear stress to 18 hours of TNF $\alpha$  treatment also significantly decreased the phospho-serine 308 DAPK fraction, as did applying 6 hours of shear stress alone to cells (see also Figure 3.1D).

These data would support the theory that shear stress has a considerable effect on regulating DAPK expression and activation. Shear stress increased overall DAPK expression and decreased serine 308 phosphorylation, indicating DAPK activation. While it is consistent that apoptosis as well as DAPK expression are both decreased with flow, shear activated DAPK, on the other hand, may serve functions other than the apoptotic signaling pathway.

#### 3.2.10 Transfection with siRNA against DAPK confirms its role in endothelial mechanotransduction

To further support our observed data so far, we also transfected BAEC with siRNA against DAPK to examine the effect of reducing DAPK expression on apoptosis in TNF $\alpha$  induced and sheared cells. First we confirmed reduced DAPK expression after transfection with DAPK siRNA using Western blot analysis (Figure 3.7A). In comparison, DAPK expression in BAEC cells transfected with control non-specific siRNA was not altered. Quantification of Western blots revealed statistically significant decrease in DAPK using siRNA ( $P < 0.01$ ) compared to control siRNA or non-transfected control BAEC (Figure 3.7B); while control siRNA did not alter overall DAPK expression

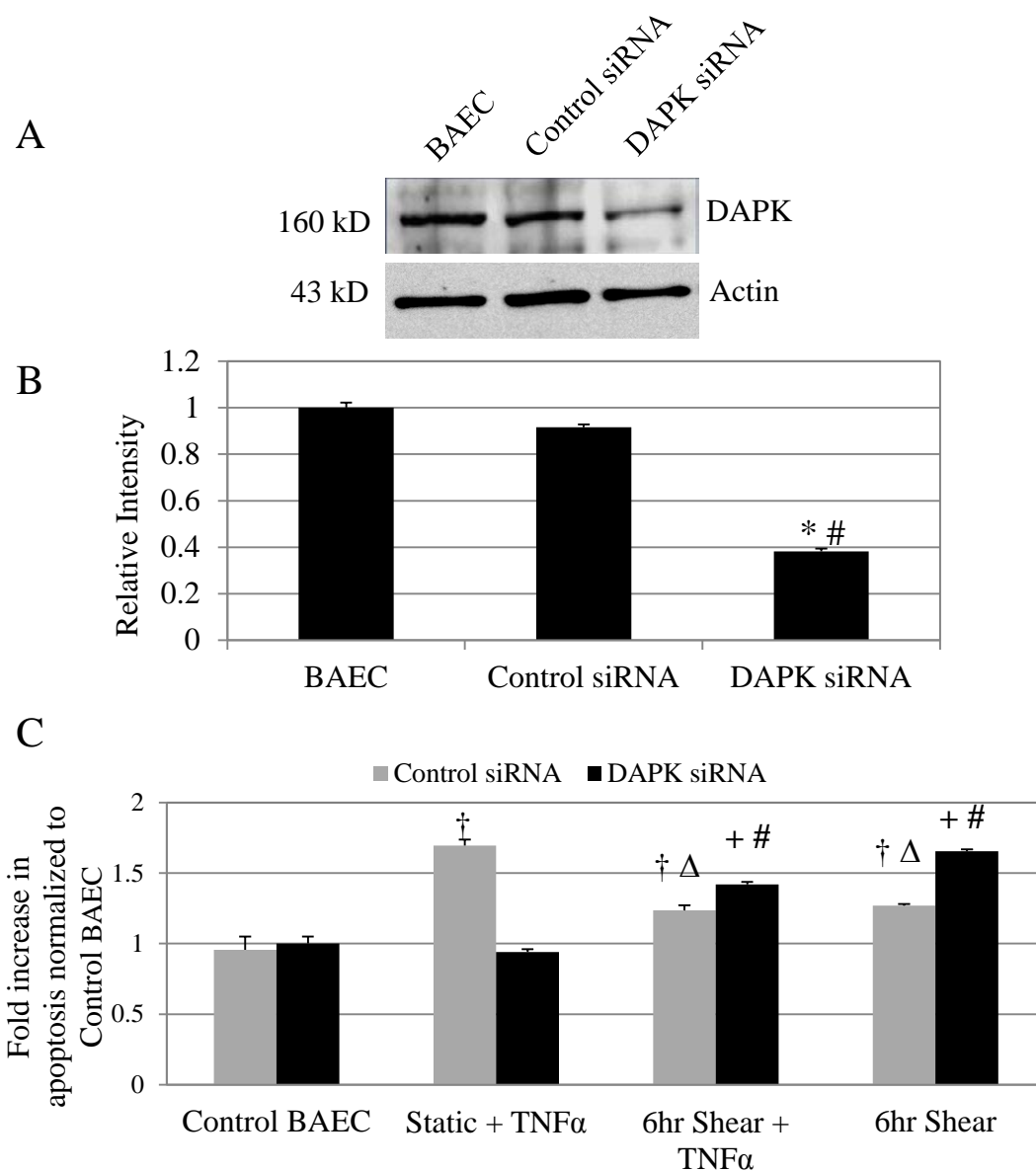


**Figure 3.7. Endothelial apoptosis after DAPK siRNA knockdown.** (A) Western analysis for total DAPK expression after transfection with siRNA. BAEC was transfected with either control siRNA or siRNA against DAPK. Relative band intensity was quantified and analyzed based on results from 3 independent experiments, and presented as fraction of control BAEC (B). (C) Apoptosis results based on flow cytometry analysis of FITC TUNEL staining with BAEC transfected w/ either control (gray) or DAPK (black) siRNA.

We repeated the apoptosis study as outlined in Figure 3.3A using BAEC transfected with either control or DAPK siRNA, and the results are presented in Figure 3.7C. Transfection alone with either siRNA does not promote apoptosis; there was only a 5% difference in apoptotic cells. Interestingly, we saw that transfecting cells with siRNA against DAPK completely eliminated TNF $\alpha$  induced apoptosis after 24-hour treatment, but with control siRNA we again saw an increase in apoptosis compared to control ( $P < 0.01$ ). With the addition of 6 hours of shear stress after 18-hour TNF $\alpha$  treatment, we observed a significant increase in apoptotic cells with DAPK siRNA treatment ( $P < 0.01$ ). These results are contrary to what we observed from non-transfected BAEC (Figure 3.3B), and together with the use of siRNA in reducing DAPK, would be consistent with our theory that DAPK plays a role in modulating shear stress reduction of TNF $\alpha$  induced apoptosis. In fact, compared to our results using non-transfected cells (Fig.3.3B), cells with control siRNA demonstrated very similar trend: we again observed significant decrease in apoptosis with the addition of 6-hour shearing ( $P < 0.01$ ) compared to TNF $\alpha$  treatment alone.

When normalized to control, a 1.27 and a 1.65 fold increase in apoptosis were observed in DAPK siRNA transfected cells sheared for 6 hours with or without TNF $\alpha$  pretreatment, respectively. Similarly, without siRNA, we observed a 1.63 fold increase in apoptosis for both cases (Fig. 3.3B). These findings are consistent with our previously observed increase in DAPK with 6 hours of shear stress (Fig. 3.1A), which would contribute to the increase in apoptosis by shearing alone. In addition, the up-regulation of DAPK with applied shear stress could compensate for DAPK siRNA treatment, again resulting in overall increased apoptosis.

Thus our siRNA data further supports our previous data suggesting an important role of DAPK in mediating endothelial apoptosis brought on by TNF $\alpha$  and shear stress.

### 3.2.11 Cytoplasm localization of GFP-DAPK on the actin network in BAEC

We also confirmed cytoplasmic presence of DAPK in endothelial cells under static and sheared conditions, specifically on the actin network. Fluorescence imaging of DAPK in cells was done using immunostaining; static or sheared (up to 6 hours) cells were fixed and stained using antibody against DAPK, as well as actin specific phalloidin probe.

Figure 3.8A shows representative fluorescence images of static control cells taken at 40X magnification: FITC labeled DAPK (left), red Phalloidin labeled actin (center), and the composite RGB image along with Hoechst stained nuclei (right). As expected, we observed cytoskeleton localization of DAPK to the actin network, as indicated by the overlapping red actin and green DAPK cytoplasmic stains. Figure 3.8B includes similar 40X images of sheared (6 hours) cells also showing localization of DAPK to the actin network. After 6 hours of shear stress, there were no discernible changes in the cytoskeleton localization of DAPK. Based on fluorescence imaging, DAPK remains in cell cytoplasm localized to the actin network either under static or sheared conditions.

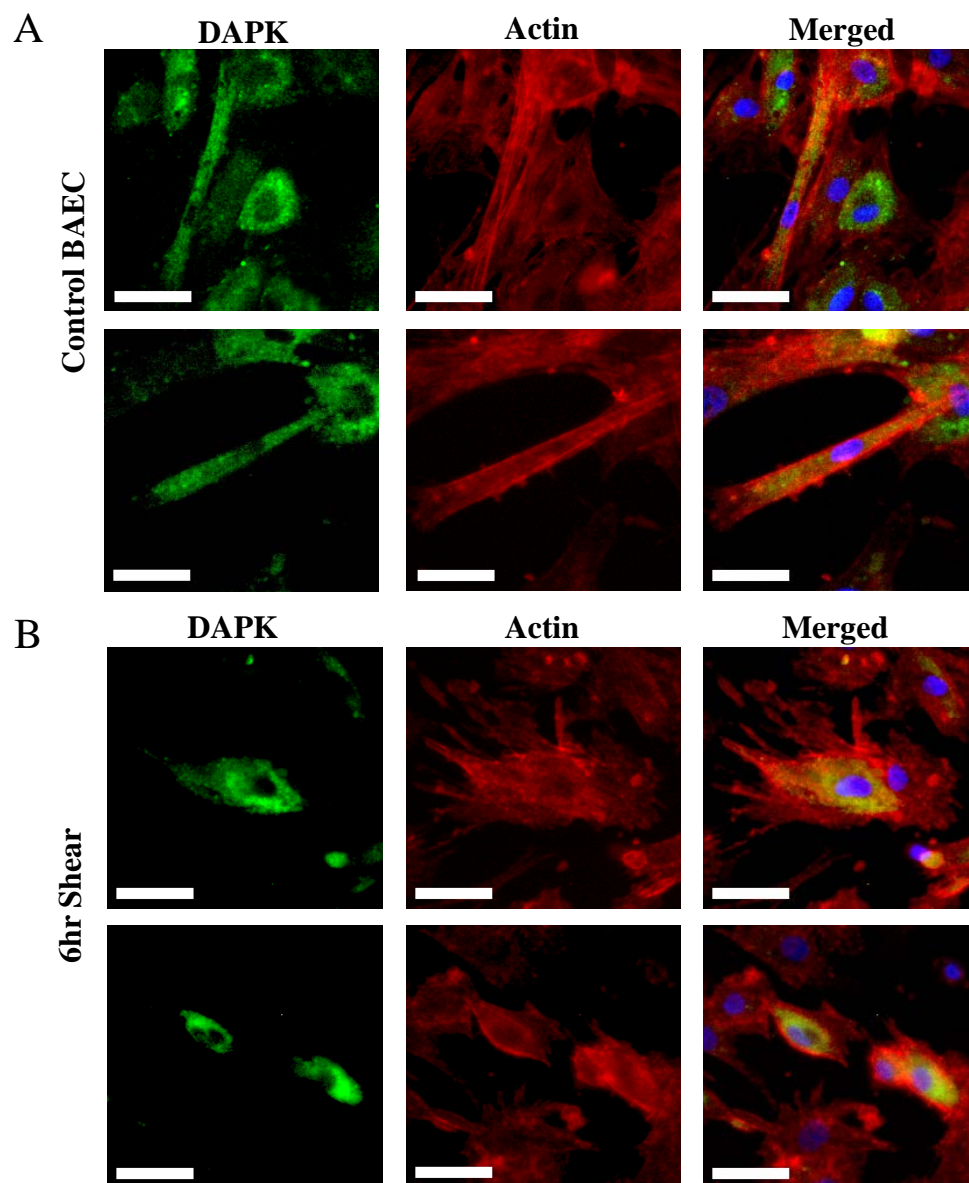


**Figure 3.8. Fluorescence microscopy images of BAEC immunostained for DAPK, actin, and nucleus:** FITC DAPK images at left panel, images of Atto 660 Phalloidin staining of actin at center, and merged RGB image of the two together with blue Hoechst nuclear stain at right. Cells are imaged at 40X for static (A) and 6-hour sheared (B) cases. Two representative images are presented for each group. White scale bar is 30  $\mu\text{m}$  for 40X images.



### 3.2.12 Long term shear stress of up to 24 hours decreased overall DAPK expression and activation

Finally, we examined effect of long term shearing on DAPK expression and activity in endothelial cells. Shear stress for up to 6 hours increased DAPK expression and as a result, increased apoptosis. However, shear stress for up to 24 hours significantly decreased DAPK level compared to static control cells ( $*P < 0.01$ ). Figure 3.9A top panel shows a Western blot probed with antibody against DAPK, and the bottom panel presents the quantitative analysis of protein expression based on multiple blots ( $n = 4$ ). This data further supports the idea that initial application of shear stress (up to 8 hours) triggers a significant but transient up regulations of DAPK, and that prolonged exposure to shear stress (up to 24 hours) ultimately resulted in decreased overall DAPK expression. We also saw a slight, not significant, decrease in phospho-serine 308 DAPK of 14% compared to static control cells after 24 hours of shearing. Figure 3.9B shows Western blot and quantitative analysis ( $n = 4$ ). This change in phospho-DAPK could be attributed to the decrease in overall DAPK after 24 hours of shearing. The ratio of phospho-DAPK to total DAPK changes, however, increased after 24 hours of shearing (Figure 3.9C), likely due to the more significant increase in overall DAPK compared to phosphor-DAPK.

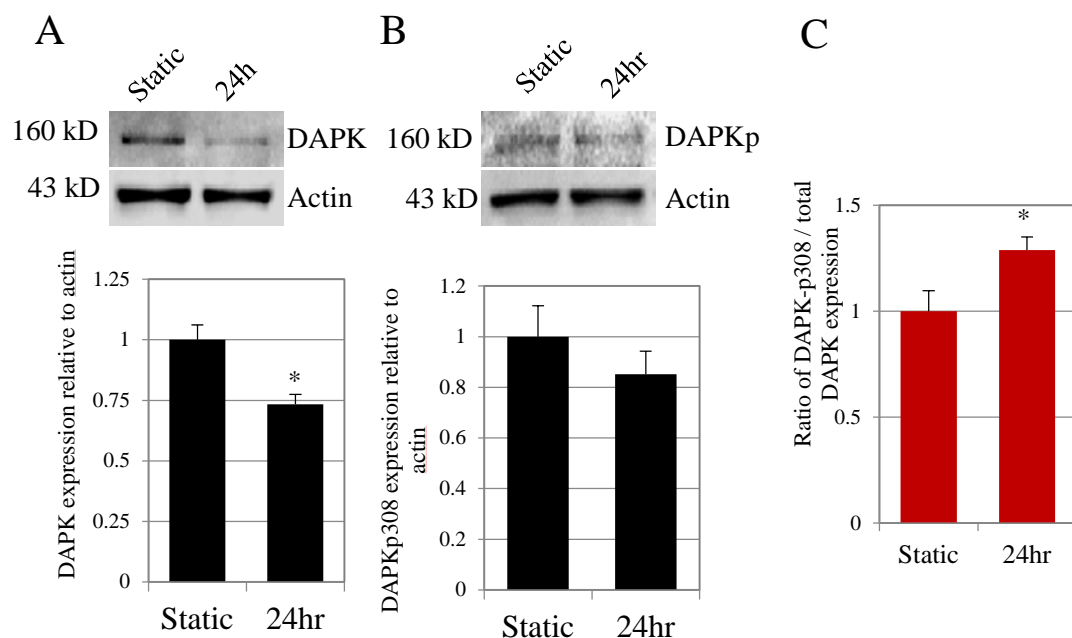


**Figure 3.9. Long-term shear effect on DAPK expression.** (A) Western blot of overall DAPK expression in control and sheared cells (24 hours). Loading control bands are probed with anti-actin antibody on the same blot. (B) Western blot of phosphorylated DAPK at serine 308, for static and sheared cells (24 hours). Phosphorylated DAPK as a fraction of total DAPK expression was calculated based Western blot analysis (C). Fraction of phospho-serine 308 DAPK increased significantly after 24 hours of shearing. \*  $P < 0.05$  compared to static BAEC.

An increase in the fraction of phosphorylated DAPK at serine 308 also indicates presence of more inactivated DAPK. The effect of short-term shearing on both overall and phospho-serine 308 DAPK seem to be transient, which would suggest that shear stress induced apoptosis is short-lived. The finding that prolonged shearing of up to 24 hours significantly decreased DAPK, further supports the role of DAPK in mediating the anti-apoptotic effects of shear stress.

### 3.3 Discussion

Understanding apoptosis, a fundamental cellular process, would have significant impact on a multitude of cell and tissue types, as well as disease and therapeutic models. In atherosclerosis, for example, increased apoptosis contributes to prolonged inflammatory response, plaque instability, rupture, and thrombus formations (32). Atherosclerotic plaques form preferentially at regions of disturbed flow and low shear stress, which are also sites of increased cell turnover rate (116). Shear stress has been shown to suppress cytokine induced apoptosis in endothelial cells (117). DAPK is an important protein kinase in modulating apoptotic pathways (109), yet its potential role in endothelial apoptosis and mechanotransduction has been largely unexplored. Identifying the role of DAPK in endothelial cell function would be important to understanding both homeostatic and diseased conditions in the vasculature.

We report, for the first time, changes in the expression of DAPK in endothelial cells exposed to up to 24 hours of laminar fluid shear stress (118). We found that shear stress induced an increase in overall DAPK protein expression, with increasing time of shear, reaching maximum level after 6 hours (Fig. 3.1A). Consistent with this finding, we observed an increase of DAPK mRNA expression early based on real time RT-PCR analysis, suggesting that DAPK transcription is at least in part regulated by a shear-sensitive mechanism (Fig. 3.1B). DAPK is auto-phosphorylated at serine 308, inside the CaM regulatory part of the protein, as an inhibitory checkpoint. Serine 308 becomes dephosphorylated when DAPK is fully activated following CaM binding. With applied shear stress, we observed a gradual decrease in phosphorylated DAPK for up to 6 hours

of shearing (Fig. 3.1C). When correlated with total DAPK expression, phosphorylated (Ser308) DAPK drops to 40% of static control after 6 hours of shearing. These data suggest that shear stress activates DAPK by dephosphorylating serine 308, with maximum effect occurring after 6 hours of shear stress (Fig. 3.1D).

The finding that shear stress alone increased mRNA and protein levels of DAPK, as well as influenced its phosphorylated state at serine 308, is significant in that DAPK could potentially play a role in the mediating effects of shear stress in endothelial cells. Though increased DAPK is more likely to promote apoptosis, shear stress has been shown to suppress cytokine induced apoptosis. To further examine DAPK activities in sheared cells, we used TNF $\alpha$  to induce apoptosis, in conjunction with shear stress stimulation. Phosphorylated DAPK at serine 308 is significantly increased with extended TNF $\alpha$  treatment of up to 48 hours (Fig. 3.2B), which suggests that DAPK activity is involved in TNF $\alpha$  induced apoptotic pathways in BAEC. With TNF $\alpha$  treatment, DAPK could trigger apoptotic mechanisms early, and returns to the inactive, phosphorylated state at serine 308.

We designed our apoptosis study (Fig. 3.3A) to combine long term TNF $\alpha$  inductions (18 hours) with subsequent applied shear stress (6 hours), in order to examine the suppression of cytokine induced apoptosis with shear stress, and the potential role for DAPK in endothelial mechanotransduction. As expected, TNF $\alpha$  induced significant apoptosis in endothelial cells kept under static conditions. However, after stimulation with TNF $\alpha$  for 18 hours, shearing cells in media containing TNF $\alpha$  for an additional 6 hours significantly decreased apoptosis (Fig. 3.3B). The same trend was observed using TUNEL stain with both flow cytometry and microscopy (Fig. 3.4C).

In addition, caspase-3 and -7 activity also increased with TNF $\alpha$  induction and decreased with subsequent shearing (Fig. 3.3B, 3.3C, 3.4C). On the other hand, shearing cells alone for 6 hours, without prior TNF $\alpha$  induction, also induced a significant increase in apoptosis compared to control (Fig. 3.3B, 3.3C, 3.4C). This is consistent with our previous finding that 6 hours of shear stress induced an increase in overall DAPK content, and dephosphorylation at serine308, which would promote DAPK activity and therefore apoptosis. Furthermore, there was no significant difference in necrosis between these experimental groups (Fig. 3.5), suggesting that shear suppression of apoptosis is independent of the necrotic pathway, and that DAPK is a specific regulator of apoptosis only.

Parallel to our apoptosis studies, TNF $\alpha$  at 25 ng/ml did in fact increase DAPK level, as well as phospho-serine 308 DAPK after 24-hour incubation in endothelial cells. We also found that in the case of 18-hour TNF $\alpha$  activation followed by 6-hour shear stress with TNF $\alpha$ , DAPK expression is attenuated compared to TNF $\alpha$  treated BAEC, but is still significantly higher than control BAEC (Fig. 3.6A, 3.6B). At the same time, phosphorylated DAPK at serine 308 also increased significantly with long term TNF $\alpha$  treatment, while adding shear stress caused a significant decrease in phosphorylated DAPK compared to both TNF $\alpha$  and control BAEC (Fig. 3.6B, 3.6C). These observed changes in DAPK are consistent our earlier findings that 6 hours of shear stress without TNF $\alpha$  increased overall DAPK expression and decreased phospho-serine 308 DAPK (Fig. 3.1). Now, in cells already exposed to TNF $\alpha$  for 18 hours, shear stress resulted in suppressed DAPK expression but increased kinase activation by dephosphorylation. In other words, in the presence of and subsequent to TNF $\alpha$  induction, shear stress induced

different effects on DAPK activity compared to shearing alone, resulting in reduced endothelial apoptosis.

Taken together, we found that shear stress at 6 hours induced endothelial apoptosis via increased expression and activation of DAPK. However, when shear stress was applied subsequent to 18 hour-treatment with TNF $\alpha$ , cells exhibited decreased expression and increased activation of DAPK, as well as attenuated apoptosis compared to TNF $\alpha$  treatment alone. The increase in DAPK by TNF $\alpha$  is consistent with its regulatory role in cytokine induced apoptosis, and the decrease of DAPK is consistent with the suppression of apoptosis by shear stress. On the other hand, increased activation of DAPK by shear after TNF $\alpha$ , in the context of reduced apoptosis, suggests that DAPK could be recruited to non-or anti-apoptotic functions. While shear stress alone activates DAPK and induces apoptosis, it has the opposite effects on apoptosis if applied in the presence or following TNF $\alpha$ . Thus shear stress regulates DAPK expression and activation through mechanisms susceptible to pro-apoptotic signals such as TNF $\alpha$ . TNF $\alpha$  and shear stress may have competing effects on the regulation of DAPK expression to either promote or suppress endothelial apoptosis respectively.

The significance of shear stress regulated DAPK in suppressing TNF $\alpha$  activated apoptosis in endothelial cells is further supported by our siRNA results. When siRNA against DAPK was used to suppress DAPK expression, apoptosis results in response to TNF $\alpha$  and shear stress stimulation was contrary to those of non-transfected cells (Fig. 3.7), while transfection with control siRNA yielded results similar to non-transfected cells. These data further demonstrate conclusively that: first, DAPK plays an essential role in mediating TNF $\alpha$  induced apoptosis, suppressing DAPK using siRNA eliminated

the increase in apoptosis with long term TNF $\alpha$  treatment; second, DAPK also plays an essential role in suppression of TNF $\alpha$  induced apoptosis by shear stress. In non-transfected cells, addition of shear stress suppressed TNF $\alpha$  induced apoptosis. With DAPK siRNA, the addition of 6 hours of shear stress again increased apoptosis in transfected BAEC. Finally, this data further confirms that shear stress alone induces apoptosis through a transient up-regulation of DAPK, since apoptosis increased with shearing independent of siRNA treatment.

These data further suggest that any interactions between TNF $\alpha$  and shear stress induced effects on DAPK pathways are critically dependent on the order and length of induction. Shear stress alone increases DAPK expression at 6 hours, but pre-treating cells with TNF $\alpha$  prior to addition of shear stress in media containing TNF $\alpha$  resulted in reduction of DAPK. As a result, the relative time of cytokine and/or shear stress inductions of DAPK in endothelial cells could also be an important determinant of their competing effects in activating and suppressing apoptosis. In fact, when we examined cells sheared for 24 hours, we saw a significant decrease in overall DAPK accompanied by an increase in fraction of phosphorylated serine 308 DAPK (Fig. 3.9). This data further indicates that DAPK expression and activation are at least in part modulated by shear stress in a time-dependent manner. Initial application of shear stress (up to 8 hours) triggers a significant but transient up-regulation of DAPK expression and activation, but with prolonged shearing (24 hours), DAPK expression is markedly attenuated while fraction of inactive DAPK is increased. This agrees with the general anti-apoptosis function of shear stress, and decreased DAPK expression could be one mechanism which shear stress modulates its athero-protective effects on endothelial cells.

Aside from its regulatory role in apoptosis, DAPK also regulates actin cytoskeleton and contributes to cytoplasmic changes associated with apoptosis such as stress fibers and membrane blebbing (94). DAPK is localized to the actin microfilament cell cytoskeleton, and phosphorylates myosin regulatory light chain (MLC) at Ser19, both *in vivo* and *in vitro* (39; 95). As a result, DAPK promotes actin-myosin contractility and stabilizes stress fibers in serum starved fibroblasts, and mediates serum-induced stress fiber formation (39). With shear stress, endothelial cells undergo morphological changes: stress fiber formation, focal adhesion reorganization, and eventual re-alignment of cytoskeleton in the direction of flow (115). DAPK could also play a role in affecting morphological changes in response to shear stress and in addition to promoting apoptosis (119). The cytoskeleton effect of DAPK occurs before apoptosis, and is independent of DAPK death domain. We confirmed cytoskeleton localization of DAPK using immunostaining of fixed BAEC (Fig. 3.8). We observed co-localization of DAPK and the actin network in the cell cytoskeleton, and there were no marked changes in DAPK intracellular location after 6 hours of shear stress compared to static control.

In summary, we have presented conclusive evidence so far that suggest an important regulatory role for DAPK in modulating the effects of shear stress in endothelial apoptotic pathways. The regulatory mechanism of DAPK gene transcription and expression is sensitive to shear stress, and DAPK is potentially controlled by mechanical cues that the endothelial cells are susceptible to TNF $\alpha$ . We demonstrated that shear stress alone for 6 hours can increase DAPK level, resulting in increased apoptosis. In long term shear stress studies, however apoptosis continues to be suppressed in the presence of death-inducing agents (112). Consistent with this finding, we saw a striking



attenuation of DAPK proteins after 24 hours of shear stress in BAEC. Shear stress, in the presence of  $\text{TNF}\alpha$ , also suppresses endothelial apoptosis by decreasing DAPK activity, or recruiting activated DAPK to other non-apoptotic functions such as cytoskeleton remodeling. Our apoptosis data based on multiple TUNEL analysis is confirmed by similar trend in caspase -3 and -7 activity which are downstream of DAPK. The role of DAPK in the competing effects of  $\text{TNF}\alpha$  and shear stress on endothelial apoptosis is further validated by siRNA knockout of DAPK, which yielded opposite results from the non-transfected case.

Our findings suggest that in endothelial cells, fluid shear stress alone can be pro-apoptotic, via DAPK activation. However, in the presences of other pro-apoptotic triggers such as  $\text{TNF}\alpha$ , shear stress actually protects against apoptosis by down regulating DAPK. Furthermore, extended shear stress of up to 24 hours induced a marked decrease in overall DAPK, again supporting the beneficial effects of long term shearing in suppressing endothelial apoptosis. The mechanisms, by which DAPK is regulated by shear stress, as well as the participating regulatory partners in the mechanotransduction pathway, are currently being elucidated. The order and duration of both shear stress and cytokine stimulation on endothelial cells need to be investigated further in the context of apoptosis and DAPK expression and activation. Time-dependent induction studies on the competing effects of shear stress and stress stimuli (cytokine, oxidative stress, etc) will shed more light on the activities of DAPK in apoptosis as well as cytoskeleton changes. The regulatory details of DAPK signal transduction in endothelial cells, particularly in modulating effects of hemodynamic shear stress, will help create a new paradigm for DAPK in mechanotransduction.

The idea that mechanical forces such as fluid shear stress may regulate DAPK activity, potentially toward a non-apoptotic direction, would have significant impacts on therapeutic mechanisms of vascular disease such as atherosclerosis.

#### 4. SHEAR STRESS ATTENUATES APOPTOSIS DUE TO TNF $\alpha$ , OXIDATIVE STRESS, AND SERUM DEPLETION VIA DAPK EXPRESSION

##### 4.1 Introduction

Endothelial apoptosis is influenced by a wide variety of signal transduction pathways. Shear stress due to fluid flow can activate or inhibit endothelial apoptosis depending on the environmental factors and local tissue-fluid flow interaction.(60) While some apoptosis signaling cascades have been investigated, endothelial apoptosis signal transduction under fluid shear stress is not fully understood. Most *in vitro* studies have tried to elucidate the key molecules that initiate apoptosis but those studies lack the concept of apoptosis signaling in the presence of shear stress.(62; 63; 67; 69; 120) On the other hand, several shear stress studies that examine inflammatory cell expression fail to quantify the subsequent endothelial apoptosis response.(70-73; 121) Understanding apoptosis activation in response to fluid flow effects may help uncover key shear stress mechanisms in both physiological and pathological conditions.

Recent research has shown that death-associated protein kinase (DAPK) is a positive mediator for apoptosis.(34) DAPK is localized to the actin extracellular network where it regulates actin and cytoplasm changes associated with programmed cell death.(77; 94; 95)

Under fluid shear, endothelial cells introduce stress fiber formation and focal adhesion realignment. As a result, the structural changes align the cell cytoskeleton in the direction of shear.(30; 115) DAPK has actin involvement that could potentially play a role in reorganization of the cytoskeleton. DAPK is shown to affect cell death cascades but its endothelial function in hemodynamic shear is still being defined.

Current research has mainly focused on DAPK function in select types of cancer (97), yet DAPK function in endothelial cells remain unclear. Galbraith *et al.* showed that sheared endothelial cells undergo various structural changes. Endothelial cells after long-term shearing facilitate cytoskeletal remodeling, stress fiber formation, increased focal adhesion activity, and eventually realignment with the flow field direction.(107; 115) Endothelial cells respond to fluid shear stress by initiating various signal transduction pathways. The DAPK regulatory role in programmed cell death and its interaction with cytoskeletal changes suggest a potential role in endothelial mechanotransduction.

In a recent *in vitro* study, the effects of fluid shear stress on endothelial DAPK expression were investigated.(118) Shear stress alone upregulated DAPK gene transcription and protein expression, which in turn increased apoptosis. Additionally, shear stress was shown to regulate DAPK activity while suppressing TNF- $\alpha$  induced apoptosis. Silencing DAPK expression through siRNA transfection resulted in increased TNF- $\alpha$  induced apoptosis as compared to non-transfected cells. This study demonstrates a mechanistic role of DAPK in suppression of TNF- $\alpha$  induced apoptosis. Two important conclusions can be taken away from this shear stress study. First, shear stress can initiate proapoptotic signaling through DAPK activation. However, long term shear stress (24 hour shear) significantly decreased DAPK expression, which confirmed the

atheroprotective effects of laminar shear. Second, shear stress regulates DAPK expression, in the presence of TNF- $\alpha$ , to protect against apoptosis activation. (118) This study exposes an interesting mechanism through which DAPK is regulated by shear stress. The competing effects of shear stress and apoptotic stimuli needs to be further explored. The temporal activation of DAPK and its correlated pathway could play a role in endothelial response to shear. Thus, shear stress effects on DAPK activation in the presence of other apoptotic inducers need to be further clarified, particularly in a time-dependent manner. The shear-apoptosis studies may explain the impact of DAPK in the endothelial mechanotransduction pathway.

**Research Objective 3: Does fluid shear stress mitigate TNF $\alpha$ , H<sub>2</sub>O<sub>2</sub>, and serum starvation induced endothelial apoptosis by modulating DAPK expression in a time-dependent manner?**

## 4.2 Results

### 4.2.1 DAPK expression is decreased in TNF $\alpha$ , H<sub>2</sub>O<sub>2</sub> treated, and serum depleted cells when exposed to shear stress before or after treatment

We observed that TNF $\alpha$  treatment (25 ng/ml), H<sub>2</sub>O<sub>2</sub> (0.5 mM), and serum depletion (0.5% FBS) all individually induced an increase in DAPK expression, which is consistent with their role in promoting apoptosis (33; 34). To examine the time-dependent effect of shear stress on apoptosis and DAPK expression, cells were categorized as one of the following groups: control BAEC, static + stimuli (24h incubation), 6h pre-shear then stimuli (18h), 6h pre-sheared then static (no stimuli), stimuli (18h) then 6hr post-shear, static then 6hr post-shear (no stimuli). First, we

explored the effect of pre-conditioning cells with shear stress exposure (12 dynes/cm<sup>2</sup>) in samples with and without each of the stimuli (TNF $\alpha$ , H<sub>2</sub>O<sub>2</sub>, and serum depletion).

Western analysis showed DAPK expression significantly decreased in cells exposed to preshearing followed by stimuli incubation compared to stimulants alone (static + stimuli) (Fig. 4.1B). DAPK expression was quantified using the relative intensity of DAPK bands normalized to a loading control, actin (Fig. 4.2A). At least three separate samples were used to confirm DAPK expression of each particular sample.

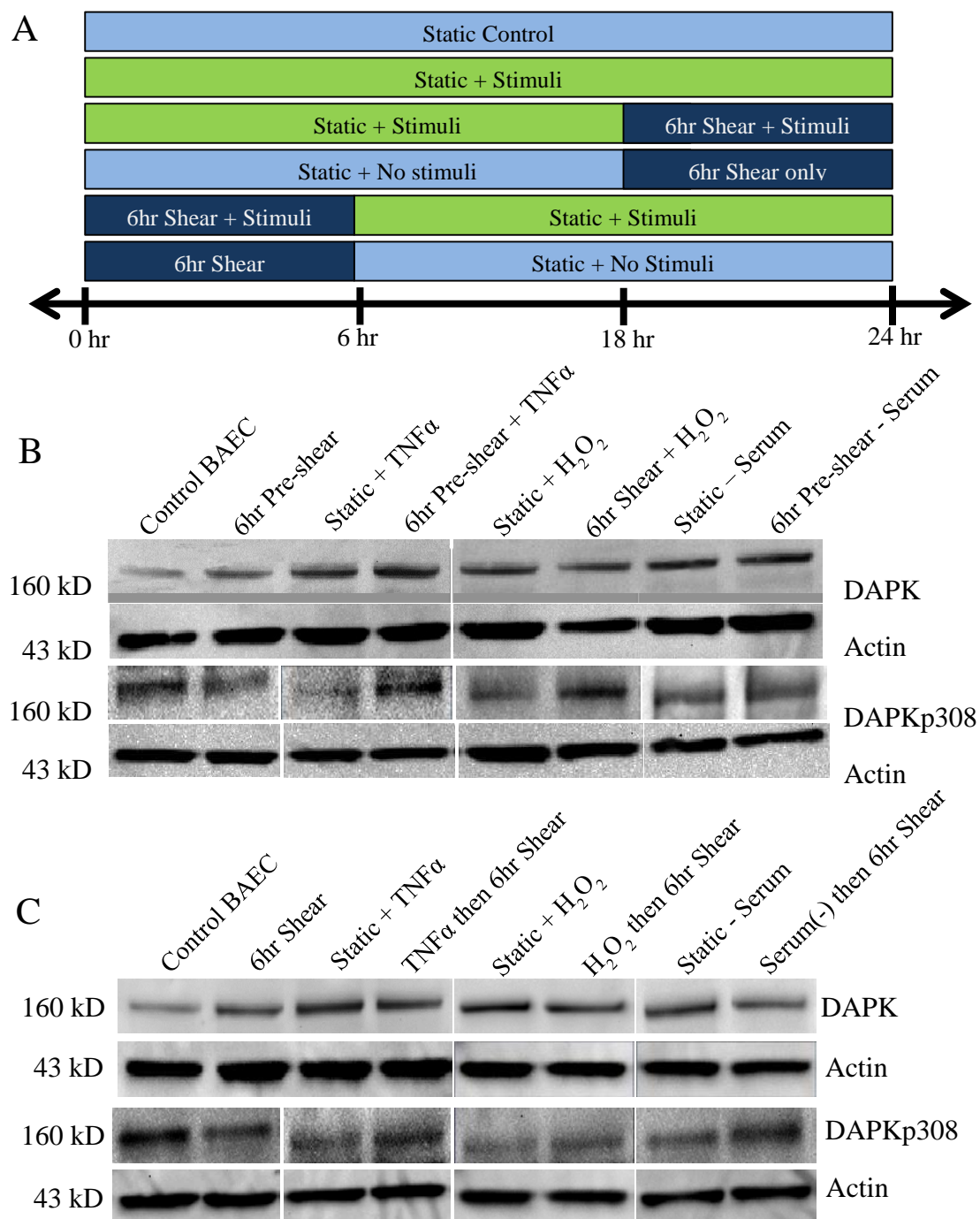


**Figure 4.1. Experimental design to investigate DAPK expression due to shear and stimulants.** A: Experimental setup for analysis of effects of simultaneous shear stress and stimulants. Cells are treated to shear stress either before or after treatment with apoptotic stimulants, which includes TNF $\alpha$ , H $_2$ O $_2$ , and serum depletion. B: Western blot of DAPK in pre-sheared cells versus cells treated with stimulus (TNF $\alpha$ , H $_2$ O $_2$ , or serum depletion). C: Western blot of DAPK in cells sheared post treatment with stimulus (TNF $\alpha$ , H $_2$ O $_2$ , or serum depletion).

After quantitative analysis, we consistently observe a significant increase in DAPK expression in static + stimuli, as compared to control BAEC ( $P < 0.05$ ). Also, we see a clear decrease in DAPK expression in cells pre-sheared prior to stimuli incubation, compared with the static cells exposed to each stimuli ( $P < 0.05$ ). After observing the effect of pre-conditioning cells, we continue to examine the time-dependent effect of shear and explore the post-shearing effects after stimuli exposure.

For the post-sheared experiments, BAEC cells were incubated with each of the stimuli for 18h prior to the 6h shear rather than pre-conditioning. Western blot were imaged and DAPK expression was quantified using the relative band intensity compared to actin (Fig. 4.1C). DAPK expression significantly decreased for apoptosis-induced then sheared cells compared to cells incubated with stimulants alone ( $P < 0.05$ ), similar to the preconditioned cells (Fig. 4.2B). Cells sheared (6hrs) after exposure to stimuli resulted in an increase of total DAPK expression, but less significantly than static cells under the same stimuli conditions (Fig. 4.2B). Overall, our data suggest that extended shearing mitigates the stimulant effect (TNF $\alpha$ , H<sub>2</sub>O<sub>2</sub> treated, and serum depletion) on endothelial DAPK expression compared to the static cases.



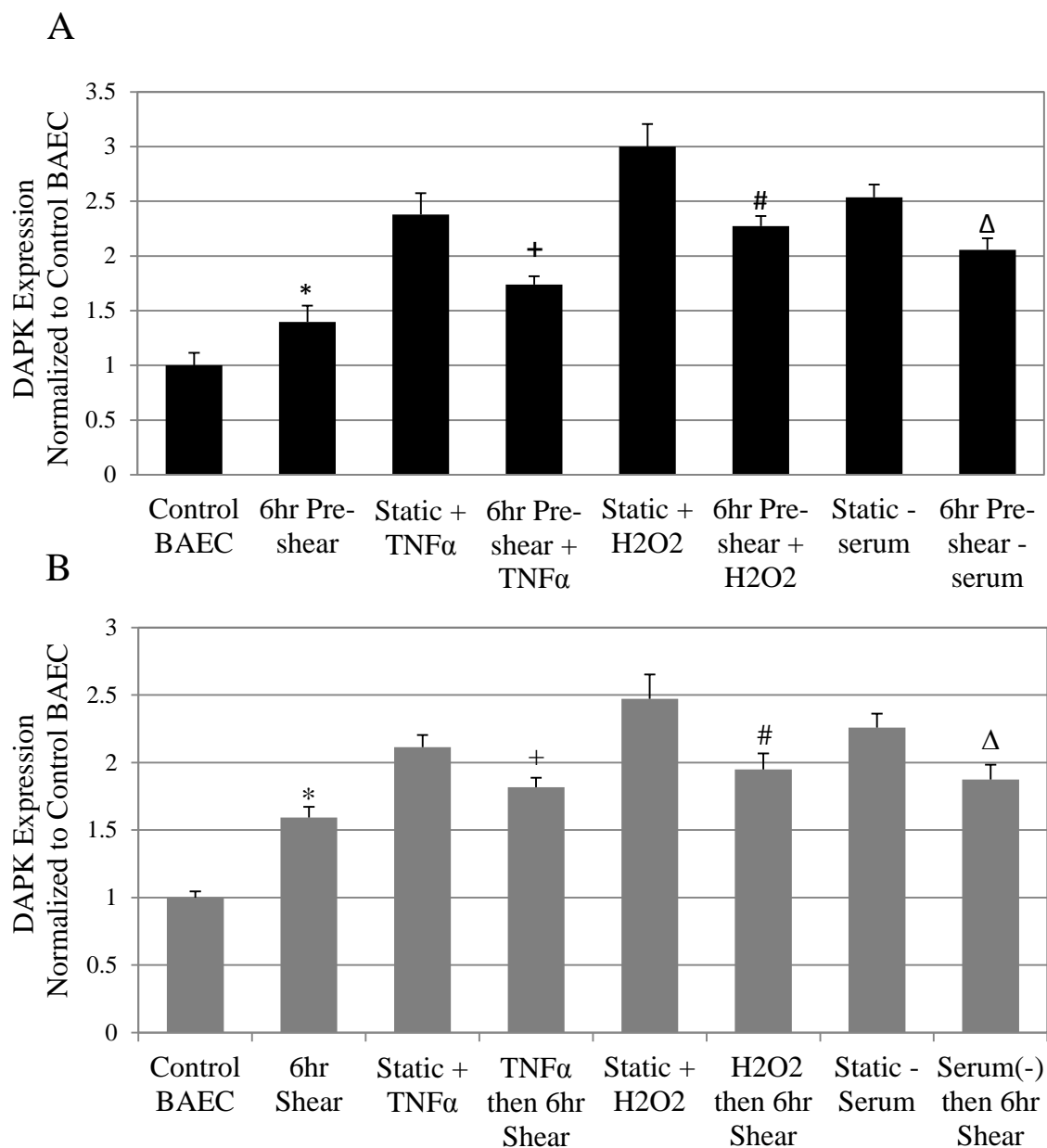


**Figure 4.2. DAPK expression due to pre- and post-conditioning and apoptosis stimulants.** A: DAPK protein expression for the treatment and pre-sheared experimental groups. B: DAPK protein expression for the treatment and post-sheared experimental groups. For all figures: \*  $P < 0.05$  compared to Control BAEC, +  $P < 0.05$  compared to Static + TNF $\alpha$ , #  $P < 0.05$  compared to Static + H<sub>2</sub>O<sub>2</sub>,  $\Delta$   $P < 0.05$  compared to Static - Serum.

#### 4.2.2 Phosphorylated serine 308 DAPK is decreased in TNF $\alpha$ , H<sub>2</sub>O<sub>2</sub> (0.5 mM), and serum depleted (0.5% FBS) and shear stress treated endothelial cells

DAPK is auto-phosphorylated in its static state as an inhibitory checkpoint. When DAPK is dephosphorylated at serine 308, in the presence of calmodulin binding, DAPK becomes fully activated for its kinase functioning. The experimental setup previously described was used to investigate the effect of time-dependent shear on phospho-serine 308 DAPK (DAPKp308). DAPKp308 decreased after 24h TNF $\alpha$ , H<sub>2</sub>O<sub>2</sub>, or serum depletion treatment in static condition (Figs. 4.1B, 4.1C). Significant decrease in phospho-308 DAPK in treated cells compared to control ( $P < 0.01$ ). The stimulants were all shown to significantly decrease phospho-DAPK in static cells, confirming the expected increased DAPK activation (Fig. 4.1B). 6h shear following 18-h induction (with each stimuli) showed significantly increased phospho-DAPK compared to each stimulant treatment alone suggesting that shear stress attenuates DAPK dephosphorylation subsequent to and in the presence of apoptosis induction ( $P < 0.05$ ). Overall DAPK activation for each experimental group is shown as a ratio of DAPKp308 / Total DAPK (Figs. 4.3).

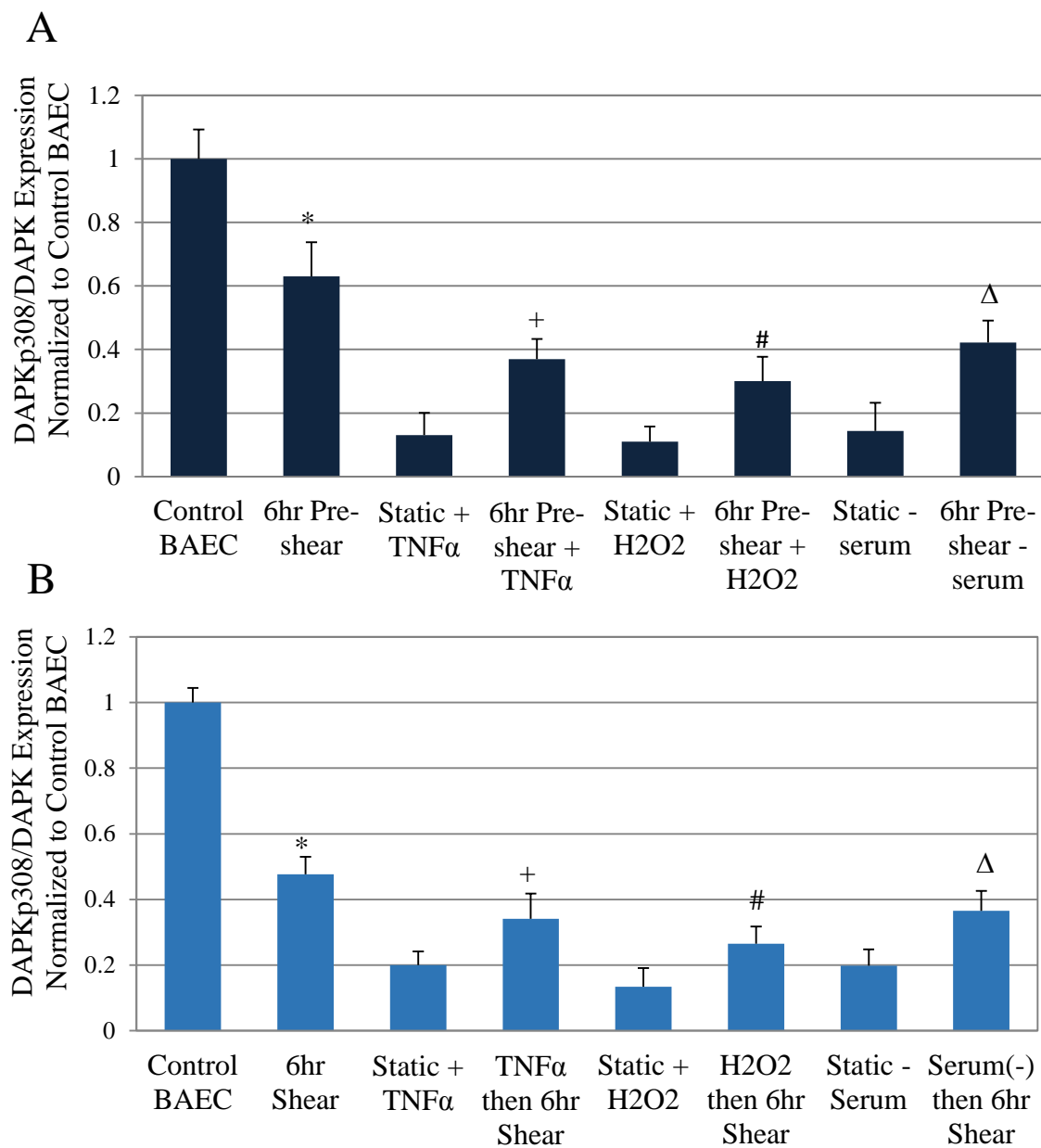


**Figure 4.3. DAPKp308/DAPK expression due to shear and stimulants.** A: Ratio of DAPKp308 / Total DAPK protein expression for the same experimental groups, pre-sheared cells treated with TNF $\alpha$ , H<sub>2</sub>O<sub>2</sub>, or serum depletion. B: Ratio of DAPKp308 /Total DAPK protein expression for the treatment and post-sheared experimental groups. For all figures: \*  $P < 0.05$  compared to Control BAEC, +  $P < 0.05$  compared to Static + TNF $\alpha$ , #  $P < 0.05$  compared to Static + H<sub>2</sub>O<sub>2</sub>, Δ  $P < 0.05$  compared to Static – Serum.

#### 4.2.3 Shear stress significantly reduced apoptosis following incubations with TNF $\alpha$ , H<sub>2</sub>O<sub>2</sub>, and low serum

Fluid shear stress has been shown to decrease apoptosis in endothelial cells induced by cytokines, such as TNF $\alpha$  (112; 118). Since our data validate that fluid shear increases DAPK activity and each apoptotic stimulant activates DAPK in a time-dependent manner, we explored the time-dependent effects of shear on TNF $\alpha$ , H<sub>2</sub>O<sub>2</sub> treated, and serum depleted induced endothelial apoptosis. We added TNF $\alpha$ , H<sub>2</sub>O<sub>2</sub> (0.5 mM), and serum depletion (0.5% FBS) to induce apoptosis, in combination with shear stress conditioning. Our apoptosis study (Fig. 4.1A) combined both long term inductions (18 h) with pre-shearing and subsequent applied post-shearing (6h), to examine the suppression of apoptosis due to shear stress, and the potential role for DAPK in endothelial mechano-transduction. Each stimulant induced an approximately two-fold increase in endothelial apoptosis kept under static conditions compared to control BAECs. On the other hand, the addition of shear decreased overall apoptosis compared to those static cells under the same stimuli conditions (Figs. 4.4).

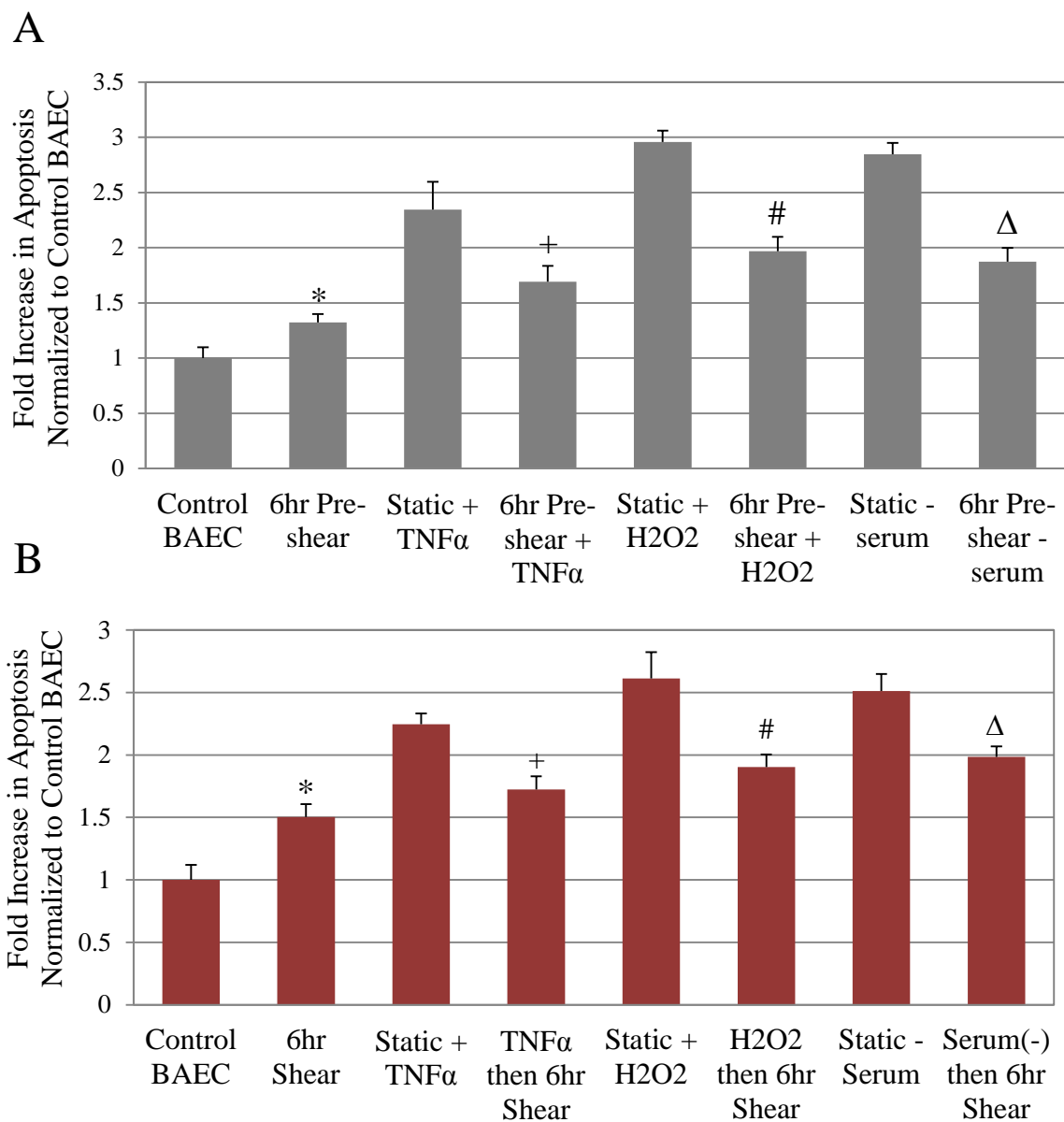


**Figure 4.4. Quantifying TUNEL positive apoptosis using flow cytometry.** A: Analysis of TUNEL in pre-sheared cells versus cells treated with stimulus (TNF $\alpha$ , H<sub>2</sub>O<sub>2</sub>, or serum depletion). B: Analysis of TUNEL results in cells sheared post treatment with stimulus (TNF $\alpha$ , H<sub>2</sub>O<sub>2</sub>, or serum depletion), for the post-treatment and sheared experimental groups. For all apoptosis data: \*  $P < 0.05$  compared to Control BAEC, +  $P < 0.05$  compared to Static + TNF $\alpha$ , #  $P < 0.05$  compared to Static + H<sub>2</sub>O<sub>2</sub>,  $\Delta$   $P < 0.05$  compared to Static - Serum.

#### 4.2.4 Preconditioning cells before apoptosis induction reduced overall apoptosis and caspase activity

Preshearing cells in media containing the same stimuli for 6h significantly decreased apoptosis at the end of 24-hr induction period, observed using TUNEL staining with flow cytometry (Fig. 4.4A). Preshearing proved to suppress overall apoptosis induced by  $\text{TNF}\alpha$ ,  $\text{H}_2\text{O}_2$ , and serum depletion. To confirm the TUNEL results, we repeated the preshearing experiments shown in Fig. 4.4A and looked at overall caspase activity in each sample (Fig. 4.5A). Caspase activity is upstream from the final steps of apoptosis initiation and confirms the subsequent results shown in the TUNEL experiments. The data suggest preshearing cells similarly decreased caspase activity when compared to each of the stimulant alone treatments, corresponding to our TUNEL results ( $P < 0.01$ ).

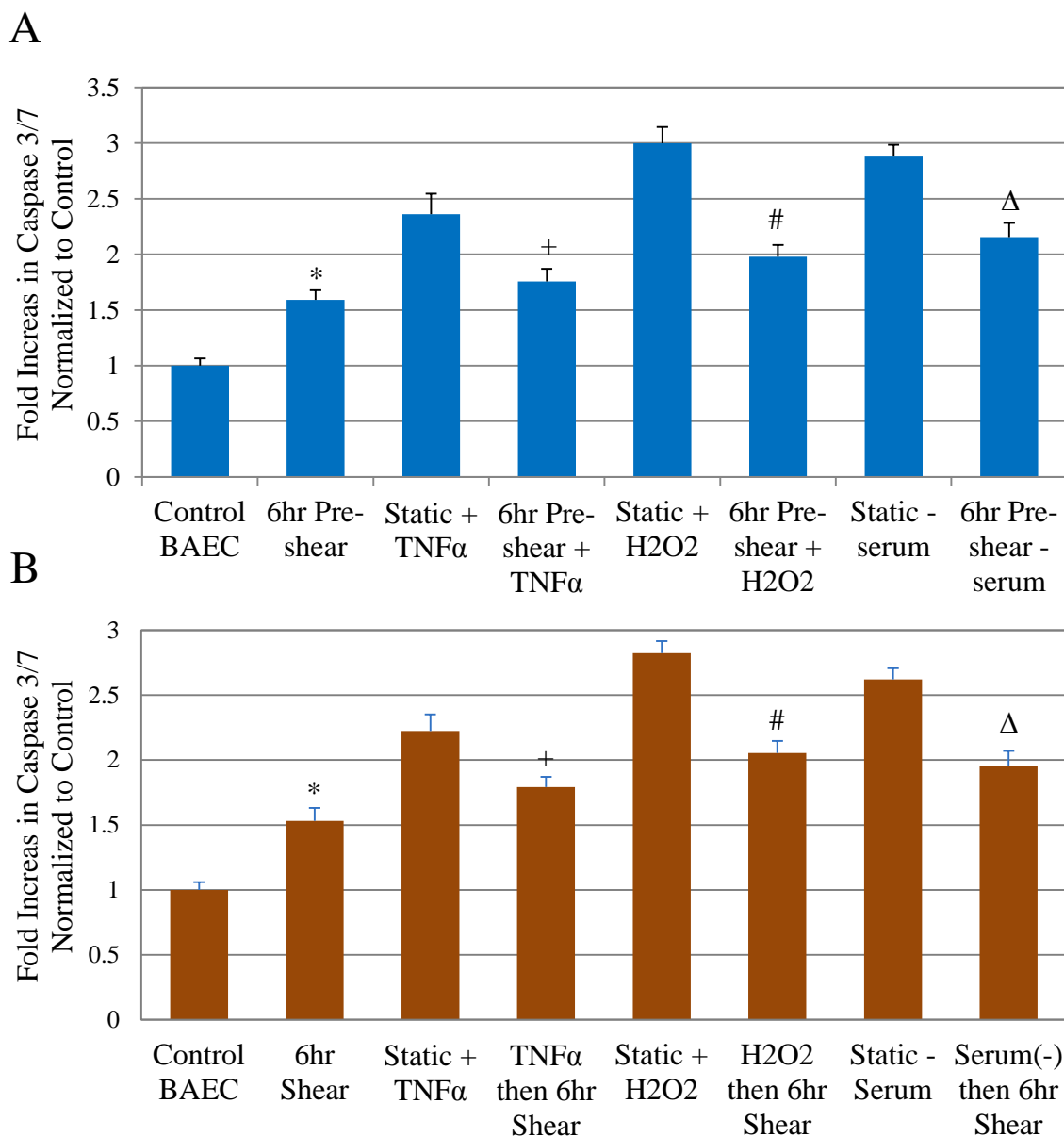


**Figure 4.5. Quantifying caspase activity in stimulated BAECs.** A: Analysis of Caspase-3 and -7 activity in pre-sheared cells versus cells treated with stimulus alone (TNF $\alpha$ , H<sub>2</sub>O<sub>2</sub>, or serum depletion). B: Analysis of Caspase-3 and -7 activity in cells sheared post treatment with stimulus versus cells treated with stimulus alone (TNF $\alpha$ , H<sub>2</sub>O<sub>2</sub>, or serum depletion). For all caspase data: \*  $P < 0.01$  compared to Control BAEC, +  $P < 0.01$  compared to Static + TNF $\alpha$ , #  $P < 0.01$  compared to Static + H<sub>2</sub>O<sub>2</sub>,  $\Delta P < 0.01$  compared to Static - Serum.

#### 4.2.5 Subsequent shearing after apoptosis induction also showed a significant decrease in apoptosis

There was a similar trend seen when cells were stimulated for 18h then subsequently sheared with each respective stimuli for 6h and observed with TUNEL staining (Fig. 4.4B). As with the preshearing samples, the post-sheared vs. static samples were collected and analyzed. The overall amount of cell apoptosis was quantified using TUNEL staining and the particular percent of apoptosis in each sample (Fig. 4.4). Shearing after incubation with  $\text{TNF}\alpha$ ,  $\text{H}_2\text{O}_2$ , and serum depletion was shown to significantly suppress apoptosis. We looked at corresponding caspase 3/7 activity in each representative sample to confirm the previous TUNEL results (Fig. 4.5B). Post-shearing cells after apoptosis induction mitigated the overall increase in caspase activity when compared to the static cells exposed to apoptosis inducers ( $P < 0.01$ ). Although, shearing cells alone for 6h, without prior stimulant induction, also induced a considerable increase in apoptosis and caspase production compared to control cells (no shearing or stimulants) (Figs. 4.4, 4.5). This is consistent with our previous finding that shear stress induced an increase in overall DAPK and decrease of phospho-DAPK, which promotes DAPK activity and subsequent apoptosis.



### 4.3 Discussion

Laminar shear stress suppresses endothelial apoptosis in the presence of various types of inducers such as cytokines (TNF $\alpha$ ), ceramide, and other stimulants (113; 122; 123). The role of DAPK in endothelial cells is unclear and to date has yet to be fully elucidated. Due to key involvement in both apoptosis and cytoskeletal remodeling, and its presence in the actin network, DAPK could play a role in endothelial mechanotransduction regulated by shear stress. Our previous study showed for the first time that shear stress affects DAPK expression and phosphorylation, as well as apoptosis following TNF $\alpha$  treatment (118; 124), suggests that shear stress uses DAPK as a mechanism of exerting its protective effect against endothelial apoptosis. Since our preliminary data showed increased DAPK and apoptosis level after 6 hr shearing alone, we decided to incorporate 6-hr shearing either before or subsequent to apoptotic stimulus, to fully evaluate its effect on DAPK and apoptosis. In combination with 6-hr exposure to shear stress (12 dynes/cm<sup>2</sup>), we used TNF $\alpha$  (25 ng/ml), H<sub>2</sub>O<sub>2</sub> (0.5 mM), and serum depletion (0.5% FBS) to induce apoptosis in an 18-hr treatment. We will apply the same 24 hour time frame to all groups to capture apoptotic and DAPK results (Figure 4.1A).

In this study, we found similar modulation of DAPK and apoptosis by shear stress with other pro-apoptotic signals such as oxidative stress and serum depletion. Onset of shearing alone increased DAPK and apoptosis, but shear stress in fact regulates DAPK expression and functions to attenuate apoptosis. We found that pre-treating cells with shear stress significantly decreased DAPK expression and downstream caspase 3/7 activation in the presence of apoptotic activators. Likewise, shearing cells after apoptosis

induction decreased DAPK activity and mitigate the apoptotic effect of each apoptosis trigger. Changes in DAPK and caspase 3/7 are directly correlated to changes in apoptosis. Thus, our data suggest that exposure to shear stress mitigates the apoptotic effect of TNF $\alpha$ , H<sub>2</sub>O<sub>2</sub> treated, and serum depletion through endothelial DAPK expression and caspase activity compared to the static cases. Comparing the effect of different apoptotic triggers, oxidative stress via addition of H<sub>2</sub>O<sub>2</sub> seemed to induce the greatest increase in DAPK expression, caspase activity, and apoptosis. Regardless of apoptosis trigger, shear stress had a similar attenuating effect on apoptosis either before or after induction. Interestingly, shear stress applied to cells prior to induction with apoptosis agents resulted in a higher suppression of apoptosis and DAPK and caspase activity, compared to applying shear stress post induction. For example, pre-shearing cells before stimulus treatment decreased apoptosis by: 28% for TNF $\alpha$ , 33.51% for H<sub>2</sub>O<sub>2</sub>, or 34.24% for serum depletion compared to static cells; while on the other hand, addition of shear stress after apoptosis stimulus decreased apoptosis by 23.56% for TNF $\alpha$ , 27.18% for H<sub>2</sub>O<sub>2</sub>, or 21% for serum depletion (Figure 4.4). These data suggest that shearing cells before addition of apoptotic trigger was more effective in suppressing apoptosis than after.

We also gained more insight into the long term effect of shear stress, independent of any apoptosis factors. Our “6hr Pre-shear” samples were maintained for 18 hrs in static condition after shearing, before samples were collected for analysis. For “6hr Post-shear”, samples were maintained under normal static condition, sheared for 6hrs, then collected for analysis. To evaluate the effect of shearing alone, we compared only the first set of two bars in each of Figure 4.2 to 4.5. The “6hr Post-shear” showed significantly increased DAPK expression and activity, as well as apoptosis, compared to the “6hr Pre-

shear”, probably because cells are collected right after shear stress. For pre-shear vs post-shear cells, there was a 39% vs. 59.3% increase in DAPK expression and 32.2% vs. 50.3% increase in apoptosis; plus a 37% vs. 52% drop in phosphor-DAPK fraction, indicating increased DAPK activity in post-shear. Only caspase 3/7 results were similar between pre- and post-shear cells 59% vs. 53.1% increase.

Thus, data on the effect of pre- or post-shear alone, without any apoptotic stimulus, suggest a direct link between shear regulated DAPK expression and activity to apoptosis. Because cells are collected right after shearing in “6hr Post-shear” cells, DAPK showed higher expression and activity, and there’s a corresponding higher level of apoptosis. The exception is caspase 3/7 activity, which is not directly linked to DAPK expression, but is downstream of DAPK expression. In this case, either shearing cells before or after apoptosis induction yielded similar level of caspase activity, though both are significantly increased compared to static cells.

Likewise, this time-dependent shear stress activation of DAPK could also explain its role in different apoptosis pathways. In examining the rest of the data in Figures 4.2-4.5, the general trend shows shear applied before the addition of apoptotic triggers, rather than after, was more effective in suppressing apoptosis. This could be explained by the opposite time-dependent effect on DAPK, when increasing DAPK expression and activity were observed in “6hr Post-shear” relative to “6hr Pre-shear.” It is possible that shear stress on cells after 18 hr apoptosis treatment had a higher, more immediate effect of increasing DAPK expression, which led to higher level of apoptosis. Therefore shear stress in the post-shear cases did not seem as effective in suppressing apoptosis, in part due to the direct increase in DAPK.

The same trend was observed in the order-dependent difference in shear stress suppression of caspase 3/7 activity: shear stress applied before treatment with apoptotic stimulus was more effective in suppressing caspase activity. Again this could also be attributed in part to the DAPK increase in cells sheared after apoptotic stimulus, and DAPK is an upstream activator of caspase activity in the apoptotic pathways. Moreover, the effects of a 6 hr exposure to shear stress alone lingered even after 18 hr incubation, and were still statistically significant compared to control cells, shown in the “6hr Pre-shear” case for Figures 4.2 to 4.5. Therefore, cells had a more immediate response to shear stress in activating DAPK and apoptosis, which was also sustained after another 18 hours, compared to static cells. Endothelial responses to shear stress can be immediate, i.e. release of nitric oxide, NO (48), short-term, such as up-regulation of tissue plasminogen activator (tPA) gene (49); and also sustained exposure to shear stress leads to endothelial cell re-alignment in the direction of flow and changes in structural organization, mechanical properties, and nuclear activities (30; 125; 126). Endothelial mechanotransduction involves a variety of signaling molecules such as heat shock proteins, transcription factors, MAP and PI3 kinases (89; 127; 128). MAPKs such as ERK, JNK and p38 have been identified to both play a role in endothelial mechanotransduction and interact with DAPK in its apoptotic activities. All three are activated by shear stress at the onset, along with increase in intracellular calcium (129). ERK is upstream of DAPK activation via phosphorylation at Ser735 (90), phospho-p38 is an apoptotic binding partner of DAPK (114); and JNK is downstream of DAPK via PKD regulation (91). As we have discussed before (3), DAPK is involved in multiple apoptotic pathways including cytokine (TNF $\alpha$ ), oxidative stress (H<sub>2</sub>O<sub>2</sub>), or serum depletion. Our

data support the theory that shear stress may target DAPK as a converging point to exert its effects of suppressing endothelial apoptosis. Regulation of DAPK expression and activity by shear stress closely mirror the effect on apoptosis.

With extended shearing (hours), endothelial cells undergo morphological changes: stress fiber formation, focal adhesion reorganization, and re-alignment in the direction of flow (115). DAPK is localized to the actin network, and promotes actomyosin contractility and stabilizes stress fibers in serum starved fibroblasts, by phosphorylation of myosin regulatory light chain (MLC) (39; 95). In endothelial cells, DAPK phosphorylates tropomyosin-1 (TM-1) at Ser283 in response to ERK activation under oxidative stress (96). DAPK could have other non-apoptotic functions in endothelial cells, for example in affecting cell morphology. A novel role for DAPK in the atherosclerosis signaling pathway may provide a realistic therapeutic target for future mechanotransduction studies. We continue to investigate the molecular responses of mechanotransduction and the role of DAPK in endothelial apoptosis.

In summary, we have shown that exposure to shear stress (12 dynes/cm<sup>2</sup> for 6hrs) suppressed endothelial apoptosis triggered by cytokine (TNF $\alpha$ ), oxidative stress (H<sub>2</sub>O<sub>2</sub>), and serum depletion, either before or after a long term (18hr) induction. This is correlated with parallel decrease of DAPK expression and caspase activity compared to non-sheared cells. Shear stress applied prior to apoptosis induction resulted in a higher suppression of apoptosis, DAPK expression, and caspase activity, opposed to applying shear stress post induction. This is correlated with a higher expression and activation of DAPK in cells sheared at the end of 24-hr experiment. Also, shear stress alone induced higher apoptosis and DAPK expression, and the effect is sustained even after 18 hrs incubation in static

condition, compared to non-sheared cells. Overall, we show that laminar shear stress inhibits various apoptosis pathways by modulating DAPK expression and activation, as well as caspase activity, in a time-dependent manner. The temporal shear stress activation of DAPK and its role in different apoptosis pathways may help identify key mechanisms of the endothelial mechanotransduction pathway. Understanding the role of DAPK and its interplay between conditioning with shear stress and apoptosis induction is important in understanding how cells respond to their chemical and mechanical environments.

## 5. EFFECT OF SHEAR STRESS AND SUBSTRATE ON ENDOTHELIAL DAPK EXPRESSION, CASPASE ACTIVITY, AND APOPTOSIS

### 5.1 Introduction

Precise mechanisms of DAPK function in endothelial cells are largely unknown. Due to its location on the cytoskeleton, DAPK expression and activity are potentially susceptible to mechanical and structural stresses. We have begun to analyze the role of DAPK in apoptosis and the subsequent cytoskeleton changes (118). We found that while cytokines such as TNF $\alpha$  induces apoptosis, adding shear stress significantly suppressed TNF $\alpha$  induced apoptosis; while shear stress alone also increased apoptosis. We also found that apoptosis was correlated with caspase activity and DAPK expression, suggesting that shear stress affected endothelial apoptosis by controlling DAPK expression. Like most *in vitro* shear stress studies, we used the conventional parallel plate flow chamber in our studies where endothelial cells were cultured on glass slides. Glass, which has elastic modulus on the order of 50 GPa, is much stiffer than what cells encounter *in vivo*, such as extracellular matrix (ECM), basement membrane, or other cells. In contrast, mechanotransduction studies that include cyclic stretch of endothelial and other cells have utilized fibronectin-coated silicone membrane as substrate, which has an average elasticity of 2 MPa (130-132).

We redesigned and constructed a flow chamber to accommodate cells plated on either glass or silicone membrane of similar size, in order to analyze the effect of different substrates on endothelial responses toward fluid shear stress. Our goal is to integrate mechanical cues such as shear stress and cyclic stretch, with mechanical properties of substrate, to fully understand the role of DAPK in apoptosis as part of endothelial mechanotransduction.

Here, we continue to investigate the effects of substrate on shear stress regulation of DAPK and apoptosis in bovine aortic endothelial cells (BAEC). We hypothesized that cells on the softer, flexible membrane substrate would be more protected from apoptosis under shear stress. We validated cell attachment and morphology on fibronectin-coated substrates, and found that shear stress induces apoptosis, through caspase and DAPK activation on both substrates. We also saw suppression of apoptosis subsequent to TNF $\alpha$  activation on membrane substrate, as we did on glass (124). Our data suggest that at least in terms of DAPK expression and apoptosis, endothelial cells respond in a similar way toward shear stress, independent of glass or silicone membrane substrates.

**Research Objective 4: Will the cell substrate impact overall DAPK activity and endothelial apoptosis in response to shear?**



## 5.2 Results

### 5.2.1 Shear stress significantly reduced apoptosis following TNF $\alpha$ activation on silicone substrate

We modified the current flow chamber to allow for use with either glass slide or a silicone membrane of similar size as substrate for cells (Figure 5.1A), and we have validated the new flow chamber with BAEC on glass slide or membrane, coated with fibronectin.

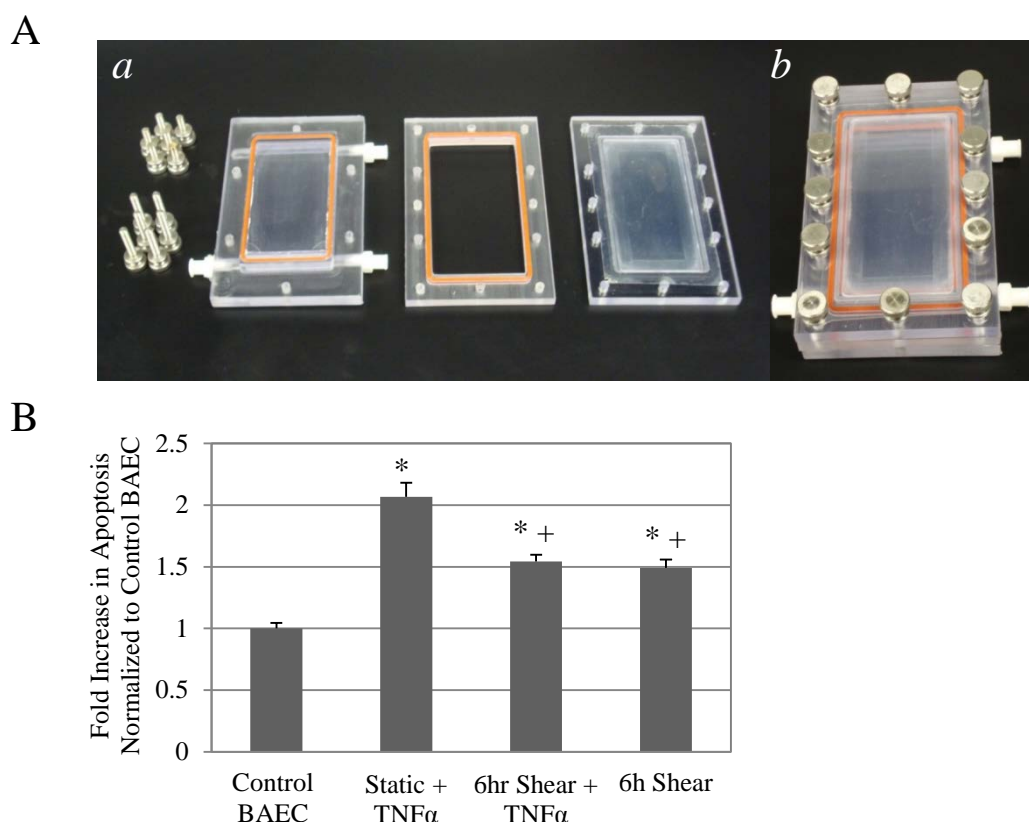


**Figure 5.1. Shear stress suppressed apoptosis subsequent to TNF $\alpha$  induction on cells plated on silicone membrane.** (A) Parallel plate design was redesigned to accommodate membrane substrate. (a) The top, middle, and bottom portion of parallel plate flow chamber, and (b) flow chamber assembled together. (B) We examined cell apoptosis using TUNEL staining. Results were quantified using FACS flow cytometry. Control groups are static (Control BAEC) and 12 dynes/cm<sup>2</sup> for 6 hours alone (6 hr Shear). Other cells were either incubated with TNF $\alpha$  (25 ng/ml) for a 24-hour period (Static + TNF $\alpha$ ) or treated with TNF $\alpha$  for 18 hours followed by 12 dynes/cm<sup>2</sup> for 6 hours (6 hr Shear + TNF $\alpha$ ).

We now confirm the same results for cells sheared on silicone membrane substrate. Cells were either incubated with TNF $\alpha$  (25 ng/ml) for a 24-hour period to fully induce apoptosis (Static + TNF $\alpha$ ) or treated with TNF $\alpha$  for 18 hours followed by shearing at 12 dynes/cm<sup>2</sup> in media containing TNF $\alpha$  for another 6 hours (6hr Shear + TNF $\alpha$ ). Control groups included static (Control BAEC) and cells sheared for 6 hours alone (6hr Shear). After TNF $\alpha$  and shear stimulation in flow chambers, apoptosis in endothelial cells was assessed by TUNEL staining with fluorescein label (Figure 5.1B). TNF $\alpha$  alone induced a significant two-fold increase in apoptotic cells compared to control BAEC on membrane (\* $P < 0.01$ ). Applying shear stress (6 hrs) to cells already activated by TNF $\alpha$  (18 hrs) significantly decreased the fraction of apoptotic cells compared to non-sheared, TNF $\alpha$  treated cells (+ $P < 0.05$ , compared to Static + TNF $\alpha$ ). We also saw a significant increase of apoptosis in cells sheared for 6 hours compared to control BAEC (\* $P < 0.01$ ); however, the result was still significantly less than TNF $\alpha$  treated static cells (+ $P < 0.05$ ). In fact, sheared BAEC, either with or without TNF $\alpha$  pretreatment, demonstrated similar levels of apoptosis that is significantly different from both static control and TNF $\alpha$  induction alone. These data correlates well with what we observed for cells on glass substrate, and suggests that while shear stress alone induces apoptosis, it also represses apoptosis subsequent to TNF $\alpha$  induction, regardless of substrate.

### 5.2.2 Shear stress reduced DAPK expression following TNF $\alpha$ treatment on membrane substrates

As previously discussed, shear stress was shown to antagonize TNF $\alpha$  induced apoptosis on silicone membrane substrates. To further examine this apoptosis pathway, we wanted to investigate the subsequent shear stress effects on a key cell death mediator, DAPK, for cells plated on membrane substrates. For each membrane experiment, cells were either incubated with TNF $\alpha$  (25 ng/ml) for a 24-hour period to induce apoptosis (Static + TNF $\alpha$ ) or treated with TNF $\alpha$  for 18 hours followed by shearing cells in media containing TNF $\alpha$  for another 6 hours (6hr Shear + TNF $\alpha$ ). Control groups included static (Control BAEC) and cells sheared for 6 hours alone (6hr Shear). In Figure 4.4A, Western blot analysis showed a significant increase in DAPK expression in Static + TNF $\alpha$ , 6hr Shear + TNF $\alpha$ , and 6hr Shear alone compared to Control BAEC (\* $P < 0.01$ ). Although, the TNF $\alpha$ -treated and then sheared cells showed a significant decrease in DAPK expression compared to cells treated with TNF $\alpha$  alone (+ $P < 0.05$ ). These results confirm that both TNF $\alpha$  and shear stress increase overall DAPK expression. Shear stress was shown to decrease DAPK expression compared to cells treated with TNF $\alpha$  alone.

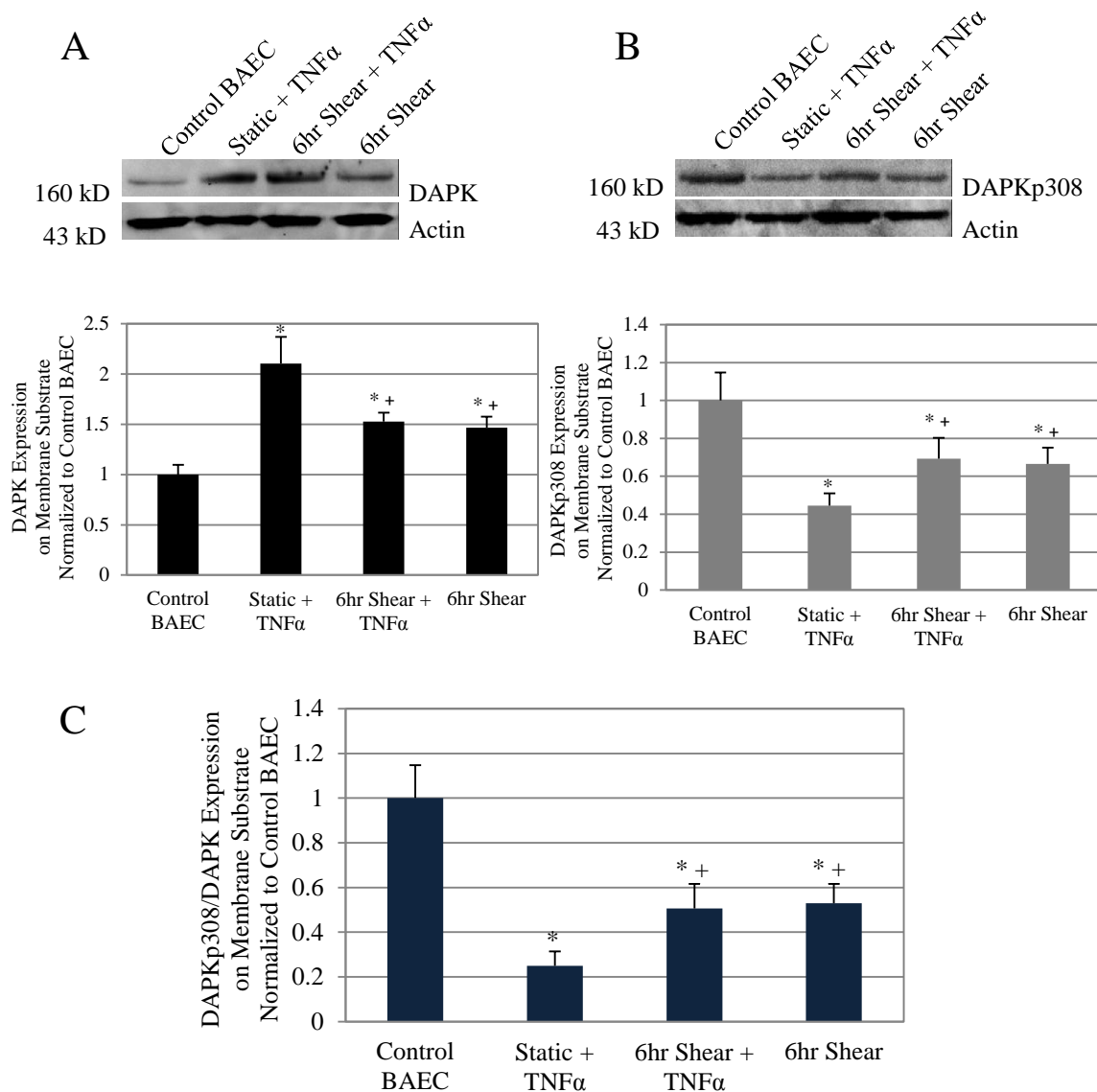


**Figure 5.2. Western analysis of DAPK expression for BAECs on membranes.** Total DAPK expression (A top) as well as phosphorylated serine 308 DAPK (B top). Relative band intensity was quantified and presented as fold increase over control BAEC for overall DAPK (A bottom) and phospho-serine 308 DAPK (B bottom). (C). Phosphorylated DAPK as a fraction of total DAPK expression was calculated for each sample group based Western blots. All data represent average  $\pm$  standard error ( $n = 3$ ). \*  $P < 0.01$  compared to control cells, and +  $P < 0.05$  compared to static TNF $\alpha$  treated cells.

### 5.2.3 Shear stress decreased phospho-DAPK in TNF $\alpha$ treated cells on membrane substrates

DAPK is dephosphorylated when it becomes activated. In Figure 5.2B, protein analysis showed significant decrease in phospho-DAPK for Static + TNF $\alpha$ , 6hr Shear + TNF $\alpha$ , and 6hr Shear alone compared to Control BAEC ( $*P < 0.01$ ). On the other hand, TNF $\alpha$  treated and then sheared cells displayed a significant increase in phospho-DAPK when compared to cells treated with TNF $\alpha$  alone ( $+P < 0.05$ ). Due to changes in both overall and phospho-DAPK, we evaluated the fraction of phospho-DAPK with respect to overall DAPK expression showing a signal ratio representative of DAPK activation for each sample set (Figure 5.2C). Compared to Control BAEC, we see a significant decrease in the fraction of phospho-DAPK to ~26% for TNF $\alpha$  alone treated cells, where only a 50% and 52% decrease in the 6hr Shear + TNF $\alpha$  and 6hr Shear alone cases, respectively ( $*P < 0.01$ ). Shear stress with TNF $\alpha$  treated cells displayed a smaller percent activation of DAPK as compared to TNF $\alpha$  alone ( $+P < 0.05$ ). This data confirms that shear stress antagonizes TNF $\alpha$  induced apoptosis on membrane substrates, possibly by modulating DAPK expression and activation.

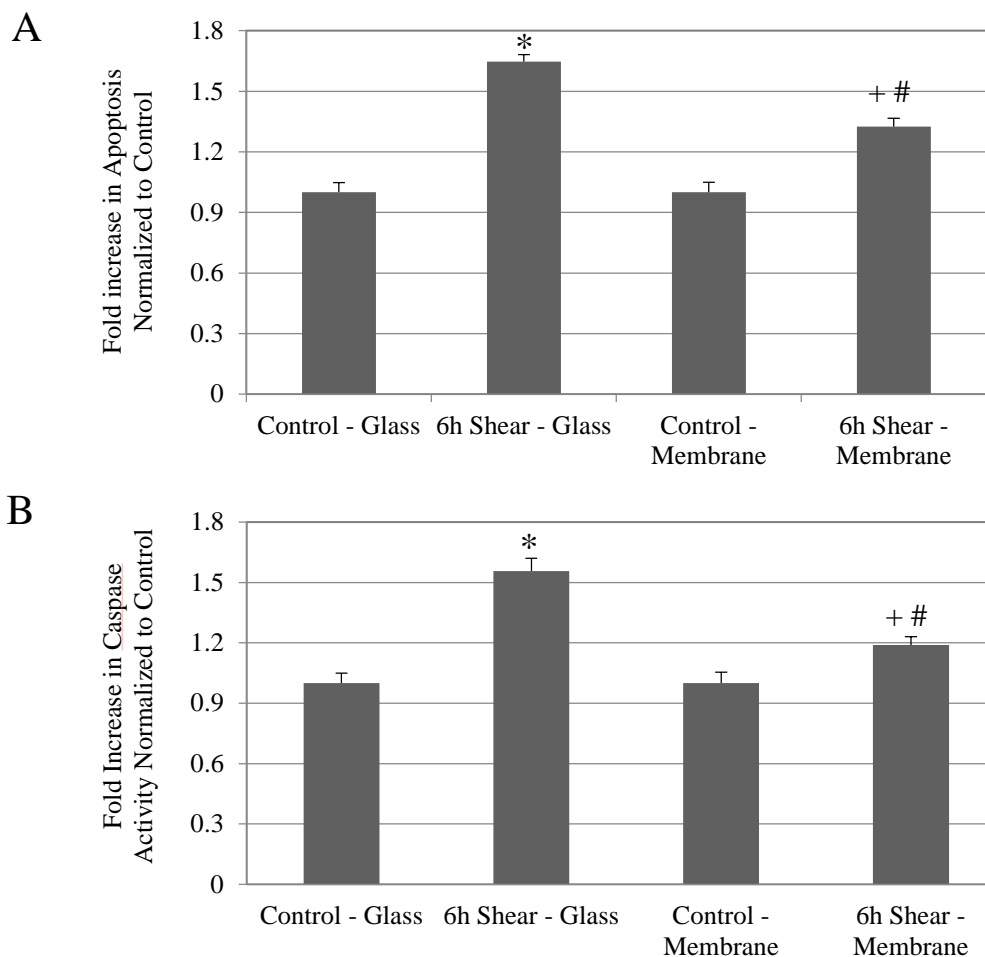


**Figure 5.3. Shear stress on membrane induced apoptosis similar to cells on glass.** (A) TUNEL positive cells are presented as fold increase over static control on either substrate. (B) Caspase-3 and -7 results are presented as fold increase over static control BAEC. Data represent average  $\pm$  standard error for  $n \geq 5$ . \* $P < 0.01$  compared to control-glass cells, + $P < 0.05$  compared to control-membrane cells, and # $P < 0.05$  compared to 6hr shear-glass.

#### 5.2.4 Shear stress alone induced apoptosis in cells on both glass and membrane substrates

To this point, we have investigated the effect of shear stress on TNF $\alpha$  induced apoptosis for silicone membrane substrates. To further investigate the effect of shear stress alone for cells on glass or membrane substrate, we compared cellular apoptosis

using TUNEL staining. We have previously shown that shear stress alone would increase apoptosis on glass slide (118). Here cells plated on either glass or silicone membrane substrates were sheared at 12 dynes/cm<sup>2</sup> for 6 hours, and after each experiment, cells were stained and quantified using flow cytometry. As shown in Figure 5.3A, there was a 1.64 fold increase in apoptosis for cells sheared on the glass substrate, when compared to control ( $*P < 0.01$ ). For the membrane substrate, there was a 1.32 fold increase in apoptosis compared to control ( $+P < 0.01$ ). Furthermore, we also observed a significant decrease in apoptosis for cells sheared on membrane compared to glass substrate ( $\#P < 0.01$ ). There was no significant difference in apoptosis, however, between static control cells on either substrate. These data suggest that while shear stress induced apoptosis in cells on either substrate, cells on the softer membrane substrate demonstrate reduced apoptosis compared to glass.

#### 5.2.5 Shear-induced apoptosis correlated with increased caspase-3 and 7 activation

To analyze shear-induced endothelial apoptosis further, we examined caspase activity. Caspases are downstream of DAPK in the apoptotic pathway, and we had previously demonstrated increase of caspase 3/7 activity by shear stress alone in cells on glass (118). Results from at least five different experiments were quantified for each case: control and sheared (12 dynes/cm<sup>2</sup>, 6 hours) on glass or on membrane. Statistical analysis showed a significant increase of caspase 3/7 activity in sheared cells for both substrates when compared to control (Figure 5.3B). For cells on glass, we saw a 1.56 fold increase in caspase activity compared to control cells ( $*P < 0.01$ ). Similarly for cells on the membrane, we saw a 1.2 fold increase compared to control ( $+P < 0.05$ ). This data suggest

that shear induced apoptosis on glass and membrane was due to increased caspase 3/7 activities. Interestingly, we also observed a significant decrease in caspase 3/7 activities in cells sheared on membrane compared to glass ( $\#P < 0.05$ ); although, there was no statistical difference between control cells on the glass and membrane subsets. Our caspase-3/7 results showed a similar trend to what was observed in our quantitative analysis of the TUNEL results. This data suggests that shearing cells on silicone substrate, instead of glass, resulted in decreased caspase activities, and that shear-induced apoptosis in endothelial cells on both glass and membrane substrate correlated with increased caspase 3/7 activities.

#### 5.2.6 Shear stress increased overall DAPK expression cells on both glass and membrane substrates

Since the increase in apoptosis after 6 hours of shear stress alone correlated with increased caspase activity, we further anticipate DAPK to play a role in shear-induced apoptosis. Western blot analysis revealed that sheared cells (12 dynes/cm<sup>2</sup>, 6 hr) on glass and membrane substrate demonstrated a significant increase in DAPK expression compared to static control cells (Figure 5.4A Top). Relative intensity of DAPK expression was quantified and normalized to the loading control, actin. Protein samples from at least 4 separate experiments were analyzed, and we saw a 1.87 fold increase on glass and a 1.46 fold increase on membrane, in sheared cells compared to their respective control cells. The increase in DAPK in sheared cells on either substrate was significant:  $*P < 0.01$  for cells on glass cells and  $\#P < 0.05$  for cells on membrane (Figure 5.4A Bottom). This result reflects what was previously reported for cells on glass substrate



(118). By comparing cells on membrane versus glass substrate, we found that there was no significant difference in DAPK expression in either the control or sheared cases. Our data suggests that, for cells on glass and membrane substrate, shear stress effectively increased DAPK expression after 6 hours.

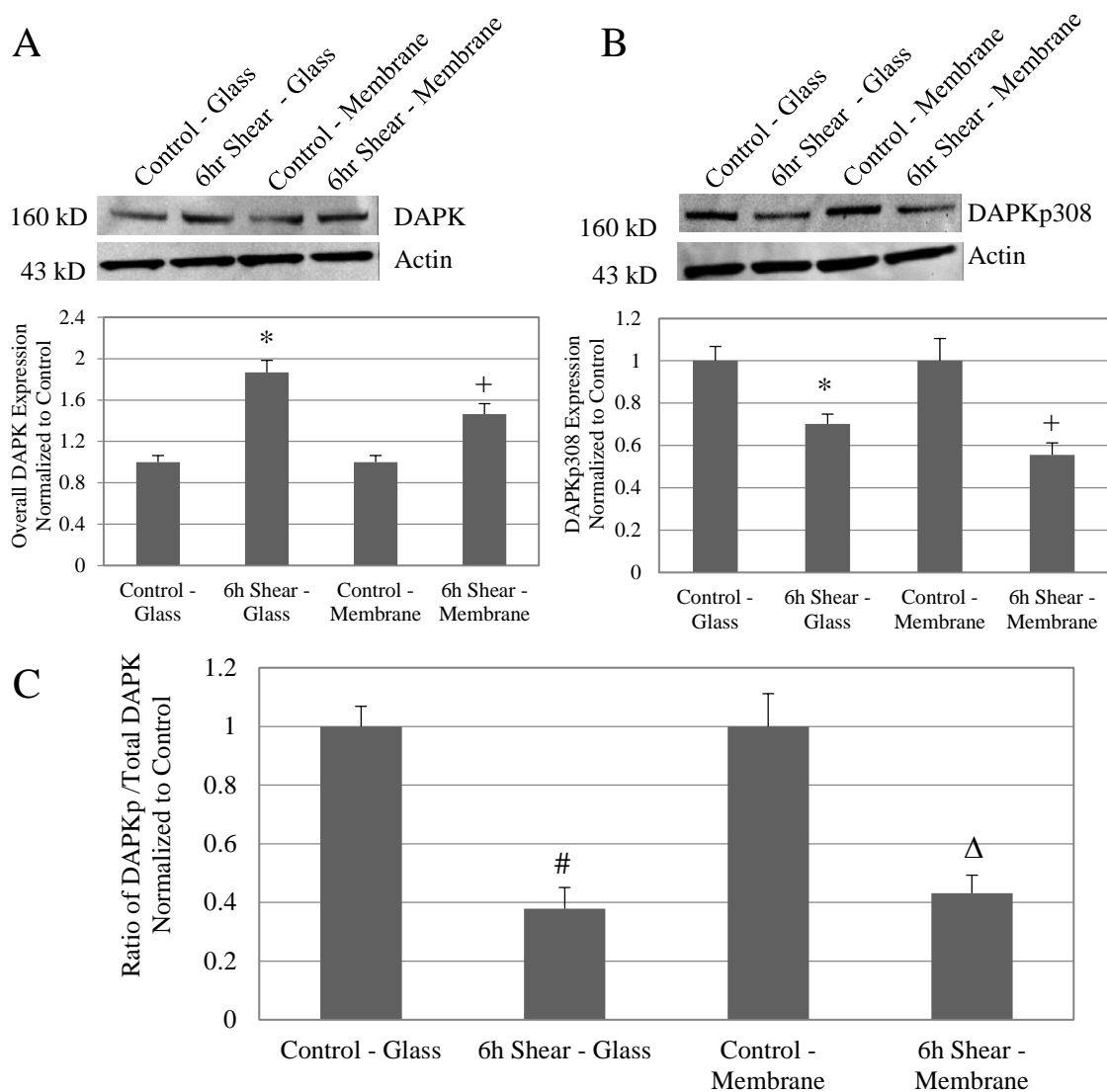


**Figure 5.4. Overall DAPK activity in BAECs for both glass and membrane substrates.** (A) Western blot of overall DAPK expression in control and sheared cells (6 hours). DAPK expression increased with extended shear (Top). Quantitative analysis of band intensities was carried out on at least 4 separate sample sets. For both glass and membrane, DAPK expression increased with extended shear (Bottom). Data represent average  $\pm$  standard error ( $n = 4$ ) with \*  $P < 0.01$  compared to control-glass cells and +  $P < 0.05$  compared to control-membrane cells. (B) Western blot of phosphorylated DAPK at serine 308, for control and sheared cells (6 hours). (C) Phosphorylated DAPK as a fraction of total DAPK expression was calculated for each sample group based Western blot analysis. Data represent average  $\pm$  standard error for 4 independent experiments ( $n = 4$ ). #  $P < 0.01$  compared to control-glass and  $\Delta P < 0.01$  compared to control-membrane.

### 5.2.7 Shear stress decreased DAPK phosphorylation at serine 308 on glass and membrane substrates

As an inhibitory checkpoint, DAPK is auto-phosphorylated in its static state. We analyzed phosphorylated DAPK expression (DAPKp308) in static and sheared cells on both glass and membrane substrates. Western blot analysis consistently showed a decrease in phosphorylated serine 308 DAPK in sheared cells (12 dynes/cm<sup>2</sup>, 6 hr) on both substrates when compared to their respective controls (Figure 5.4B Top). After quantifying repeated western blots, we found that sheared cells showed an average 30% decrease in DAPKp308 on glass (\* $P < 0.01$ ) and 45% decrease on membrane (# $P < 0.05$ ), when normalized to static control (Figure 5.4B Bottom). Again, there was no significant difference between substrates in either static or sheared case.

Due to changes in both total and phosphorylated DAPK, we evaluated DAPKp308 as a fraction of total DAPK, which is an indication of overall DAPK activation, not just expression (Figure 5.4C). For both overall and phosphorylated DAPK western blots, protein loading was normalized based on the concentration of protein in each representative sample, determined using a Bradford protein assay. Also, western blot loading and transfer procedures were identical, and each antibody (DAPK55 and DAPKp308) was incubated at a 1:1000 ratio with 5% milk blotto for each blot. The protein signal ratio of both DAPK55 and DAPKp308 is proportional to overall DAPK expression and amount of phosphorylated DAPK, respectively. The signal ratio of phosphorylated DAPK with respect to the total DAPK signal ratio demonstrates the overall DAPK activation in each respective sample subset. We saw that the fraction of phospho-DAPK decreased to 38% on glass and to 43% on membrane in sheared cells, as

compared to their respective control cells ( $P < 0.01$ ). These results are comparable to what was observed previously for cells on glass (118). However, we saw no significant changes in DAPK activation between cells on glass and membrane in both control and sheared conditions. These data suggests that shear stress induced DAPK activation on membrane surfaces, similar to DAPK activation on glass surfaces. The expression and activation of DAPK, via p308 dephosphorylation, therefore are increased by fluid shear stress, regardless of substrate.

### 5.3 Discussion

Understanding apoptosis, a fundamental cellular process, fully would have major impact on a multitude of cell and tissue types, as well as disease and therapeutic models. In atherosclerosis, for example, increased apoptosis contributes to prolonged inflammatory response, plaque instability, rupture, and thrombus formations (32). Atherosclerosis develops preferentially at regions of disturbed flow and low shear stress, which are also sites of increased cell turnover rate (116), and shear stress has been shown to suppress cytokine induced apoptosis in endothelial cells (117). DAPK is an important protein kinase in modulating apoptotic pathways (109). Its potential role in endothelial apoptosis and mechanotransduction has been largely unexplored. Identifying the role of DAPK in endothelial cell function would be important to understanding apoptosis under both homeostatic and diseased conditions in the vasculature.

We have shown previously that DAPK is a mechano-sensitive regulator of apoptosis, in cells cultured on glass and sheared in parallel plate flow chambers (118).

Both apoptosis and DAPK expression and activation are sensitive to fluid shear stress. Here we extend the study to cells cultured on a different substrate, silicone membrane, typically used for cyclic stretch studies. We again saw shear stress significantly attenuated TNF $\alpha$  activated apoptosis, and that shear stress alone also increased apoptosis (Figure 5.1B). This observation corresponds well to the results for cells on glass substrate. We continued to investigate further the effect of shear stress alone on cells plated on different substrates. We found that on either glass or membrane, shearing cells resulted in elevated apoptosis (Figure 5.3). Furthermore, shear-induced apoptosis on both substrates corresponded to an increase in caspase 3/7 activities, and increased DAPK expression and activation via dephosphorylation of serine 308 (Figure 5.4). These data suggest that that in terms of apoptosis and DAPK expression, endothelial cells respond to shear stress similarly on either glass or silicone membrane substrate, and that DAPK expression in endothelial cells is more influenced by shear stress, rather than the substrate cells are on.

Overall, regardless of substrate, we found that shear stress alone induced apoptosis, through a mechanism that involves increased DAPK expression and activation, upstream of caspase 3 and 7 activities. These findings agree well with our previous study, and further confirm that expression and activation of DAPK are regulated in part by fluid shear stress alone on both glass and membrane substrates. While we saw that adding shear stress subsequent to TNF $\alpha$  induction suppressed apoptosis, the increase in apoptosis by shear alone suggests that there is a time-dependent effect of shear stress on TNF $\alpha$  induced apoptosis – which we are currently investigating.

When apoptosis or caspase results of Figure 5.3 were evaluated for statistical difference between substrates, instead of comparing static vs. shear, we did observe statistically significant differences between substrates. Both TUNEL and caspase-3 and 7 activities were significantly lower in cells sheared on membrane, compared to cells sheared on glass. There was no difference between the substrates under static condition. Furthermore, cells sheared on membrane substrate also demonstrated reduced DAPK expression and activation compared to cells sheared on glass, although the differences were not statistically significant (Figure 5.4). The reduced apoptosis and caspase activities in cells sheared on membrane suggest that while shear stress induced apoptosis overall, membrane substrate is more protective against apoptosis compared to glass substrate. The finding that shear-induced apoptosis was attenuated on membrane compared to glass suggests that there is at least some substrate-dependent differences in how endothelial cells respond to fluid shear stress.

Aside from its primary role in downstream activation in the death cascade, DAPK also regulates other cytoskeleton changes associated with apoptosis such as stress fibers and membrane blebbing (94). DAPK also phosphorylates myosin regulatory light chain (MLC) at Ser19 (39; 95), and promotes actomyosin contractility and stabilizes stress fibers in serum starved fibroblasts (39). Thus, under shear, DAPK might be utilized for non-apoptotic functions such stress fiber formation, focal adhesion reorganization, and eventual re-alignment of cytoskeleton in the direction of flow (115). Shear stress may induce structural changes in cells that are dependent on substrate. Other non-apoptotic functions of DAPK in endothelial cells would also be influenced by both shear stress and substrate.

In addition, mechanical properties of the substrate could also affect the substrate-dependent differences in apoptosis. Substrate stiffness is an important factor in behavior and functions of fibroblasts, smooth muscle cells, and neurons (133-135), and affects cell adhesion, shape, and cytoskeleton structure of endothelial cells (136). Thus, substrate stiffness could be an important factor in determining how cells respond to external forces, and should be considered in conjunction with other mechanical cues such as shear stress. In addition to fluid shear stress, endothelial cells *in vivo* are also subject to cyclic stretch and reside on much softer substrate than glass. While most *in vitro* substrate studies have focused on cell behaviors under static conditions, other mechanotransduction studies have used cells cultured on glass surfaces for shear stress, or flexible silicone membrane for cyclic stretch devices.

This study bridges the gap between shear stress studies on cells plated on glass, to substrates of a more physiologically relevant stiffness. Our investigation on the mechanotransduction role of DAPK in endothelial apoptosis will continue in two fronts. We will examine the effect of shear stress on cells on substrates of varying mechanical properties, on the order of kPa. We plan to generate polyacrylamide hydrogels of different stiffness according to published protocols (137), which can be anchored to a base and accommodated into our flow chamber. We will also continue to use silicone membrane as substrate in a cyclic stretch device to examine the effect of substrate strain on endothelial apoptosis.

In summary, we have shown that cells plated on either glass or silicone substrate showed increased apoptosis in response to fluid shear stress that also correlates with increased DAPK expression and activation, and caspase 3/7 activities (124). Cells are

actively sensing and responding to their environment, which includes not only external and internal forces, but also mechanical properties of their surroundings (138). This study provides the basis for continued research to further examine cellular apoptosis and DAPK activity in cells exposed to different substrate stiffness or to cyclic stretch. This study lays the groundwork for our goal to elucidate the simultaneous effect of multiple mechanical stresses (shear stress, cyclic stretch, and substrate stiffness) on endothelial functions such as apoptosis.



## 6. FLUID SHEAR INCREASES ENDOTHELIAL APOPTOSIS AND DAPK ACTIVITY IN LAMIN-DEFICIENT CELLS

### 6.1 Introduction

The cellular nuclear envelope is composed of two membranes, inner and outer, connected by nuclear pore complexes. The nuclear lamina structure is made of type V intermediate filaments, lamin, that lies underneath the nuclear envelope and provides nuclear support. Recent research has shown that lamins are not only located externally but also in the nucleoplasm. This lamin network links to the cytoskeletal network through nesprin and SUN-domain proteins and provide functional support for gene transcription, chromatin organization, and DNA replication (139). A family of nuclear proteins are localized in the nuclear lamina (Fig 6.1). Mutations in lamin or lamin-binding proteins result in a number of diseases in human known as laminopathies (140). These mutations potentially change the protein constituents of the inner membrane, nucleoplasm, and cytoplasm. They are thought to either compromise the structural integrity of the nucleus, where disrupted nuclear lamin demonstrate a deformed and fragile nucleus structure; or disrupt normal cellular regulation of gene transcription. On the other hand, a defective lamina and its associated proteins can lead to a disconnected network of signal transduction pathways in and out of the cell nucleus, and altered response to both external and internal cellular stresses.

The weakened cell nucleus and surrounding network make cells more susceptible to external stimuli that may initiate cell death processes. In healthy cells, mechanical stress initiates the survival response activating NF- $\kappa$ B pathway via signal transduction to the nucleus (67; 68). Also, long-term shear stress exposure leads to cell alignment with the flow and an increase in protective cell signaling initiated by mechanotransduction response (30). Figure 6.1B highlights lamin's role in nuclear signal transduction from outside influence but the role of lamin in the mechanotransduction pathway is not fully understood. Further cell studies need to investigate the impact of nuclear lamin loss on endothelial mechanotransduction response and the subsequent apoptosis due to environmental stresses.

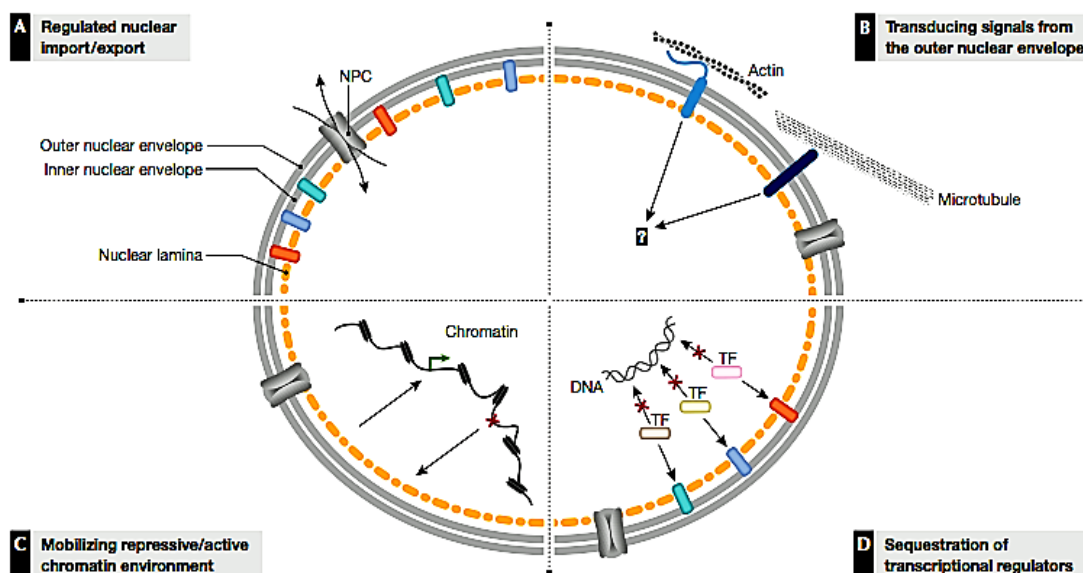


**Figure 6.1. The various roles of nuclear lamina in cells (2).**

The nuclear lamina is surrounded by an actin network directly connected to the nuclear envelope through nesprin proteins in LINC complex. A small amount of lamin is

solubilized before the acute apoptosis onset. Thereafter, the chromatin condensation is subsequently accompanied by lamin A and B degradation (141). Lamin proteolysis is a significant early step prior to nuclear degradation and eventual cell death. Caspase activation is a key upstream step in the apoptosis process. Caspase-3 and -6 activate each other and amplify downstream apoptosis, and caspase activation leads to proteolysis of nuclear protein and DNA degradation. Furthermore, caspase 6 cleaves lamin A subsequent to increased apoptosis post-seizure in rat neuronal cells (142).

Lamin A is cleaved to a signature apoptotic fragment length necessary to proceed with the multi-step cell death process (143). Similarly, DAPK is simultaneously cleaved by caspase-1 and -6 (144). DAPK mediates apoptosis through the p19<sup>ARF</sup>/p53 protein dependent pathway. Co-immunoprecipitation studies show that DAPK and p53 binding activity significantly increases after the onset of apoptotic seizure events (144).

Additionally, DAPK is co-localized in cytoskeletal network and plays a necessary role in apoptosis events. DAPK phosphorylates MLCs leading to a weakening of the actin network and membrane blebbing (95). Likewise, DAPK is a downstream effector in the Protein kinase C (PKC)/ERK pathway during cell apoptosis (145). Specifically, caspase-3 activates ROCK leading to an activation of the PKC/ERK pathway, where ERK phosphorylates DAPK at serine 735, shown both *in vitro* and *in vivo*. The increased DAPK ser735 phosphorylation *in vivo* correlated with greater phosphorylation of DAPK substrate, MLC, and increased apoptosis with the overexpressed DAPK (90). In TNF $\alpha$ -induced apoptosis, caspase-3 cleaves Rho kinase (ROCK) leading to myosin light chains (MLC) phosphorylation (146). ROCK, an effector of small GTPase Rho protein, is shown to contribute to MLC activation. The phosphorylation of MLCs is mediated by

MLC kinase (MLCK), a calcium/calmodulin dependent kinase and is regulated by MLC phosphatase (147). Furthermore, ROCK activation and MLC phosphorylation subsequently lead to lamin proteolysis and apoptosis (146). Figure 6.2 summarizes the apoptosis activation pathway based on our current understanding of caspase activation, DAPK phosphorylation, and lamin cleavage leading to nuclear membrane blebbing and apoptosis. Recent research highlights important DAPK and lamin involvement in cell apoptosis (40; 93; 145; 148). To date, our studies have identified a substantial role for DAPK in both the mechanotransduction and apoptosis signaling cascades. Our previous data show that laminar shear stress attenuates TNF $\alpha$ -induced endothelial apoptosis by modulating DAPK expression (118). With the loss of nuclear lamin A/C expression, it is not fully understood whether the cells are protected by shear or more susceptible to external stress and apoptosis activation. Nuclear lamin play an important role in the apoptotic pathway in connection to DAPK activity, as seen in Figure 6.2. Understanding the loss of lamin A/C expression in both static and shear studies can further provide a mechanistic role of nuclear lamin in endothelial cells. This pathway may further elucidate competing effects between endothelial mechanotransduction and apoptosis activation involving DAPK modulation at the nucleus level.

**Research Objective 5: Does the loss of nuclear lamina affect endothelial apoptosis via the DAPK pathway in both static and shear conditions?**

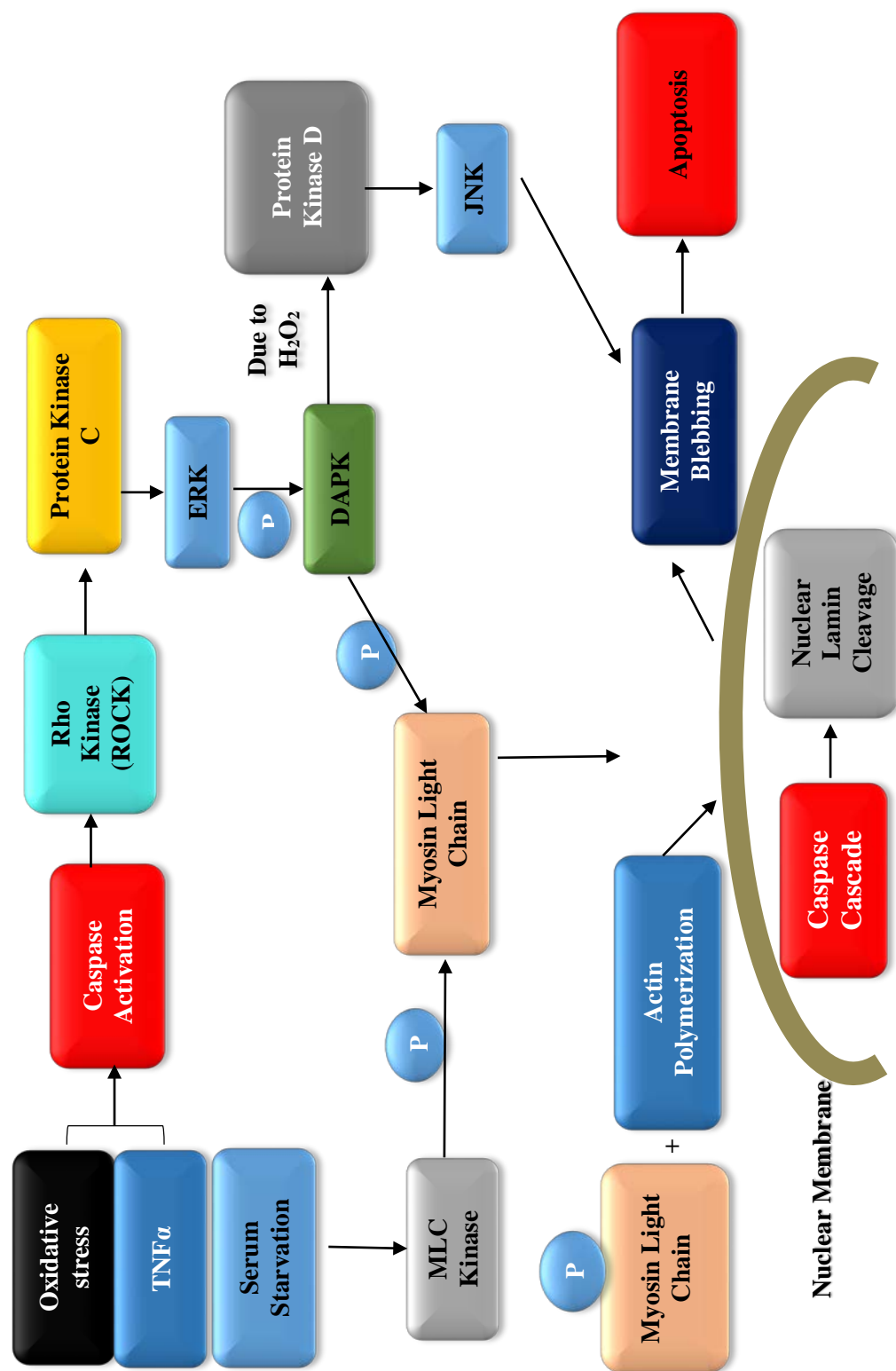


**Figure 6.2. Current understanding of apoptosis activation involving DAPK and nuclear lamin signaling.** Caspase activation leads to ROCK cleavage and MLC phosphorylation. This complex and actin-myosin polymerization results in lamin cleavage and membrane blebbing necessary for apoptosis.

## 6.2 Results

### 6.2.1 DAPK expression and apoptosis in lamin-deficient cells under shear and TNF $\alpha$

Various laminopathies are known to negatively affect fibroblast cell function and stress response, potentially relating to previous shear stress-apoptosis study (149-151). Therefore, the initial study investigated the effect of lamin A/C loss in mouse embryonic fibroblasts (MEF) for both static and shear conditions. Both wild-type and LMNA(-) MEF cell lines were provided by Jan Lammerding at Cornell University, originally derived from intercrossed LMNA(+/-) mouse embryos. We examined the corresponding time-dependent effects of shear stress on TNF $\alpha$  induced apoptosis in wild-type and lamin-deficient (LMNA-) MEF cells. Cells were either incubated with TNF $\alpha$  (25 ng/ml) for a 24hr period to fully induce apoptosis (Static + TNF $\alpha$ ) or treated with TNF $\alpha$  for 18 hr followed by shearing cells in media containing TNF $\alpha$  for another 6hr (6hr Shear + TNF $\alpha$ ). Control groups included static (Control) and cells sheared for 6 hours alone (6hr Shear), similar to our previous studies. Quantitative western analysis was performed for both cell sets and each individual sample was repeated at least 3 times, n = 3. First, we examined DAPK expression in MEF's with or without lamin (Fig. 6.3A, 6.3B). In the wild-type MEFs, we saw a similar trend to our previous BAEC studies, in that TNF $\alpha$  incubation increased DAPK expression compared to control. The 6h shear and 6h shear + TNF $\alpha$  samples displayed a decrease of DAPK expression compared to control and significantly reduced compared to Static + TNF $\alpha$ , further confirming the suppressive effect of shear stress on DAPK expression (Fig. 6.3C). Interestingly, TNF $\alpha$  little or no effect on the lamin-deficient MEF cells. The control and static + TNF $\alpha$  samples

approximately expressed the same amount of DAPK. Both sheared cases had reduced DAPK expression when compared to LMNA- control MEF. There is a 1.67 fold increase in DAPK expression in the wild-type MEFs when compared with the LMNA- static + TNF $\alpha$  samples.

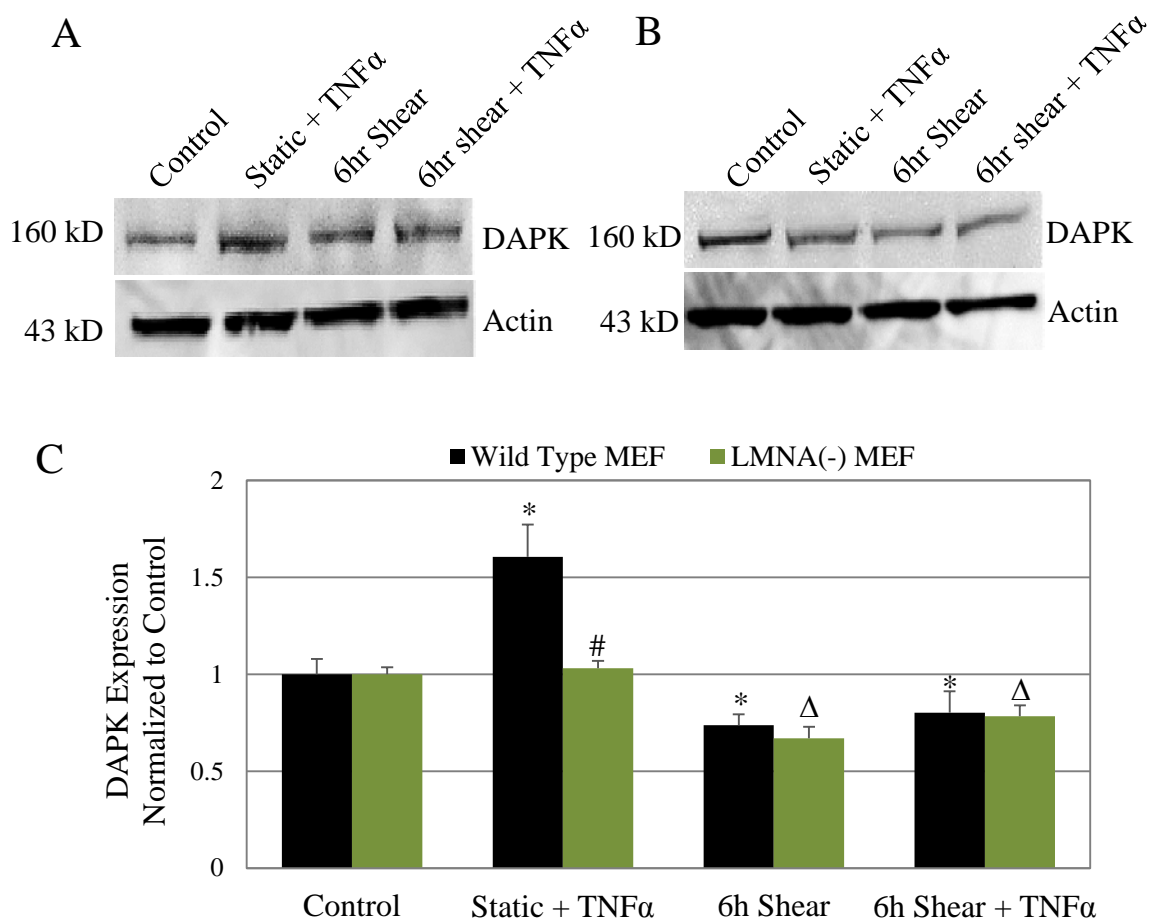


**Figure 6.3. DAPK expression in MEFs under shear and TNF $\alpha$  exposure.** (A) Western analysis for total DAPK expression in Wild-type MEF cells for each respective sample set. (B) Western analysis for total DAPK expression in LMNA(-) MEF cells for each respective sample set. (C) Relative band intensity was quantified and analyzed based on results from 3 independent experiments, and presented as fraction of control BAEC, either wild-type (black) or LMNA(-) (gray) MEFs. \*P < 0.05 compared to WT-Control, #P < 0.05 compared to WT-Static + TNF $\alpha$ ,  $\Delta$ P < 0.05 compared to LMNA-Control.

Apoptosis in both MEF cell sets was assessed using TUNEL with fluorescein label and quantified with flow cytometry. After TNF $\alpha$  and shear stimulation, cells were gently collected from slides and were fixed for staining. Each sample was TUNEL labeled and quantified using flow cytometry. TNF $\alpha$  alone (wild-type static + TNF $\alpha$ ) induced a significant 2.5-fold increase in apoptotic cells over control MEFs (Figure 6.4). We found that applying 6 hours of shear stress to cells already activated by TNF $\alpha$  for 18 hours, significantly decreased the fraction of apoptotic cells ( $P < 0.05$ ), compared to TNF $\alpha$  treatment under static condition. At the same time, we also saw a significant increase of apoptosis from wild-type control MEF with 6 hours of shear stress alone; however, the result was still significantly less than that of TNF $\alpha$  treated static cells. As a result, sheared MEF, with or without TNF $\alpha$  induction, demonstrated similar levels of apoptosis that is significantly different from both static control and TNF $\alpha$  induction alone. In LMNA(-) MEF cells, apoptosis activation correlated to the DAPK expression, in that TNF $\alpha$  did not significantly affect the static + TNF $\alpha$  sample. There was no significant increase between control and static + TNF $\alpha$  subsets; however shearing LMNA(-) MEF cells significantly increased apoptosis. In all cases where MEF were exposed to shear stress, the apoptosis fold increase was higher than static case, but significantly less than the wild-type static + TNF $\alpha$  subset. This data clearly suggest that while shear stress alone induces apoptosis, it also suppresses apoptosis subsequent to TNF $\alpha$  induction, but only in the wild-type MEF. There is a distinct difference in how MEFs with or without lamina respond to TNF $\alpha$  activation in apoptosis. These data suggest further studies are needed to fully understand the role of nuclear lamina in TNF $\alpha$ -induced apoptosis and DAPK expression for fibroblasts.



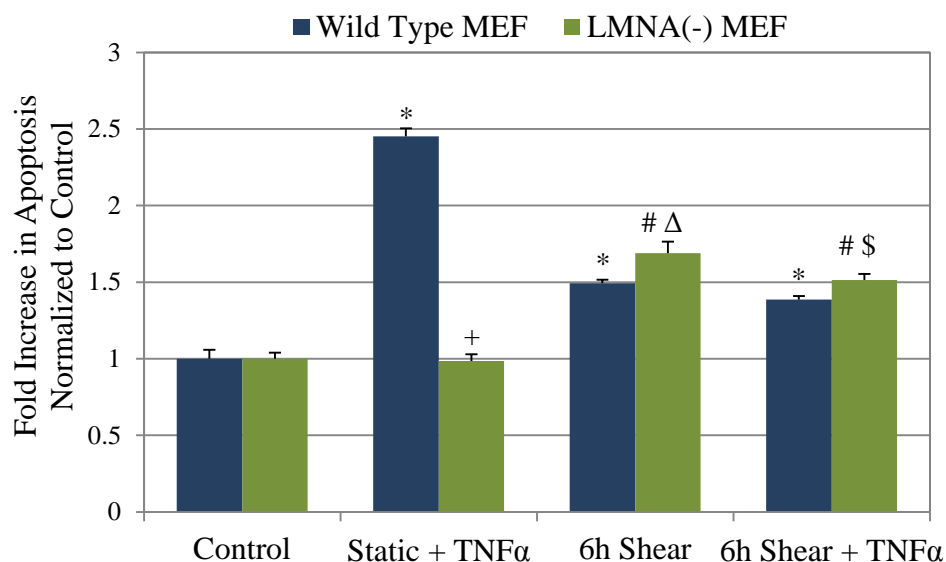


**Figure 6.4. Apoptosis results based on flow cytometry analysis of TUNEL in MEFs.** MEFs normalized to Control of each respective cell set, either Wild-type (blue) or LMNA(-) (green) (n = 3). LMNA(-) MEFs show increased apoptosis due to shear exposure compared to sheared wild type MEFs. Also, TNF $\alpha$  does not impact apoptosis in LMNA(-) MEFs compared to TNF $\alpha$  treated wild type MEFs, suggesting a vital role of lamin in the TNF $\alpha$ -induced apoptosis pathway. \* $P < 0.01$  compared to WT Control, + $P < 0.01$  compared to WT Static + TNF $\alpha$ , # $P < 0.01$  compared to LMNA(-) Control,  $\Delta P < 0.05$  compared to WT 6h Shear,  $\$P < 0.05$  compared to WT 6h Shear + TNF $\alpha$ .

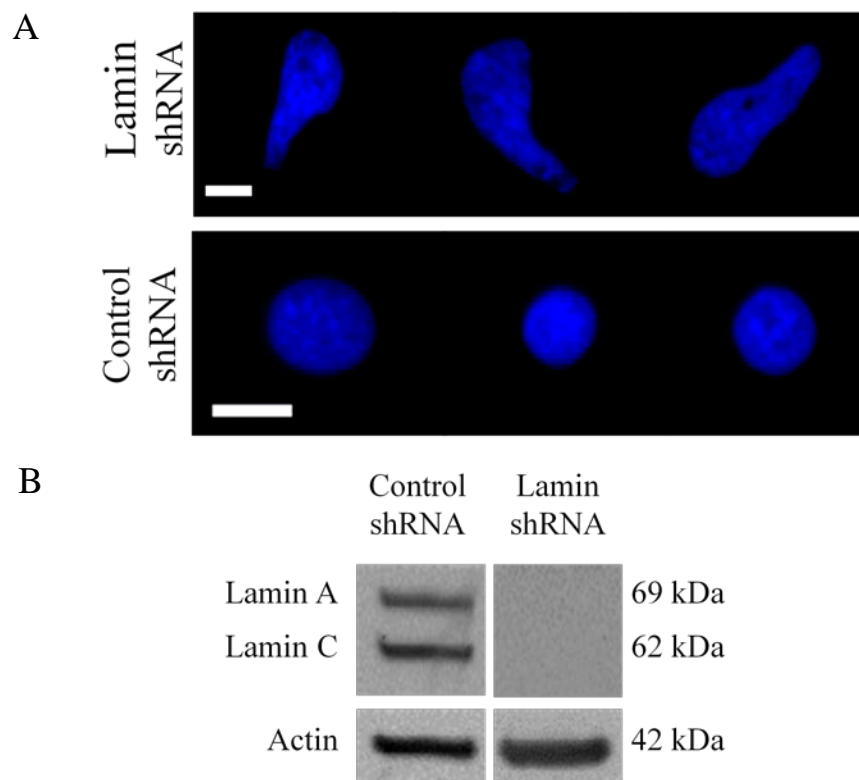


**Figure 6.5. Lamin A/C silencing in BAECs (1).** A. Hoechst stained live cell nuclei images that show significant nuclear deformation in lamin shRNA cells. Images are taken at 40X magnification, and scale bar represents 15  $\mu$ m. B. Western Blot of lamin expression in control and lamin short hairpin RNA cell lines. The blot confirms the presence of lamin in control shRNA cells and the absence of lamin in lamin shRNA cells against a loading control, actin.

After investigating the role of lamin in a well-established model such as MEFs, we wanted to continue our study of endothelial cells. Lamin A/C silencing in BAEC was carried out using short-hairpin RNA (shRNA) in stable transfections with lentivirals. Lamin A/C gene was successfully silenced in BAEC cells (Fig. 6.5). The experiment groups to analyze DAPK expression in control and lamin shRNA cells are categorized as follows: Control, TNF $\alpha$  treated, TNF $\alpha$  plus 6hr shear, and 6hr shear alone conditions. In control shRNA cells, we observed that TNF $\alpha$  treatment alone (25 ng/ml) induced an increase in DAPK expression, which would be consistent with its role in promoting apoptosis. Western analysis also showed that DAPK expression significantly decreased in TNF $\alpha$ -treated then sheared cells compared to TNF $\alpha$  alone (Fig. 6.6A). For lamin shRNA cells, TNF $\alpha$  treatment alone (Static + TNF $\alpha$ ) showed no significant increase in overall DAPK expression, when compared to Control-lamin shRNA cells (Fig. 6.6B). Quantitative analysis of relative band intensity revealed that the decrease in DAPK for TNF $\alpha$  treated then sheared cells was significant ( $P < 0.01$ ) (Fig. 6.6C). Further DAPK analysis is needed to show overall DAPK activity where phosph-DAPK expression is normalized to overall DAPK expression. These data suggest that control shRNA cells again confirmed out earlier studies, and behaved similar to untreated BAEC in response to shear stress and TNF $\alpha$ . However in lamin deficient BAEC, we observed higher DAPK expression with shear stress, particularly in combination with TNF $\alpha$  treatment.

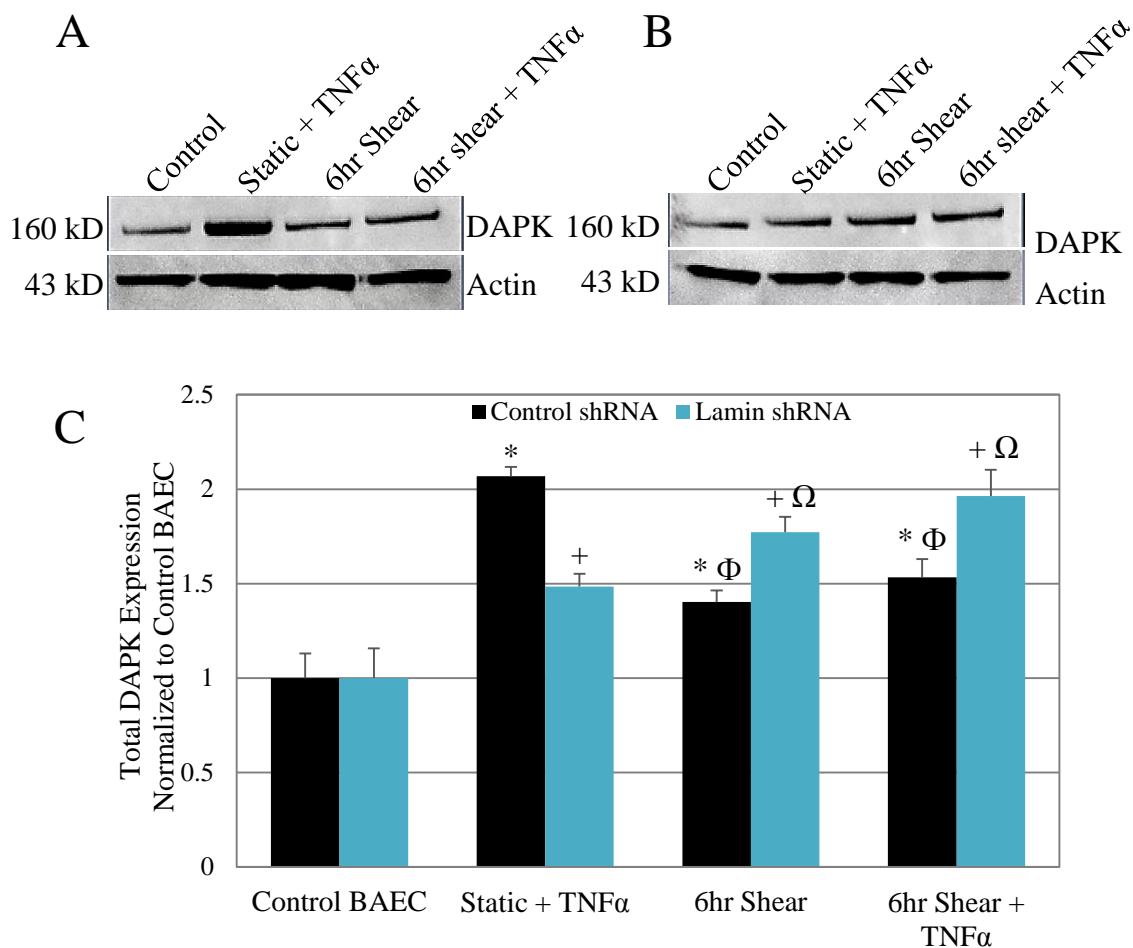


**Figure 6.6. DAPK western analysis in control and lamin shRNA BAECs.** A. Western analysis for total DAPK expression in Control shRNA cells for each respective sample set. B. Western analysis for total DAPK expression in Lamin shRNA cells for each respective sample set. (C) Relative band intensity was quantified and analyzed based on results from 3 independent experiments, and presented as fraction of control BAEC. \* $P < 0.05$ , compared to Control shRNA, - Control BAEC,  $\Phi P < 0.05$ , compared to Control shRNA - Static + TNF $\alpha$ . + $P < 0.05$ , compared to Lamin shRNA, - Control BAEC,  $\Omega P < 0.05$ , compared to Lamin shRNA - Static + TNF $\alpha$ .

We then analyzed apoptosis using control and lamin(-) shRNA BAEC, and the results are presented in Figure 6.7. The control shRNA cells alone show that the shRNA transduction process does not promote apoptosis. Interestingly, we saw that the loss of lamin A/C expression significantly eliminated TNF $\alpha$  induced apoptosis after 24-hour treatment compared to the control shRNA + TNF $\alpha$  sample ( $P < 0.01$ ). With the addition of 6 hours of shear stress after 18-hour TNF $\alpha$  treatment, we observed a significant increase in apoptotic cells with both control and lamin(-) shRNA cells ( $P < 0.01$ ). These results are complimentary to what we observed from the DAPK expression results with respect to shear suppression of TNF $\alpha$ -induced apoptosis. The loss of lamin A/C expression again attenuated the effects of TNF $\alpha$  induction of apoptosis. This data suggest lamin A/C expression is necessary for TNF $\alpha$ -induced endothelial apoptosis.

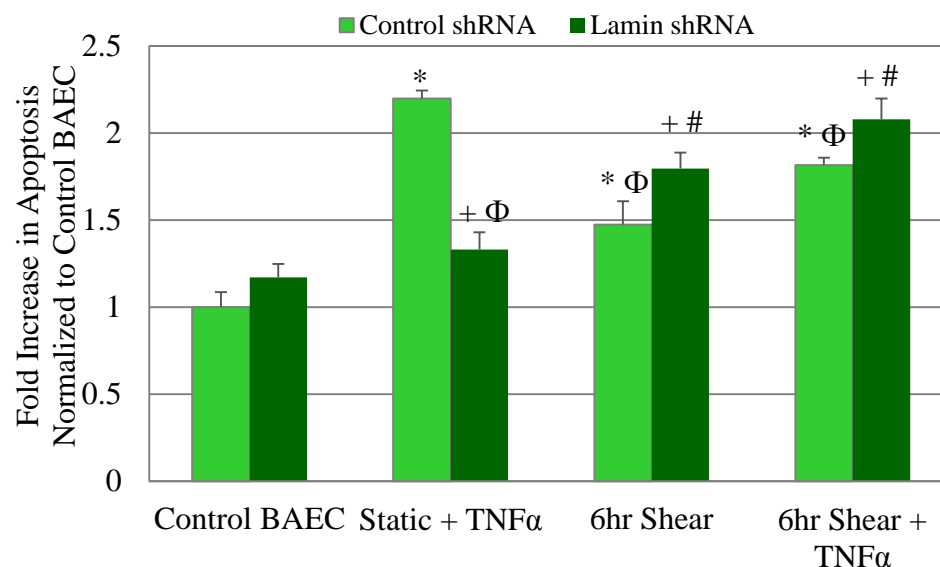


**Figure 6.7. TUNEL positive apoptosis results using flow cytometry analysis in shRNA BAECs.** shRNA BAECs normalized to Control BAEC, either control (light green) or lamin (dark green). (n = 3) \* $P < 0.01$  compared to Control BAEC - control, + $P < 0.01$  compared to Control BAEC - lamin, # $P < 0.01$  compared to Static+ TNF $\alpha$  - lamin,  $\Phi P < 0.05$  compared to Static + TNF $\alpha$  - control. Lamin shRNA cells are more susceptible to mechanical stress as seen with increased apoptosis in sheared lamin shRNA samples. Also, TNF $\alpha$  incubation did not elicit apoptosis activation in lamin knockdown cells as significantly as in control shRNA cells.

### 6.2.2 DAPK expression in lamin-deficient cells under shear stress and other environmental stimulus

This study explores the effect of shear stress and nuclear lamina on endothelial apoptosis and DAPK in response to environmental apoptosis stimulants. Given that the lamina provides structural support to the nucleus, it would be expected to play a role in shear induced changes in endothelial cells. Our previous data suggest that nuclear lamina impacts how endothelial cells respond to fluid shear stresses, especially nuclear import of activated receptors and subsequent gene transcription regulation (1). To further examine the effects of lamin loss, the inducers of apoptosis to be evaluated will be: cytokine (TNF $\alpha$ ), oxidative stress (H<sub>2</sub>O<sub>2</sub>), or serum depletion. They are common apoptotic triggers and all are shown to activate DAPK. Also, ECs were exposed to fluid shear in the absence and presence of each apoptotic inducer. Control and lamin shRNA samples were categorized in each of the following groups: Control BAEC, Static + TNF $\alpha$ , 6h Shear, 6h + TNF $\alpha$ , Static + H<sub>2</sub>O<sub>2</sub>, 6h + H<sub>2</sub>O<sub>2</sub>, Static – Serum, 6h – Serum.

Western analysis showed DAPK expression significantly decreased in sheared control shRNA cells compared to static + stimulant samples. DAPK expression significantly increased in both sheared and stimulant lamin shRNA cells compared to control BAEC ( $P < 0.05$ ) (Fig. 6.8). Once again TNF $\alpha$  exposure did not affect DAPK expression as significantly in lamin shRNA cells. These data also suggest different DAPK expression pattern in response to TNF $\alpha$  as compared to oxidative stress or serum depletion. Both H<sub>2</sub>O<sub>2</sub> and serum depletion yielded higher DAPK expression compared to TNF $\alpha$ . At the same time, the ability of shear stress to suppress DAPK expression was also reduced with H<sub>2</sub>O<sub>2</sub> and serum depletion treatment. In control cells, there was a

consistent reduction of DAPK expression with the addition of shear stress, which is not observed in lamin deficient cells. The results suggest a potential role of nuclear lamin in the inflammatory cytokine pathway, possibly regulated via DAPK expression and activity. However, the effect of nuclear lamina is also dependent on the specific apoptosis trigger and the subsequent DAPK pathway.

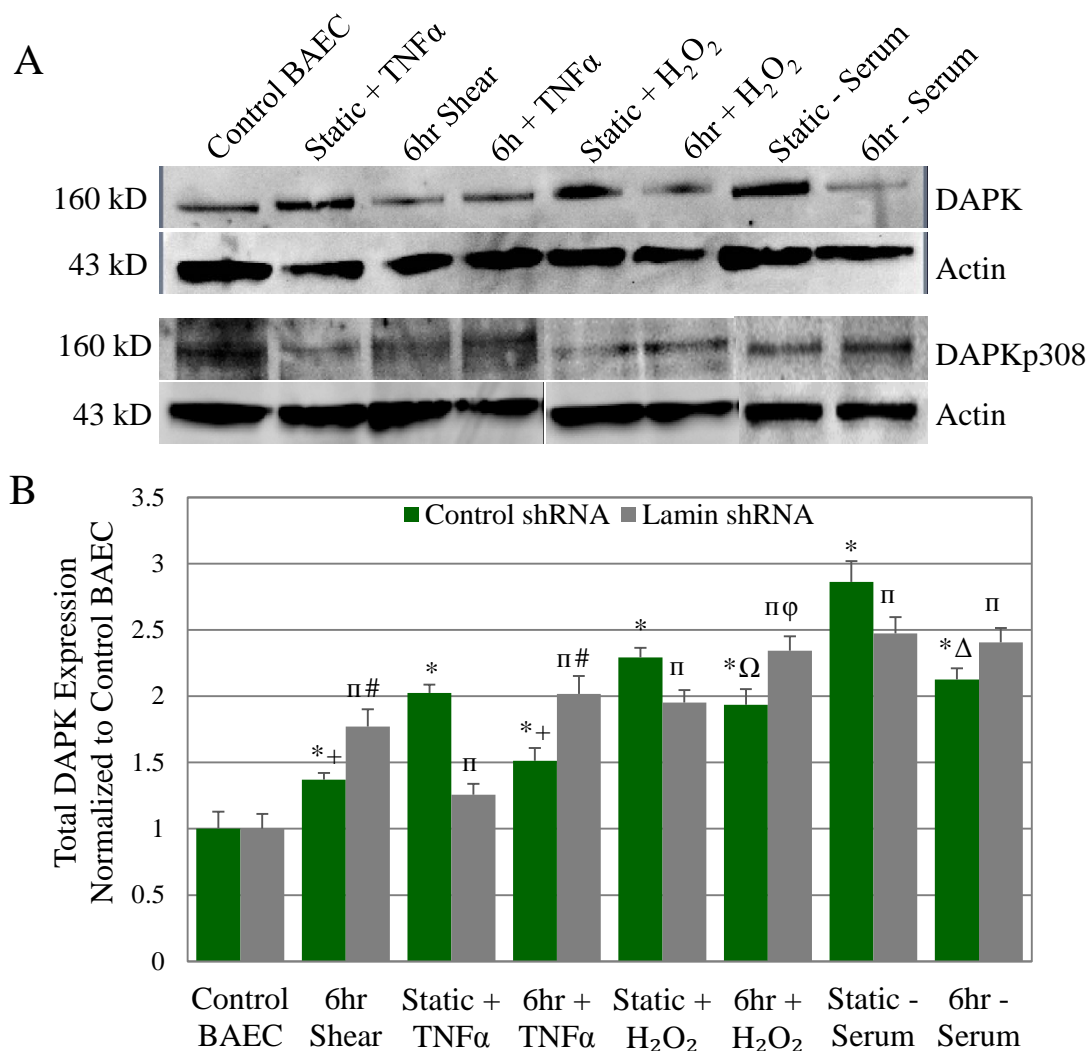


**Figure 6.8. DAPK activity in shRNA cells under shear and stimulants.** A. Representative Western Blot for DAPK Expression in Control shRNA Samples. B. Total DAPK Protein Expression in Control and Lamin shRNA cells. \* $P < 0.05$ , compared to Control shRNA, Control BAEC. + $P < 0.05$ , compared to Control shRNA, Static + TNF $\alpha$ .  $\Omega P < 0.05$ , compared to Control shRNA, Static + H<sub>2</sub>O<sub>2</sub>.  $\Delta P < 0.05$ , compared to Control shRNA, Static - Serum.  $\pi P < 0.05$ , compared to Lamin shRNA, Control BAEC. # $P < 0.05$ , compared to Lamin shRNA, Static + TNF $\alpha$ .  $\phi P < 0.05$  compared to Lamin shRNA, Static + H<sub>2</sub>O<sub>2</sub>.



Overall DAPK activation was determined using DAPKp308/total DAPK expression. A decrease in DAPKp308 corresponds to overall increase in kinase activity. All stimulants significantly decreased DAPKp308 in both control and lamin shRNA cells. Also, DAPKp308 decreased in each sheared sample compared to Control BAEC (Fig. 6.9A). The ratio of DAPKp308/DAPK was quantified to determine changes in DAPK activity for each sample (Fig. 6.9B). DAPK activity increased in every sample set compared to each respective “Control BAEC” group. In control shRNA groups, shear significantly decreased DAPK activity compared to static, apoptosis induced subsets. Sheared lamin shRNA cells showed significantly higher DAPK activation when compared to sheared control shRNA cells (Fig. 6.9B). The lamin-deficient cells displayed nearly the opposite trend as seen in the control shRNA group comparing DAPK activation between the sheared and static, induced cell sets. Shear stress without the presence of nuclear lamin leads to more DAPK activation in each sheared group compared to the respective static, stimulated cells. This data suggest that nuclear lamin may play a key role in the DAPK-dependent mechanotransduction pathway necessary to regulate endothelial apoptosis in the presence of apoptosis inducing agents.

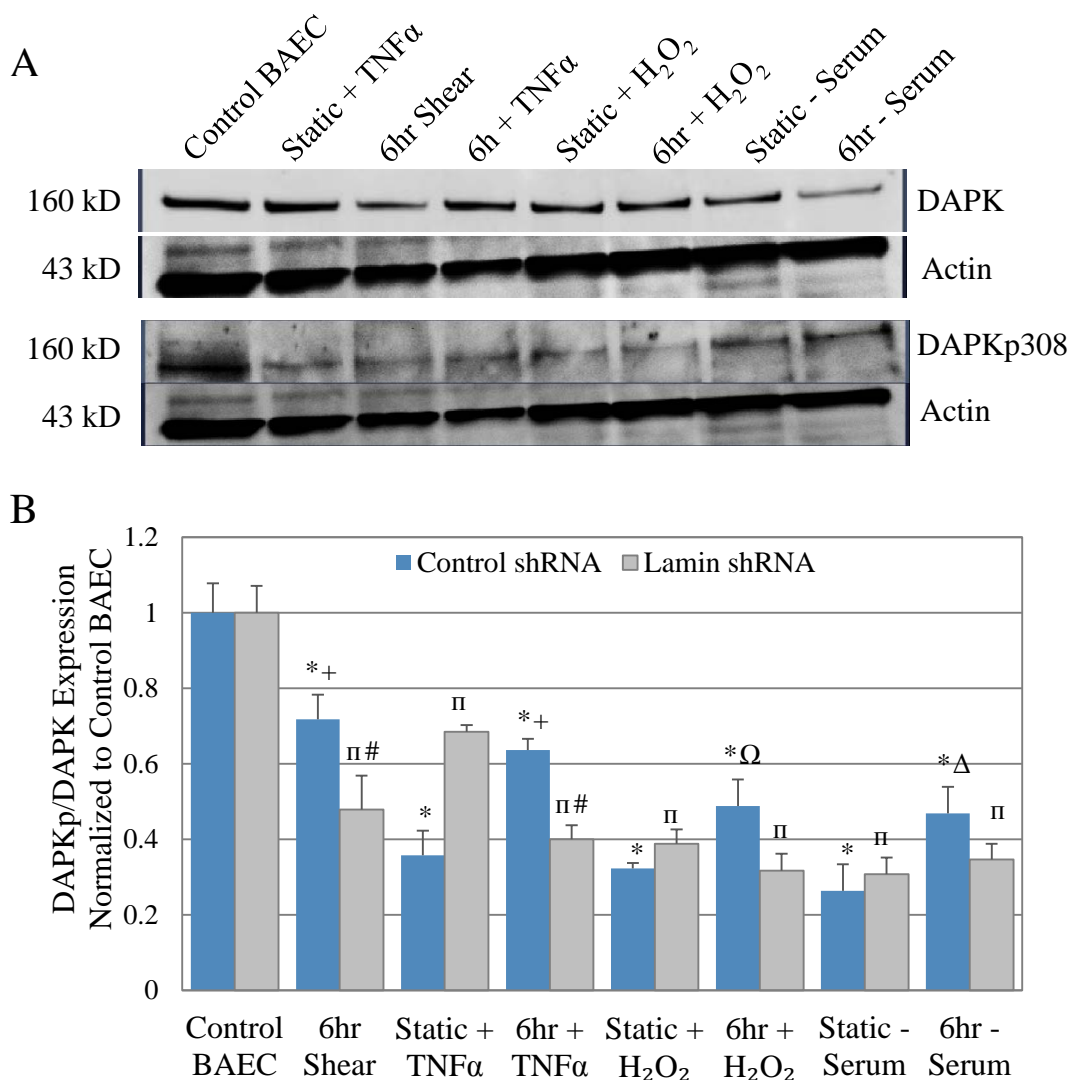


**Figure 6.9. DAPKp308/DAPK activity in shRNA cells under shear and stimulation.** A. Representative Western Blot for DAPK expression in lamin shRNA samples. B. DAPKp308 versus total DAPK protein expression for control and lamin shRNA subsets (n=3). \* $P < 0.05$ , compared to Control shRNA, control BAEC. + $P < 0.05$ , compared to control shRNA, Static + TNF $\alpha$ .  $\Omega P < 0.05$ , compared to control shRNA, Static + H<sub>2</sub>O<sub>2</sub>.  $\Delta P < 0.05$ , compared to control shRNA, Static - Serum.  $\Pi P < 0.05$ , compared to lamin shRNA, Control BAEC. # $P < 0.05$ , compared to lamin shRNA, Static + TNF $\alpha$ .  $\phi P < 0.05$  compared to lamin shRNA, Static + H<sub>2</sub>O<sub>2</sub>

### 6.2.3 Apoptosis in shRNA cells

Our previous studies show fluid shear decreases DAPK expression and endothelial apoptosis in the presence of apoptosis inducers. For the shRNA cell sets, this study continues to investigate the impact of lamin loss on apoptosis with respect to the previous experimental setup. So far, control shRNA cells have shown a similar DAPK expression profile in response to shear and stimulants.

Phase images of shRNA cells in each experimental group following shear and apoptosis triggers are analyzed for changes in cell morphology. Control shRNA cells looked as expected based on our previous studies with shear and each of the three apoptotic inducers (Fig. 6.10). Static + TNF $\alpha$ , Static + H<sub>2</sub>O<sub>2</sub>, and Static – Serum samples exhibit stressed cell phenotypes including cell disorganization, increase in cell size, and overall decrease in adhered cell numbers compared to the untreated Control BAEC (left column Fig. 6.10). Compared to the corresponding static samples, each sheared sample set displays increased healthier looking cells. These cells displayed better morphology and organization, and cells begin to elongate and align in the direction of fluid flow. There also seem to be higher percentage of adherent cells (right column Fig. 6.10). These representative cell images correlate well with our previous molecular studies showing the impact of shear to counter the effects of various apoptotic stimulants. On the other hand, lamin shRNA cells show an increase in cell monolayer organization even in the static BAEC groups treated with apoptotic triggers (left column, Fig. 6.11). Cells treated under static condition, are still affected by each apoptotic inducer but to a lesser extent based on the images. However, the lack of nuclear lamin did appear to increase susceptibility to shear stress (right column, Fig. 6.11). We observed little to no elongation of cells and

alignment in the fluid flow direction. However, most cells remained attached. These images provide a glimpse into the morphological changes in cells due to shear and environmental stimulates in both control and lamin shRNA cells.

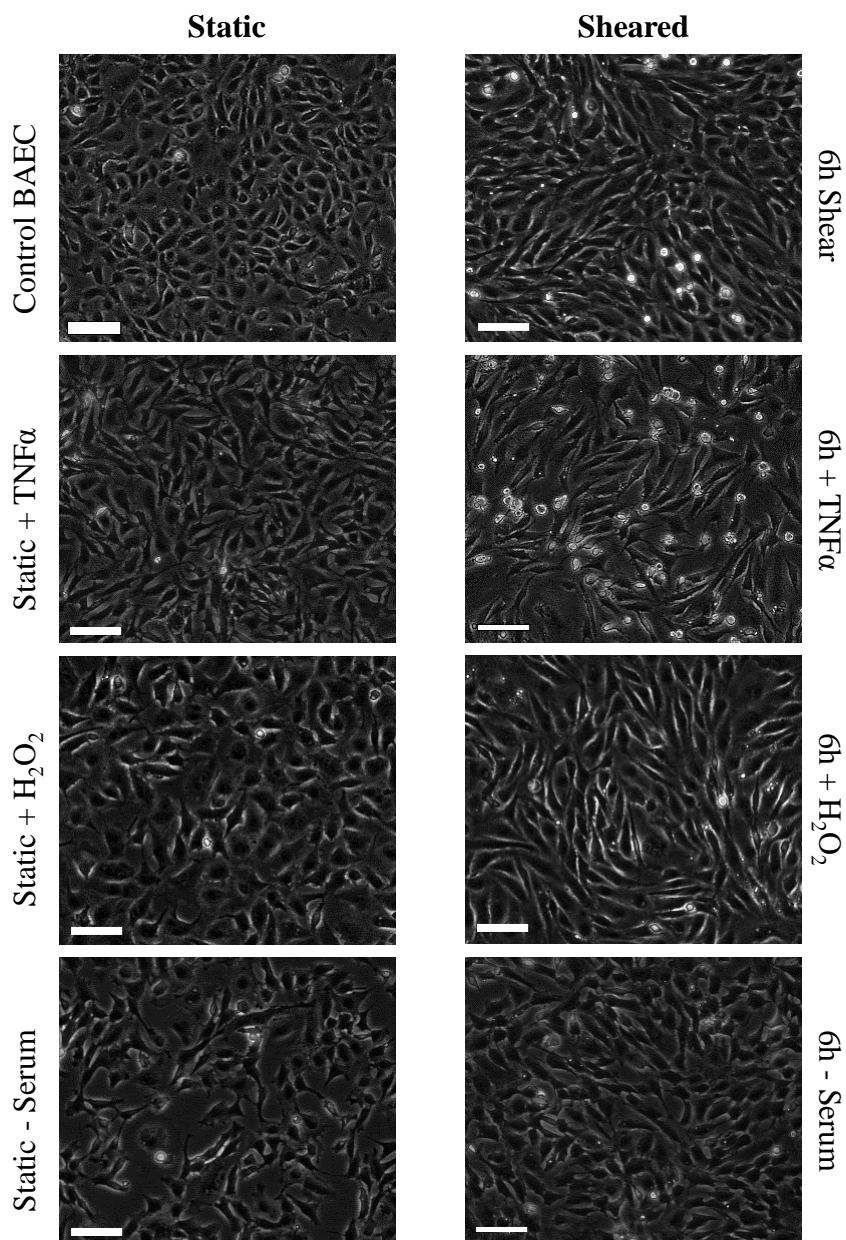


**Figure 6.10. Control shRNA cells in representative 10X phase images.** Images were taken post-experiment, either after 24hr incubation or following shearing as described in our experimental design. Sheared control shRNA cells show more cell confluency, organization, and alignment compared to the static + stimulant cells. These images correlates well with the current understanding that laminar shear provides a protective cell response in the presence of apoptotic stimulants. Each scale bar represents 50 $\mu$ m.

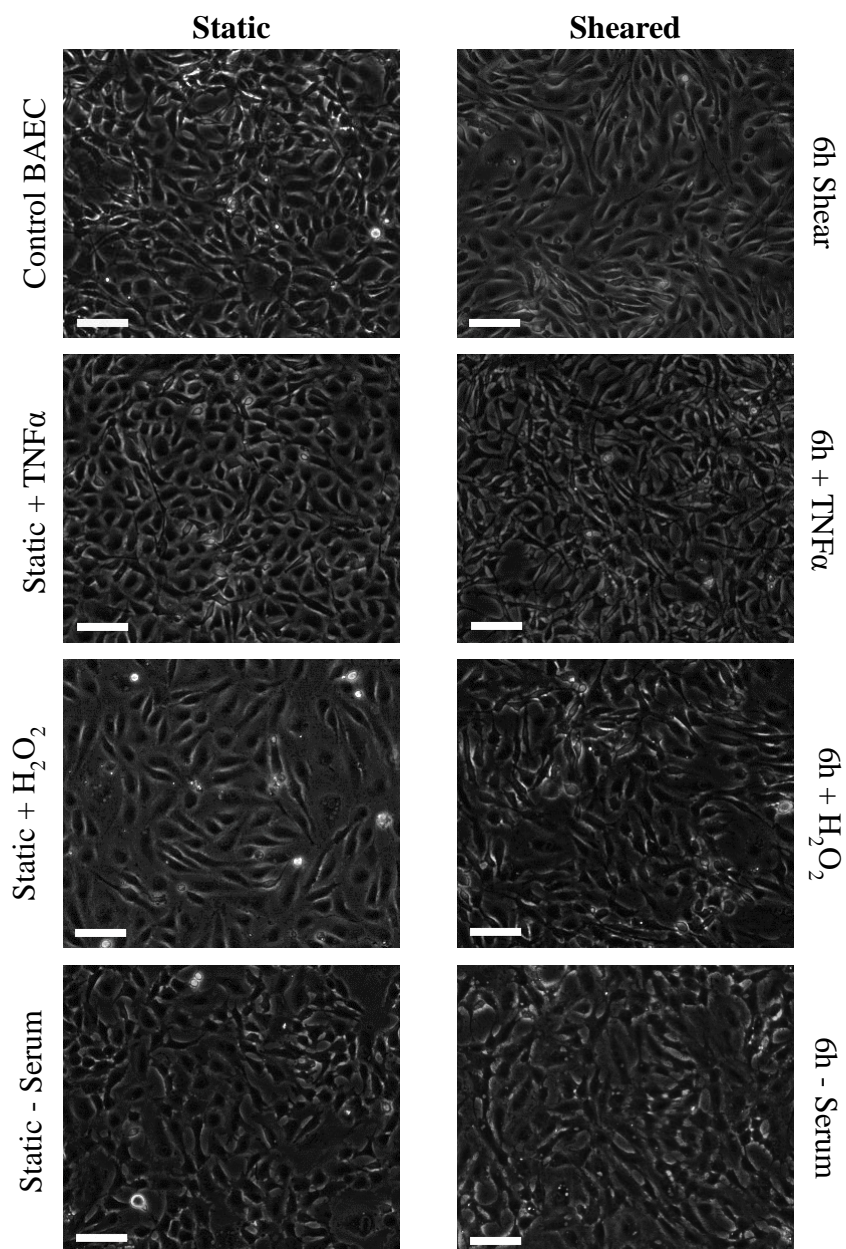


**Figure 6.11. Lamin shRNA cells in representative 10X phase images.** Images were taken post-experiment, either after 24hr incubation or following shearing as described in our experimental setup. Sheared cells show more susceptibility to mechanical stress, and lack the positive response to shear seen in the control shRNA sheared cells. The loss of lamin presents disconnect in the endothelial mechanotransduction response pathway resulting in a stressed, atypical cell phenotype. Each scale bar represents 50 $\mu$ m.

In order to truly evaluate cell apoptosis and the molecular response in lamin-deficient cells, apoptosis was quantified in each shRNA sample group using TUNEL staining. Endothelial apoptosis was quantified using flow cytometry protocols, the results are presented in Figure 6.12. Addition of apoptosis triggers increased apoptosis across all groups, as expected. When comparing cells treated with apoptosis trigger in static or sheared cells, sheared control shRNA cells displayed significantly decreased cell death compared to stimulus alone in static condition. On the other hand, compared to control cells, lamin shRNA cells showed decreased apoptosis when cells are treated by apoptosis stimulus in static condition, suggesting that lack of lamin suppresses apoptosis.

However these cells were negatively affected by shear stress exposure compared to sheared control shRNA cells. Shear stress did not suppress apoptosis activated by  $\text{TNF}\alpha$ ,  $\text{H}_2\text{O}_2$ , and serum depletion. These results suggest lamin-deficient cells have a different susceptibility to shear and apoptosis. We still saw a good correlation between DAPK expression, activation and endothelial apoptosis.

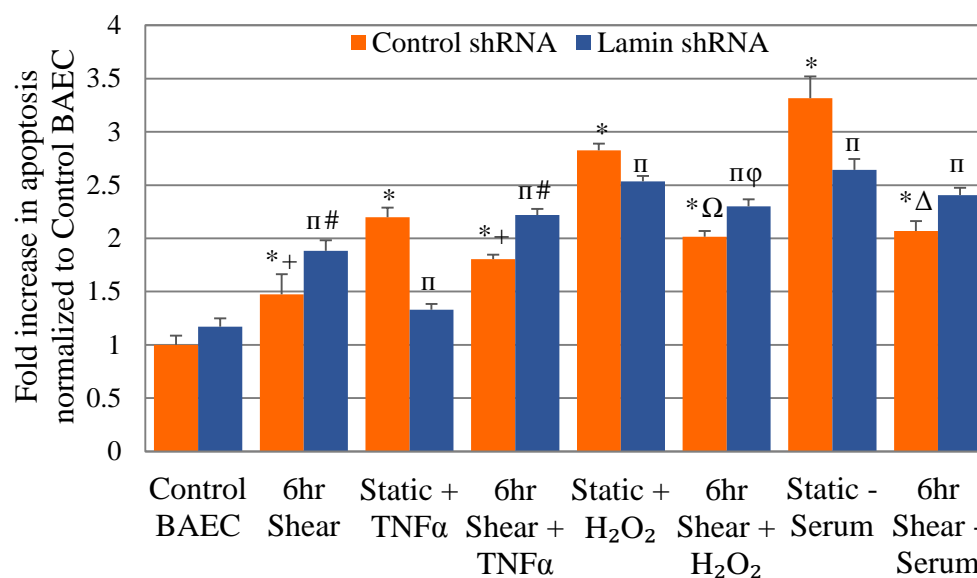


**Figure 6.12. Fold Increase in apoptosis for control and lamin shRNA cells.** TUNEL stained cells were analyzed with flow cytometry. Lamin shRNA cells were significantly affected by shear stress showing increased apoptosis compared to sheared control shRNA cells. \*P < 0.01, compared to Control shRNA, Control BAEC. +P < 0.01, compared to control shRNA, Static + TNF $\alpha$ . ΩP < 0.01, compared to Static + H<sub>2</sub>O<sub>2</sub>. ΔP < 0.01, compared to control shRNA, Static - Serum. #P < 0.01, compared to lamin shRNA, Control BAEC. #P < 0.01, compared to lamin shRNA, Static + TNF $\alpha$ . φP < 0.01 compared to lamin shRNA, Static + H<sub>2</sub>O<sub>2</sub>.



### 6.3 Discussion

Nuclear lamins were initially thought to only be structural support proteins based on their external nuclear envelope location. Recent research has shown a broader role for lamins in overall nuclear function. Lamins are involved in nuclear envelope assembly, DNA synthesis, gene transcription, and even apoptosis (127). Lamin degradation is a significant step in the apoptosis pathway and necessary for nuclear degradation.

The nuclear lamina is connected to the actin cytoskeleton and directly associated with the nuclear envelope. The actin network plays an important role in nuclear degradation and necessary to regulate apoptosis events. DAPK is localized in the cytoskeleton and interacts with MLC to mediate membrane blebbing in apoptosis. DAPK phosphorylates MLC leading to a weakening of the actin network. MLC phosphorylation in combination with ROCK activation lead to lamin proteolysis and cell death. ROCK is activated by caspase up-regulation that lead to nuclear protein proteolysis and DNA degradation. In  $\text{TNF}\alpha$ -induced apoptosis,  $\text{TNF}\alpha$  stimulates caspase activation which cleave downstream ROCK leading to lamin degradation and eventual apoptosis. Figure 6.2 depicts the detailed schematic of this apoptosis cascade.

We begin to investigate relationship between the nuclear lamina and cellular apoptosis. First, we examined the  $\text{TNF}\alpha$ -induced apoptosis pathway in wild-type and LMNA- MEF cells (Fig. 6.3). These are MEFs that have knock out of the lamin gene.  $\text{TNF}\alpha$  increased both DAPK and apoptosis induction in wild-type MEFs. However,  $\text{TNF}\alpha$  did not increase DAPK expression in LMNA- MEFs. There was no statistically significant difference between control and  $\text{TNF}\alpha$  treated LMNA- cells. Also, shearing

cells decreased DAPK expression and significantly attenuated MEF apoptosis in both wild-type and LMNA- cells (Fig. 6.4).

To confirm our results in non-MEF cells, we repeated the experiments in BAECs. Using shRNA transfections, we created two stable shRNA cell lines: control shRNA and lamin shRNA. Shear stress alone also increased both DAPK and apoptosis for both control and lamin shRNA cells compared to their respective control BAEC samples. Also, TNF $\alpha$ , H<sub>2</sub>O<sub>2</sub>, and serum starvation increased DAPK activation and endothelial apoptosis compared to each control BAEC subset.

The results show shear stress significantly attenuated TNF $\alpha$ , H<sub>2</sub>O<sub>2</sub>, and serum starvation activated DAPK expression and activity, and apoptosis in control shRNA cells (Fig. 6.8, 6.9, and 6.12). Although, the lamin-deficient cells showed an opposite trend between sheared and static, stimulated cells. Sheared cells displayed higher DAPK activity and apoptosis compared to the static, stimulated cell subsets. TNF $\alpha$  incubation increased both DAPK expression and apoptosis in lamin shRNA, although to a substantially lesser degree compared to TNF $\alpha$ -treated control shRNA groups. Also, H<sub>2</sub>O<sub>2</sub> and serum deprivation significantly increased DAPK and apoptosis, but to a lesser extent than the shear exposed lamin shRNA groups.

Lamin shRNA cells proved to be more susceptible to shear, showing significantly increased DAPK expression and apoptosis compared to sheared control shRNA cells. Increased apoptosis correlates with the current understanding that lamin deficient cells maintain low survival rates due to cell stress (131). These results suggest lamin plays a prominent role in TNF $\alpha$ , H<sub>2</sub>O<sub>2</sub>, and serum deprivation induced endothelial apoptosis.

Particularly in the case with TNF $\alpha$  induction, apoptosis was attenuated in the absence of lamin suggesting that lamin is crucial for modulating TNF $\alpha$ -induced apoptosis.

Various nuclear proteins are lamin-dependent complexes with roles ranging from gene transcription to signal transduction. A deeper understanding of the nuclear membrane mechanisms require a detailed signal transduction study of vital constituents that interact with lamin, such as DAPK. Ongoing studies of lamin modulation will help clarify its role in laminopathies, endothelial mechanotransduction and apoptosis.

## 7. CONCLUSIONS AND RECOMMENDATIONS

### 7.1 Summary

There are key gaps in the current research with regards to DAPK activity and the competing effects between hemodynamic shear stress and apoptosis. Hemodynamic shear stress continuously engages the endothelium layer that line the vascular walls. The type of fluid flow ultimately determines endothelial cell phenotype and function.

Atherosclerosis preferentially develops in regions of disturbed flow where increased endothelial apoptosis disrupts the endothelium barrier and structural integrity. DAPK is involved in positively regulating apoptosis in various cell types.(36; 79) DAPK expression is also upregulated in atherosclerotic plaques and silenced by DNA hypermethylation in some types of cancer (97).

Mechanotransduction in endothelial cells includes a variety of pathways that bring about changes in cellular functions such as proliferation and apoptosis. Excessive apoptosis leads to unfavorable environmental inflammation and cell turnover, while laminar shear stress is protective against apoptosis (118). DAPK interacts with MAPK and its pathways, which become transiently activated via laminar shear stress (19).

Laminar shear stress elicits morphological changes in endothelial cells including stress fiber formation, focal adhesion reorganization, cell motility, and eventual cell alignment in the direction of flow. DAPK is localized to the actin network, and promotes acto-myosin contractility. DAPK stabilizes stress fibers by phosphorylation of MLC (39; 95). In endothelial cells DAPK phosphorylates TM-1 at Ser283 in response to ERK activation under oxidative stress (96). TM-1 is important in maintaining cardiovascular homeostasis, and its expression is lost in tumor cells (41). Furthermore, DAPK-regulated apoptosis pathway is suppressed during the angiogenic process. Netrin-1 was recently discovered to promote endothelial cell survival and angiogenesis by inhibiting its pro-apoptotic receptor UNC5B and its downstream regulator DAPK (152). Complete functions of DAPK are still being elucidated, which would further emphasize the importance of DAPK. Thus, DAPK could have other non-apoptotic functions in endothelial cells. The role of DAPK in apoptosis and its association with the actin cytoskeleton suggest it as a regulator of endothelial responses in mechanotransduction. DAPK can be potentially utilized by endothelial cells in affecting morphological changes in response to shear stress. The cytoskeleton effect of DAPK occurs before onset of apoptosis, and is independent of DAPK death domain (39). One potential model for this dual role of DAPK is that shear stresses regulate apoptotic function of DAPK in a time-dependent manner: the onset of shear stress will sequester DAPK to its cytoskeleton activities, and attenuate its ability to interact with subsequent stress-activated apoptotic binding partners. For example, shear stress increases binding of DAPK with cytoskeleton components TM-1 and MLC, while apoptotic cytokine will increase binding of DAPK with cytoplasmic partners to induce apoptosis (39; 96).

Understanding endothelial DAPK expression and function will help elucidate overlaps between the apoptotic and shear stress signaling pathways. This dissertation assesses the effect of shear stress on endothelial cell phenotype, apoptosis, and DAPK. The potential role of DAPK and its corresponding signaling pathway for endothelial mechanotransduction and endothelial apoptosis is further evaluated. Specifically, the following research objectives were investigated in our study of the role of DAPK in mechanotransduction and endothelial apoptosis:

**Research Objective 1: Does fluid shear stress regulate DAPK expression?**

**Research Objective 2: Will fluid shear stress attenuate TNF $\alpha$  endothelial apoptosis via DAPK activity?**

**Research Objective 3: Does fluid shear stress mitigate TNF $\alpha$ , H<sub>2</sub>O<sub>2</sub>, and serum starvation induced endothelial apoptosis by modulating DAPK expression in a time-dependent manner?**

**Research Objective 4: Will the cell substrate impact overall DAPK activity and endothelial apoptosis in response to shear?**

**Research Objective 5: Does the loss of nuclear lamina affect endothelial apoptosis via the DAPK pathway in both static and shear conditions?**

To achieve the specific research objectives, we first examined expression and activity of DAPK in endothelial cells under fluid shear stress alone. We showed that shear stress increased overall DAPK and decreased phosphor-DAPK endothelial expression with extended time sheared. Also, we used real time RT-PCR analysis to show DAPK mRNA activation correlated with the overall increase in DAPK protein expression. Next, laminar shear proved to antagonize TNF $\alpha$ -induced endothelial

apoptosis by modulating DAPK activity. We confirmed that long term shear stress decreased DAPK activity corresponding with the expected athero-protective response. Furthermore, the competing effects of both mechanotransduction and endothelial apoptosis were investigated using DAPK siRNA knockdown studies. Our results suggest DAPK is important for both TNF $\alpha$ -induced apoptosis and endothelial response mechanisms to shear stress exposure.

To further elucidate the role of DAPK in apoptosis, we explored TNF $\alpha$ , H<sub>2</sub>O<sub>2</sub>, and serum starvation induced endothelial apoptosis under the presence of shear stress. We show that laminar shear stress inhibited various apoptotic pathways by modulating DAPK expression, potentially regulating both pro- and anti-apoptotic DAPK activity in a time-dependent manner. Also, pre-shearing of cells decreased overall apoptosis prior to stimulant incubation more so than post-shearing cells after each stimulant incubation.

To extend our previous study to include different substrates, we investigated how cells respond to being cultured and treated on a different substrate, silicone membrane, normally used in cyclic stretch experiments. Here we begin to bridge the gap between shear stress and cyclic stretch studies by using a more physiologically relevant softer substrate, silicone. We showed that DAPK expression and activation is influenced by shear stress more than cell substrate. Overall, TUNEL and caspase 3/7 activities were lower when sheared on membrane compared to glass. Here we confirm substrate-dependent differences in how endothelial cells respond to fluid shear stress in apoptosis.

Finally, we investigate the role of nuclear lamin in endothelial apoptosis and mechanotransduction, and how DAPK is modulated in lamin-deficient cells. In lamin knockout cells (MEFs), TNF $\alpha$  did not significantly increase either DAPK expression or

apoptosis in lamin shRNA cells when compared to control shRNA samples. We found that lamin-deficient cells are more susceptible to shear stress. Overall, lamin A/C is crucial for TNF $\alpha$ -induced MEF and endothelial apoptosis, as well as how cells respond to mechanical stress.

Currently, our group is investigating key players of mechanotransduction in endothelial apoptosis by incorporating other mechanical cues such as substrate stiffness variations, different extracellular matrix ligands, and cyclic stretch to better understand cell response mechanisms. Results obtained from such studies will advance our knowledge of not only endothelial mechano-biology and apoptosis, but also functions of key signaling pathways in other cellular processes. Due to an involvement in both apoptosis and cytoskeletal remodeling, a novel role for DAPK in the atherosclerosis signaling pathway may provide a potential therapeutic target for future endothelial studies. Likewise, many nuclear proteins depend on nuclear lamin for localization. The disruption of lamin composition can affect signal transduction processes and overall cell function (153). The role of lamin function in mechanotransduction and apoptosis is still being elucidated and further lamin studies are needed to determine its part in nuclear and overall cell function.

Future experimental research will pursue a mechanistic study of the DAPK and mechanotransduction pathways, and determine further the effect of shear stress and nuclear lamina on endothelial apoptosis and DAPK. Cells with and without intact nuclear lamina are used to evaluate the effect of mechanical and environmental stresses on apoptosis and DAPK. The work set forth in this dissertation has highlighted the role of DAPK in both mechanotransduction and endothelial apoptosis. To advance these



findings, continued studies should investigate DAPK binding partners and the resultant cell response to varying mechanical and chemical stimulation. This work may provide a better understanding of these competitive pathways in physiological and pathological situations. By understanding how cells regulate phenotypic and genotypic changes in response to stimulation, we can better address disease and develop effective therapeutics.

## 7.2 Potential Limitations

There are a few limitations in this study to address moving forward. One limitation is using cultured cells in an *in vitro* setting cannot mimic all the complexities of *in vivo* systems. We used a parallel plate flow chamber expose endothelial cells to laminar fluid shear, while *in vivo* fluid flow is more complex. Also, the complete vasculature would consist of other types of cells such as smooth muscle cells simultaneously exposed to other hemodynamic forces. Although the entire system cannot be easily simulated, the *in vitro* parallel plate flow studies allows research to investigate and identify important signal transduction mechanisms. The parallel plate flow chamber is a well-know and widely used *in vitro* system. Our novel results show DAPK has a key role in the endothelial mechanotransduction pathway and plays a part in shear attenuating apoptosis in the presence of different environmental stimulants.

Another limitation is the use of one particular target protein, DAPK. The mechanisms that activate DAPK were not fully defined. Other DAPK activators or mechnao-sensitive targets, specifically MAPK expression, binding and activity, should be explored in correlation to the current study.

Our recent studies incorporated lamin and how DAPK interacts in the mechanotransduction and apoptosis pathways in the absence of this key nuclear membrane protein.

### **7.3 Future Research Directions**

#### **7.3.1 Endothelial and smooth muscle cell mechanotransduction due to cyclic stretch**

Our lab group will utilize a custom designed stretch device incorporating silicone membrane substrates to mimic and study another important hemodynamic force, cyclic stretch of the vessel wall in the vasculature. Endothelial and/or smooth muscle cells are plated on strips of silicone and secured in the device. The stretch device is connected to a linear actuator to move the membranes back and forth. A physiologically relevant cyclic strain, approximately 10 percent at 1 Hz frequency, is applied to cells in a time-dependent manner. The frequency and strain applications can be controlled and varied depending on the experimental design. Cells can be collected post-stretch and analyzed using the various techniques and protocols previously described in this dissertation. These cyclic stretch studies may help elucidate the overarching cardiovascular mechanotransduction response in combination with our fluid shear stress experiments. Using both force applications, our group will utilize inhibition studies with different mechano-sensitive signal transduction pathways, such as MAPKs, to identify potential interacting partners with DAPK, as well as nuclear lamin.

We hypothesize also that mechanical stresses promotes DAPK to its cytoskeleton activities, and attenuate its ability to interact with stress-activated apoptotic binding partners. Shear stress will increase binding of DAPK with cytoskeleton components TM-1 and MLC.

### 7.3.2 The effect of mechanical stress on lamin expression in cells

Hemodynamics play an important role in endothelial cell function where laminar shear attenuates cell turnover and suppresses apoptosis triggered by environmental factors (118). External forces, such as shear or strain, lead to changes in nuclear membrane signal transduction and structure. Modifications in nuclear membrane properties may result in systematic reformation within the cell nucleus. The nuclear membrane shape and stiffness adapt and reorganize in response to external forces. Although, the resultant changes in gene and protein expression remain unclear (154). Lamin functions to control cell homeostasis and fate through nuclear membrane regulation. Cell protection mechanisms and the role of lamin in response to mechanical stimulation are not fully understood.

Lamin is a key player in a system of proteins that communicate external signals into transcriptional changes in the cell nucleus. Specifically, lamin A contains stress sensitive domains altered by dynamic phosphorylation (155). The phosphorylated lamin protein variations alter nuclear membrane and the response to external forces. Lamin A levels adjust to the cell microenvironment, cell-cell interactions and environmental stresses. Lamin A overexpression or a high lamin A: lamin B ratio show a flattened, elongated cell phenotype with a limited susceptibility to migration (148). These cells

have a stiffer nuclear membrane associated with increased cell survival rates. Lamin knockdown cells or a low lamin A: lamin B ratio portray a more rounded cell phenotype with significantly increased likelihood for cell migration compared to control cells (156). These lamin-deficient cells have soft nuclear membrane mechanics leading to short cell half-lives and diminished cell survival rate.

Lammerding et. al show significant nuclear deformations, decreased signal response and cell viability in LMNA  $-/-$  cells exposed to mechanical strain. Particularly, the NF- $\kappa$ B-regulated signaling pathway in LMNA  $-/-$  cells is attenuated in response to strain or cytokine stimulation (153). This study shows the central role lamin plays in nuclear membrane mechanics as well as gene transcription changes in response to mechanical stimulation. Similarly, our recent study of lamin-deficient cells shows significantly increased endothelial apoptosis due to shear compared to control cells. This correlates well with previous studies portraying decreased cell viability. Also, our recent experiments show shear down modulates lamin A/C expression in control shRNA cells compared to Control BAEC (Figure 7.1). On the other hand, lamin-deficient cells exhibit significant lamin A/C upregulation when exposed to fluid shear (Figure 7.2).

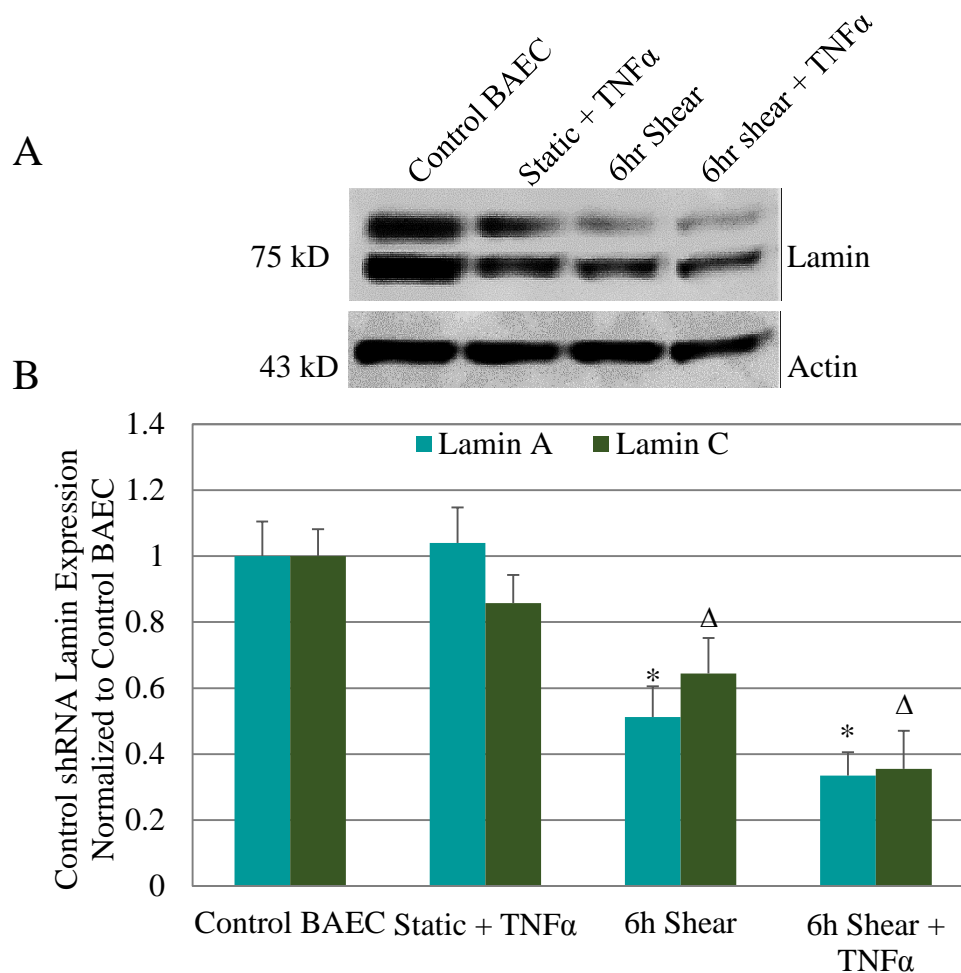


**Figure 7.1. Lamin expression in control shRNA cells.** A. Western blot of lamin A/C expression in control shRNA samples. B. Graph of quantified lamin A/C protein expression in each sample set (n=3). \* $P < 0.05$ , compared to Control BAEC (lamin A),  $\Delta P < 0.05$ , compared to Control BAEC (lamin C). Shearing control shRNA cells elicits a significant decrease in lamin A/C expression, signifying lamin is modulated in endothelial mechanotransduction response to fluid shear stress.

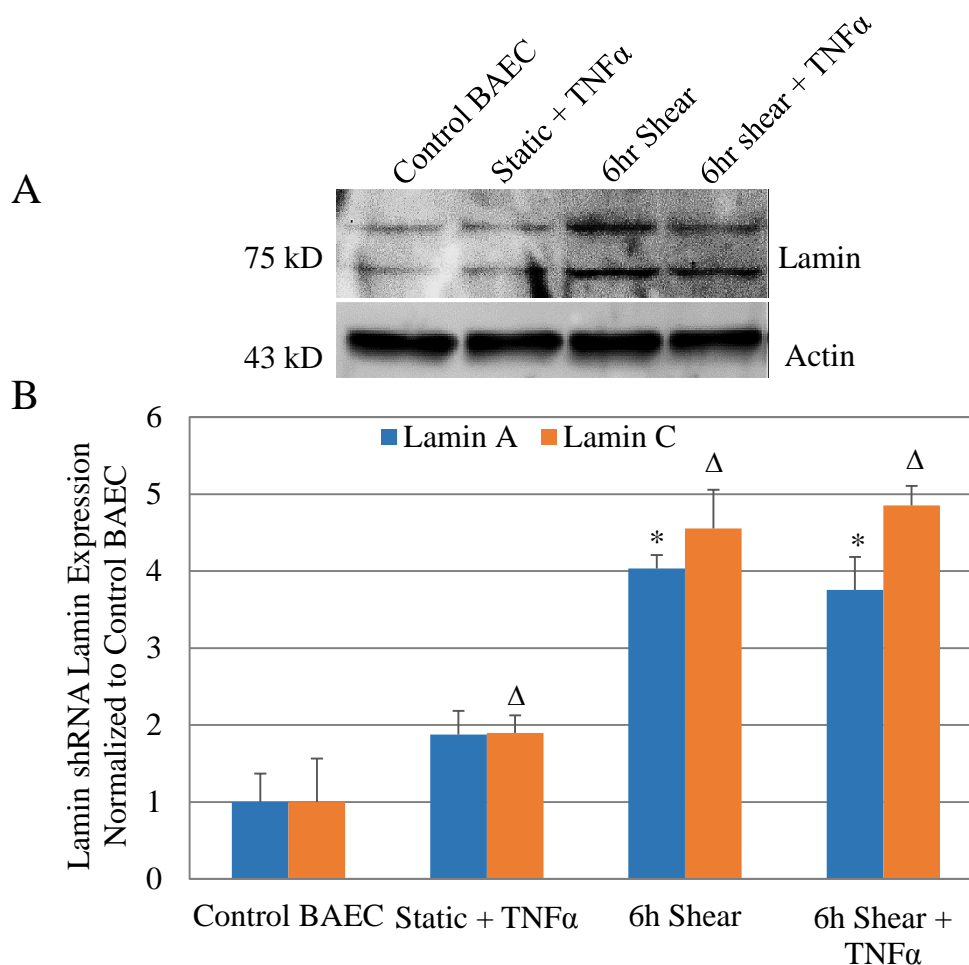


**Figure 7.2. Lamin expression in lamin shRNA cells.** A. Western blot of lamin A/C expression in lamin shRNA samples. B. Graph of quantified lamin A/C protein expression in each sample set (n=3). \* $P < 0.05$ , compared to Control BAEC (lamin A),  $\Delta P < 0.05$ , compared to Control BAEC (lamin C). Shearing lamin shRNA cells elicits a significant increase in lamin A/C expression originally knocked down in control BAECs. The activation of lamin expression in response to mechanical stress is not fully understood in lamin-deficient cells.

The shear stress exposure leads to significant changes in lamin expression in both control and lamin shRNA cells. The current literature does not fully address translational modification of lamin due to fluid shear. Also, the mechanisms of lamin regulation under mechanical stress are not fully understood. Therefore, do mutations in lamin permit nuclear deformation by modifying nuclear membrane stiffness, resulting in DNA transcriptional changes? Further shear stress studies may help elucidate underlying lamin expression and activity in nuclear membrane biomechanics, particularly in how lamin A/C regulate nuclear deformation and gene reorganization during various laminopathies. Future mechanotransduction studies will focus on the cytoskeleton-nucleus interface that lead to cell signal transduction activation, transcriptional changes in gene expression, and nuclear protein modulation.

## REFERENCES



## REFERENCES

1. Nayebosadri A, Ji JY. 2013. Endothelial nuclear lamina is not required for glucocorticoid receptor nuclear import but does affect receptor-mediated transcription activation. *American journal of physiology. Cell physiology* 305:C309-22
2. Heesen C, Mohr DC, Huitinga I, Bergh FT, Gaab J, et al. 2007. Stress regulation in multiple sclerosis: current issues and concepts. *Multiple sclerosis* 13:143-8
3. Rennier K, Ji JY. 2013. The role of death-associated protein kinase (DAPK) in endothelial apoptosis under fluid shear stress. *Life sciences* 93:194-200
4. Ross R. 1999. Atherosclerosis--an inflammatory disease. *The New England journal of medicine* 340:115-26
5. Maton A. 1993. *Human Biology and Health*. Upper Saddle River, N.J.: Prentice Hall
6. Berliner JA, Navab M, Fogelman AM, Frank JS, Demer LL, et al. 1995. Atherosclerosis: basic mechanisms. Oxidation, inflammation, and genetics. *Circulation* 91:2488-96
7. Glaudemans AW, Slart RH, Bozzao A, Bonanno E, Arca M, et al. 2010. Molecular imaging in atherosclerosis. *European journal of nuclear medicine and molecular imaging* 37:2381-97
8. Rennier K, Ji JY. 2010. *The role of DAP-kinase in modulating vascular endothelial cell function under fluid shear stress*. Purdue University, Ann Arbor. 85 pp.
9. Arab A, Kuemmerer K, Wang J, Bode C, Hehrlein C. 2008. Oxygenated perfluorochemicals improve cell survival during reoxygenation by pacifying mitochondrial activity. *The Journal of pharmacology and experimental therapeutics* 325:417-24
10. Hahn C, Schwartz MA. 2009. Mechanotransduction in vascular physiology and atherogenesis. *Nature reviews. Molecular cell biology* 10:53-62
11. Li YS, Haga JH, Chien S. 2005. Molecular basis of the effects of shear stress on vascular endothelial cells. *Journal of biomechanics* 38:1949-71
12. Gimbrone MA, Jr., Resnick N, Nagel T, Khachigian LM, Collins T, Topper JN. 1997. Hemodynamics, endothelial gene expression, and atherogenesis. *Annals of the New York Academy of Sciences* 811:1-10; discussion -1

13. Garcia-Cardena G, Comander J, Anderson KR, Blackman BR, Gimbrone MA, Jr. 2001. Biomechanical activation of vascular endothelium as a determinant of its functional phenotype. *Proceedings of the National Academy of Sciences of the United States of America* 98:4478-85
14. Kaiser D, Freyberg MA, Friedl P. 1997. Lack of hemodynamic forces triggers apoptosis in vascular endothelial cells. *Biochemical and biophysical research communications* 231:586-90
15. Masuda H, Kawamura K, Tohda K, Shozawa T, Sageshima M, Kamiya A. 1989. Increase in endothelial cell density before artery enlargement in flow-loaded canine carotid artery. *Arteriosclerosis* 9:812-23
16. Malek AM, Izumo S. 1994. Molecular aspects of signal transduction of shear stress in the endothelial cell. *Journal of hypertension* 12:989-99
17. Ando J, Tsuboi H, Korenaga R, Takada Y, Toyama-Sorimachi N, et al. 1994. Shear stress inhibits adhesion of cultured mouse endothelial cells to lymphocytes by downregulating VCAM-1 expression. *The American journal of physiology* 267:C679-87
18. Helmlinger G, Berk BC, Nerem RM. 1995. Calcium responses of endothelial cell monolayers subjected to pulsatile and steady laminar flow differ. *The American journal of physiology* 269:C367-75
19. Shyy JY, Li YS, Lin MC, Chen W, Yuan S, et al. 1995. Multiple cis-elements mediate shear stress-induced gene expression. *Journal of biomechanics* 28:1451-7
20. Hishikawa K, Nakaki T, Marumo T, Suzuki H, Kato R, Saruta T. 1995. Pressure enhances endothelin-1 release from cultured human endothelial cells. *Hypertension* 25:449-52
21. Malek A, Izumo S. 1992. Physiological fluid shear stress causes downregulation of endothelin-1 mRNA in bovine aortic endothelium. *The American journal of physiology* 263:C389-96
22. Fleming I, Bauersachs J, Busse R. 1997. Calcium-dependent and calcium-independent activation of the endothelial NO synthase. *Journal of vascular research* 34:165-74
23. Palmer RM, Ashton DS, Moncada S. 1988. Vascular endothelial cells synthesize nitric oxide from L-arginine. *Nature* 333:664-6
24. Ranjan V, Xiao Z, Diamond SL. 1995. Constitutive NOS expression in cultured endothelial cells is elevated by fluid shear stress. *The American journal of physiology* 269:H550-5
25. Topper JN, Cai J, Falb D, Gimbrone MA, Jr. 1996. Identification of vascular endothelial genes differentially responsive to fluid mechanical stimuli: cyclooxygenase-2, manganese superoxide dismutase, and endothelial cell nitric oxide synthase are selectively up-regulated by steady laminar shear stress. *Proceedings of the National Academy of Sciences of the United States of America* 93:10417-22
26. Korenaga R, Ando J, Kosaki K, Isshiki M, Takada Y, Kamiya A. 1997. Negative transcriptional regulation of the VCAM-1 gene by fluid shear stress in murine endothelial cells. *The American journal of physiology* 273:C1506-15

27. Diamond SL, Eskin SG, McIntire LV. 1989. Fluid flow stimulates tissue plasminogen activator secretion by cultured human endothelial cells. *Science* 243:1483-5
28. Resnick N, Collins T, Atkinson W, Bonthron DT, Dewey CF, Jr., Gimbrone MA, Jr. 1993. Platelet-derived growth factor B chain promoter contains a cis-acting fluid shear-stress-responsive element. *Proceedings of the National Academy of Sciences of the United States of America* 90:4591-5
29. Ohno M, Cooke JP, Dzau VJ, Gibbons GH. 1995. Fluid shear stress induces endothelial transforming growth factor beta-1 transcription and production. Modulation by potassium channel blockade. *The Journal of clinical investigation* 95:1363-9
30. Dewey CF, Jr., Bussolari SR, Gimbrone MA, Jr., Davies PF. 1981. The dynamic response of vascular endothelial cells to fluid shear stress. *Journal of biomechanical engineering* 103:177-85
31. Zebda N, Dubrovskiy O, Birukov KG. 2012. Focal adhesion kinase regulation of mechanotransduction and its impact on endothelial cell functions. *Microvascular research* 83:71-81
32. Martinet W, Schrijvers DM, De Meyer GR, Thielemans J, Knaapen MW, et al. 2002. Gene expression profiling of apoptosis-related genes in human atherosclerosis: upregulation of death-associated protein kinase. *Arterioscler Thromb Vasc Biol* 22:2023-9
33. Woodside KJ, Hernandez A, Smith FW, Xue XY, Hu M, et al. 2003. Differential gene expression in primary and recurrent carotid stenosis. *Biochemical and biophysical research communications* 302:509-14
34. Cohen O, Kimchi A. 2001. DAP-kinase: from functional gene cloning to establishment of its role in apoptosis and cancer. *Cell death and differentiation* 8:6-15
35. Raveh T, Kimchi A. 2001. DAP kinase-a proapoptotic gene that functions as a tumor suppressor. *Experimental cell research* 264:185-92
36. Raveh T, Droguett G, Horwitz MS, DePinho RA, Kimchi A. 2001. DAP kinase activates a p19ARF/p53-mediated apoptotic checkpoint to suppress oncogenic transformation. *Nature cell biology* 3:1-7
37. Inbal B, Cohen O, Polak-Charcon S, Kopolovic J, Vadai E, et al. 1997. DAP kinase links the control of apoptosis to metastasis. *Nature* 390:180-4
38. Bialik S, Kimchi A. 2004. DAP-kinase as a target for drug design in cancer and diseases associated with accelerated cell death. *Seminars in cancer biology* 14:283-94
39. Bialik S, Bresnick AR, Kimchi A. 2004. DAP-kinase-mediated morphological changes are localization dependent and involve myosin-II phosphorylation. *Cell death and differentiation* 11:631-44
40. Shohat G, Spivak-Kroizman T, Cohen O, Bialik S, Shani G, et al. 2001. The proapoptotic function of death-associated protein kinase is controlled by a unique inhibitory autophosphorylation-based mechanism. *The Journal of biological chemistry* 276:47460-7

41. Bharadwaj S, Shah V, Tariq F, Damartoski B, Prasad GL. 2005. Amino terminal, but not the carboxy terminal, sequences of tropomyosin-1 are essential for the induction of stress fiber assembly in neoplastic cells. *Cancer Lett* 229:253-60
42. Packard RR, Libby P. 2008. Inflammation in atherosclerosis: from vascular biology to biomarker discovery and risk prediction. *Clinical chemistry* 54:24-38
43. Teichert AM, Scott JA, Robb GB, Zhou YQ, Zhu SN, et al. 2008. Endothelial nitric oxide synthase gene expression during murine embryogenesis: commencement of expression in the embryo occurs with the establishment of a unidirectional circulatory system. *Circ Res* 103:24-33
44. Malek AM, Alper SL, Izumo S. 1999. Hemodynamic shear stress and its role in atherosclerosis. *JAMA : the journal of the American Medical Association* 282:2035-42
45. Davies PF, Polacek DC, Shi C, Helmke BP. 2002. The convergence of haemodynamics, genomics, and endothelial structure in studies of the focal origin of atherosclerosis. *Biorheology* 39:299-306
46. Volger OL, Fledderus JO, Kisters N, Fontijn RD, Moerland PD, et al. 2007. Distinctive expression of chemokines and transforming growth factor-beta signaling in human arterial endothelium during atherosclerosis. *The American journal of pathology* 171:326-37
47. Passerini AG, Polacek DC, Shi C, Francesco NM, Manduchi E, et al. 2004. Coexisting proinflammatory and antioxidative endothelial transcription profiles in a disturbed flow region of the adult porcine aorta. *Proceedings of the National Academy of Sciences of the United States of America* 101:2482-7
48. Kuchan M, Frangos J. 1994. Role of calcium and calmodulin in flow-induced nitric oxide production in endothelial cells. *Am J Physiol* 266:C628-36
49. Diamond S, Sharefkin J, Dieffenbach C, Frasier-Scott K, McIntire L, Eskin S. 1990. Tissue plasminogen activator messenger RNA levels increase in cultured human endothelial cells exposed to laminar shear stress. *J Cell Physiol* 143:364-71
50. Surapisitchat J, Hoefen RJ, Pi X, Yoshizumi M, Yan C, Berk BC. 2001. Fluid shear stress inhibits TNF-alpha activation of JNK but not ERK1/2 or p38 in human umbilical vein endothelial cells: Inhibitory crosstalk among MAPK family members. *Proceedings of the National Academy of Sciences of the United States of America* 98:6476-81
51. Choy JC, Granville DJ, Hunt DW, McManus BM. 2001. Endothelial cell apoptosis: biochemical characteristics and potential implications for atherosclerosis. *Journal of molecular and cellular cardiology* 33:1673-90
52. Munoz-Chapuli R. 2011. Evolution of angiogenesis. *The International journal of developmental biology* 55:345-51
53. Riedl SJ, Shi Y. 2004. Molecular mechanisms of caspase regulation during apoptosis. *Nature reviews. Molecular cell biology* 5:897-907
54. Kumar V. 2010. *Robbins and Cotran Pathological Basis of Disease*. Philadelphia, PA: Saunders, an Imprint of Elsevier

55. Slee EA, Harte MT, Kluck RM, Wolf BB, Casiano CA, et al. 1999. Ordering the cytochrome c-initiated caspase cascade: hierarchical activation of caspases-2, -3, -6, -7, -8, and -10 in a caspase-9-dependent manner. *The Journal of cell biology* 144:281-92
56. Zou H, Li Y, Liu X, Wang X. 1999. An APAF-1.cytochrome c multimeric complex is a functional apoptosome that activates procaspase-9. *The Journal of biological chemistry* 274:11549-56
57. Nicholson DW. 2000. From bench to clinic with apoptosis-based therapeutic agents. *Nature* 407:810-6
58. Yu T, Li J, Qiu Y, Sun H. 2012. 1-phenyl-2-decanoylamino-3-morpholino-1-propanol (PDMP) facilitates curcumin-induced melanoma cell apoptosis by enhancing ceramide accumulation, JNK activation, and inhibiting PI3K/AKT activation. *Molecular and cellular biochemistry* 361:47-54
59. Mallat Z, Tedgui A. 2000. Apoptosis in the vasculature: mechanisms and functional importance. *British journal of pharmacology* 130:947-62
60. Lev N, Melamed E, Offen D. 2003. Apoptosis and Parkinson's disease. *Progress in neuro-psychopharmacology & biological psychiatry* 27:245-50
61. Savill J. 2000. Apoptosis in resolution of inflammation. *Kidney & blood pressure research* 23:173-4
62. Winn RK, Harlan JM. 2005. The role of endothelial cell apoptosis in inflammatory and immune diseases. *Journal of thrombosis and haemostasis : JTH* 3:1815-24
63. Stupack DG, Cheresh DA. 2002. Get a ligand, get a life: integrins, signaling and cell survival. *Journal of cell science* 115:3729-38
64. Stupack DG, Cheresh DA. 2003. Apoptotic cues from the extracellular matrix: regulators of angiogenesis. *Oncogene* 22:9022-9
65. Munoz-Chapuli R, Perez-Pomares JM. 2010. Cardiogenesis: an embryological perspective. *Journal of cardiovascular translational research* 3:37-48
66. Munoz-Chapuli R, Quesada AR, Angel Medina M. 2004. Angiogenesis and signal transduction in endothelial cells. *Cellular and molecular life sciences : CMLS* 61:2224-43
67. Scatena M, Almeida M, Chaisson ML, Fausto N, Nicosia RF, Giachelli CM. 1998. NF-kappaB mediates alphavbeta3 integrin-induced endothelial cell survival. *The Journal of cell biology* 141:1083-93
68. Zen K, Karsan A, Stempien-Otero A, Yee E, Tupper J, et al. 1999. NF-kappaB activation is required for human endothelial survival during exposure to tumor necrosis factor-alpha but not to interleukin-1beta or lipopolysaccharide. *The Journal of biological chemistry* 274:28808-15
69. Li JH, Kirkiles-Smith NC, McNiff JM, Pober JS. 2003. TRAIL induces apoptosis and inflammatory gene expression in human endothelial cells. *J Immunol* 171:1526-33
70. Resnick N, Yahav H, Khachigian LM, Collins T, Anderson KR, et al. 1997. Endothelial gene regulation by laminar shear stress. *Advances in experimental medicine and biology* 430:155-64

71. Wasserman SM, Mehraban F, Komuves LG, Yang RB, Tomlinson JE, et al. 2002. Gene expression profile of human endothelial cells exposed to sustained fluid shear stress. *Physiological genomics* 12:13-23
72. Wentzel JJ, Gijssen FJ, Stergiopoulos N, Serruys PW, Slager CJ, Krams R. 2003. Shear stress, vascular remodeling and neointimal formation. *Journal of biomechanics* 36:681-8
73. Zakkar M, Chaudhury H, Sandvik G, Enesa K, Luong le A, et al. 2008. Increased endothelial mitogen-activated protein kinase phosphatase-1 expression suppresses proinflammatory activation at sites that are resistant to atherosclerosis. *Circ Res* 103:726-32
74. Bialik S, Kimchi A. 2006. The death-associated protein kinases: structure, function, and beyond. *Annual review of biochemistry* 75:189-210
75. Deiss LP, Feinstein E, Berissi H, Cohen O, Kimchi A. 1995. Identification of a novel serine/threonine kinase and a novel 15-kD protein as potential mediators of the gamma interferon-induced cell death. *Genes & development* 9:15-30
76. Chen RH, Wang WJ, Kuo JC. 2006. The tumor suppressor DAP-kinase links cell adhesion and cytoskeleton reorganization to cell death regulation. *J Biomed Sci* 13:193-9
77. Cohen O, Feinstein E, Kimchi A. 1997. DAP-kinase is a Ca<sup>2+</sup>/calmodulin-dependent, cytoskeletal-associated protein kinase, with cell death-inducing functions that depend on its catalytic activity. *The EMBO journal* 16:998-1008
78. Cohen O, Inbal B, Kissil JL, Raveh T, Berissi H, et al. 1999. DAP-kinase participates in TNF-alpha- and Fas-induced apoptosis and its function requires the death domain. *The Journal of cell biology* 146:141-8
79. Pelled D, Raveh T, Riebeling C, Fridkin M, Berissi H, et al. 2002. Death-associated protein (DAP) kinase plays a central role in ceramide-induced apoptosis in cultured hippocampal neurons. *The Journal of biological chemistry* 277:1957-61
80. Jang CW, Chen CH, Chen CC, Chen JY, Su YH, Chen RH. 2002. TGF-beta induces apoptosis through Smad-mediated expression of DAP-kinase. *Nature cell biology* 4:51-8
81. Yamamoto M, Hioki T, Ishii T, Nakajima-Iijima S, Uchino S. 2002. DAP kinase activity is critical for C(2)-ceramide-induced apoptosis in PC12 cells. *European journal of biochemistry / FEBS* 269:139-47
82. Gozuacik D, Bialik S, Raveh T, Mitou G, Shohat G, et al. 2008. DAP-kinase is a mediator of endoplasmic reticulum stress-induced caspase activation and autophagic cell death. *Cell death and differentiation* 15:1875-86
83. Kissil JL, Feinstein E, Cohen O, Jones PA, Tsai YC, et al. 1997. DAP-kinase loss of expression in various carcinoma and B-cell lymphoma cell lines: possible implications for role as tumor suppressor gene. *Oncogene* 15:403-7
84. Irby RB, Mao W, Coppola D, Kang J, Loubeau JM, et al. 1999. Activating SRC mutation in a subset of advanced human colon cancers. *Nature genetics* 21:187-90
85. Wang WJ, Kuo JC, Ku W, Lee YR, Lin FC, et al. 2007. The tumor suppressor DAPK is reciprocally regulated by tyrosine kinase Src and phosphatase LAR. *Molecular cell* 27:701-16

86. Jin Y, Gallagher PJ. 2003. Antisense depletion of death-associated protein kinase promotes apoptosis. *The Journal of biological chemistry* 278:51587-93
87. Dimmeler S, Rippmann V, Weiland U, Haendeler J, Zeiher AM. 1997. Angiotensin II induces apoptosis of human endothelial cells. Protective effect of nitric oxide. *Circ Res* 81:970-6
88. Jalali S, Li YS, Sotoudeh M, Yuan S, Li S, et al. 1998. Shear stress activates p60src-Ras-MAPK signaling pathways in vascular endothelial cells. *Arterioscler Thromb Vasc Biol* 18:227-34
89. Ishida T, Peterson T, Kovach N, Berk B. 1996. MAP kinase activation by flow in endothelial cells. Role of beta 1 integrins and tyrosine kinases. *Circ Res* 79:310-6
90. Chen CH, Wang WJ, Kuo JC, Tsai HC, Lin JR, et al. 2005. Bidirectional signals transduced by DAPK-ERK interaction promote the apoptotic effect of DAPK. *EMBO J* 24:294-304
91. Eisenberg-Lerner A, Kimchi A. 2007. DAP kinase regulates JNK signaling by binding and activating protein kinase D under oxidative stress. *Cell death and differentiation* 14:1908-15
92. Anjum R, Roux PP, Ballif BA, Gygi SP, Blenis J. 2005. The tumor suppressor DAP kinase is a target of RSK-mediated survival signaling. *Current biology : CB* 15:1762-7
93. Shohat G, Shani G, Eisenstein M, Kimchi A. 2002. The DAP-kinase family of proteins: study of a novel group of calcium-regulated death-promoting kinases. *Biochimica et biophysica acta* 1600:45-50
94. Inbal B, Bialik S, Sabanay I, Shani G, Kimchi A. 2002. DAP kinase and DRP-1 mediate membrane blebbing and the formation of autophagic vesicles during programmed cell death. *The Journal of cell biology* 157:455-68
95. Kuo JC, Lin JR, Staddon JM, Hosoya H, Chen RH. 2003. Uncoordinated regulation of stress fibers and focal adhesions by DAP kinase. *Journal of cell science* 116:4777-90
96. Houle F, Poirier A, Dumaresq J, Huot J. 2007. DAP kinase mediates the phosphorylation of tropomyosin-1 downstream of the ERK pathway, which regulates the formation of stress fibers in response to oxidative stress. *Journal of cell science* 120:3666-77
97. Tanaka T, Bai T, Yukawa K. 2010. Death-associated protein kinase is essential for the survival of various types of uterine cancer cells. *International journal of oncology* 37:1017-22
98. Frangos JA, McIntire LV, Eskin SG. 1988. Shear stress induced stimulation of mammalian cell metabolism. *Biotechnology and bioengineering* 32:1053-60
99. Pavalko FM, Gerard RL, Ponik SM, Gallagher PJ, Jin Y, Norvell SM. 2003. Fluid shear stress inhibits TNF-alpha-induced apoptosis in osteoblasts: a role for fluid shear stress-induced activation of PI3-kinase and inhibition of caspase-3. *J Cell Physiol* 194:194-205
100. Papavassiliou AG. 1994. Preservation of protein phosphoryl groups in immunoprecipitation assays. *Journal of immunological methods* 170:67-73
101. Penna A, Cahalan M. 2007. Western Blotting using the Invitrogen NuPage Novex Bis Tris minigels. *Journal of visualized experiments : JoVE*:264

102. Hawkes WC, Wang TT, Alkan Z, Richter BD, Dawson K. 2009. Selenoprotein W modulates control of cell cycle entry. *Biological trace element research* 131:229-44
103. Hoffmann AC, Kaifi JT, Vallbohmer D, Yekebas E, Grimminger P, et al. 2009. Lack of prognostic significance of serum DNA methylation of DAPK, MGMT, and GSTPI in patients with non-small cell lung cancer. *Journal of surgical oncology* 100:414-7
104. Rozen S, Skaletsky H. 2000. Primer3 on the WWW for general users and for biologist programmers. *Methods in molecular biology* 132:365-86
105. Richards GP, Watson MA, Kingsley DH. 2004. A SYBR green, real-time RT-PCR method to detect and quantitate Norwalk virus in stools. *Journal of virological methods* 116:63-70
106. Jin Y, Blue EK, Dixon S, Hou L, Wysolmerski RB, Gallagher PJ. 2001. Identification of a new form of death-associated protein kinase that promotes cell survival. *The Journal of biological chemistry* 276:39667-78
107. Davies PF, Spaan JA, Krams R. 2005. Shear stress biology of the endothelium. *Annals of biomedical engineering* 33:1714-8
108. Michie AM, McCaig AM, Nakagawa R, Vukovic M. 2010. Death-associated protein kinase (DAPK) and signal transduction: regulation in cancer. *The FEBS journal* 277:74-80
109. Kimchi A. 1999. DAP kinase and DAP-3: novel positive mediators of apoptosis. *Ann Rheum Dis* 58 Suppl 1:I14-9
110. Caplan BA, Schwartz CJ. 1973. Increased endothelial cell turnover in areas of in vivo Evans Blue uptake in the pig aorta. *Atherosclerosis* 17:401-17
111. Ku DN, Giddens DP, Zarins CK, Glagov S. 1985. Pulsatile flow and atherosclerosis in the human carotid bifurcation. Positive correlation between plaque location and low oscillating shear stress. *Arteriosclerosis* 5:293-302
112. Dimmeler S, Haendeler J, Rippmann V, Nehls M, Zeiher AM. 1996. Shear stress inhibits apoptosis of human endothelial cells. *FEBS letters* 399:71-4
113. Hermann C, Zeiher AM, Dimmeler S. 1997. Shear stress inhibits H<sub>2</sub>O<sub>2</sub>-induced apoptosis of human endothelial cells by modulation of the glutathione redox cycle and nitric oxide synthase. *Arterioscler Thromb Vasc Biol* 17:3588-92
114. Bajbouj K, Poehlmann A, Kuester D, Drewes T, Haase K, et al. 2009. Identification of phosphorylated p38 as a novel DAPK-interacting partner during TNF $\alpha$ -induced apoptosis in colorectal tumor cells. *The American journal of pathology* 175:557-70
115. Galbraith CG, Skalak R, Chien S. 1998. Shear stress induces spatial reorganization of the endothelial cell cytoskeleton. *Cell Motil Cytoskeleton* 40:317-30
116. Berk BC, Abe JI, Min W, Surapisitchat J, Yan C. 2001. Endothelial atheroprotective and anti-inflammatory mechanisms. *Annals of the New York Academy of Sciences* 947:93-109; discussion -11



117. Malek A, Jiang L, Lee I, Sessa W, Izumo S, Alper S. 1999. Induction of nitric oxide synthase mRNA by shear stress requires intracellular calcium and G-protein signals and is modulated by PI 3 kinase. *Biochemical and biophysical research communications* 254:231-42
118. Rennie K, Ji JY. 2012. Shear stress regulates expression of death-associated protein kinase in suppressing TNF $\alpha$ -induced endothelial apoptosis. *J Cell Physiol* 227:2398-411
119. Macario DK, Entersz I, Abboud JP, Nackman GB. 2008. Inhibition of apoptosis prevents shear-induced detachment of endothelial cells. *The Journal of surgical research* 147:282-9
120. Robaye B, Mosselmans R, Fiers W, Dumont JE, Galand P. 1991. Tumor necrosis factor induces apoptosis (programmed cell death) in normal endothelial cells in vitro. *The American journal of pathology* 138:447-53
121. Malek AM, Izumo S. 1995. Control of endothelial cell gene expression by flow. *Journal of biomechanics* 28:1515-28
122. Dimmeler S, Haendeler J, Nehls M, Zeiher AM. 1997. Suppression of apoptosis by nitric oxide via inhibition of interleukin-1 $\beta$ -converting enzyme (ICE)-like and cysteine protease protein (CPP)-32-like proteases. *J Exp Med* 185:601-7
123. Buttgereit F, Dimmeler S, Neugebauer E, Burmester GR. 1996. [Mechanisms of action of high-dosage glucocorticoid therapy]. *Deutsche medizinische Wochenschrift* 121:248-52
124. Rennie K, Ji JY. 2013. Effect of shear stress and substrate on endothelial DAPK expression, caspase activity, and apoptosis. *BMC research notes* 6:10
125. Flaherty JT, Pierce JE, Ferrans VJ, Patel DJ, Tucker WK, Fry DL. 1972. Endothelial nuclear patterns in the canine arterial tree with particular reference to hemodynamic events. *Circ Res* 30:23-33
126. Sato M, Ohshima N, Nerem RM. 1996. Viscoelastic properties of cultured porcine aortic endothelial cells exposed to shear stress. *J Biomech* 29:461-7
127. Li Y, Shyy J, Li S, Lee J, Su B, et al. 1996. The Ras-JNK pathway is involved in shear-induced gene expression. *Mol Cell Biol* 16:5947-54
128. Tseng H, Peterson T, Berk B. 1995. Fluid shear stress stimulates mitogen-activated protein kinase in endothelial cells. *Circ Res* 77:869-78
129. Davies P. 1995. Flow-mediated endothelial mechanotransduction. *Physiol Rev* 75:519-60
130. Peng X, Recchia FA, Byrne BJ, Wittstein IS, Ziegelstein RC, Kass DA. 2000. In vitro system to study realistic pulsatile flow and stretch signaling in cultured vascular cells. *American journal of physiology. Cell physiology* 279:C797-805
131. Punchard MA, Stenson-Cox C, O'Ceirbhail E D, Lyons E, Gundy S, et al. 2007. Endothelial cell response to biomechanical forces under simulated vascular loading conditions. *Journal of biomechanics* 40:3146-54
132. Lammerding J, Fong LG, Ji JY, Reue K, Stewart CL, et al. 2006. Lamins A and C but not lamin B1 regulate nuclear mechanics. *The Journal of biological chemistry* 281:25768-80
133. Lo CM, Wang HB, Dembo M, Wang YL. 2000. Cell movement is guided by the rigidity of the substrate. *Biophys J* 79:144-52

134. Peyton SR, Putnam AJ. 2005. Extracellular matrix rigidity governs smooth muscle cell motility in a biphasic fashion. *J Cell Physiol* 204:198-209
135. Flanagan LA, Ju YE, Marg B, Osterfield M, Janmey PA. 2002. Neurite branching on deformable substrates. *Neuroreport* 13:2411-5
136. Yeung T, Georges PC, Flanagan LA, Marg B, Ortiz M, et al. 2005. Effects of substrate stiffness on cell morphology, cytoskeletal structure, and adhesion. *Cell Motil Cytoskeleton* 60:24-34
137. Tse JR, Engler AJ. 2010. Preparation of hydrogel substrates with tunable mechanical properties. *Curr Protoc Cell Biol* Chapter 10:Unit 10 6
138. Discher DE, Janmey P, Wang YL. 2005. Tissue cells feel and respond to the stiffness of their substrate. *Science* 310:1139-43
139. Han Y, Wang L, Yao QP, Zhang P, Liu B, et al. 2015. Nuclear envelope proteins Nesprin2 and LaminA regulate proliferation and apoptosis of vascular endothelial cells in response to shear stress. *Biochimica et biophysica acta* 1853:1165-73
140. Gruenbaum Y, Margalit A, Goldman RD, Shumaker DK, Wilson KL. 2005. The nuclear lamina comes of age. *Nature reviews. Molecular cell biology* 6:21-31
141. Oberhammer FA, Hochegger K, Froschl G, Tiefenbacher R, Pavelka M. 1994. Chromatin condensation during apoptosis is accompanied by degradation of lamin A+B, without enhanced activation of cdc2 kinase. *The Journal of cell biology* 126:827-37
142. Kawahara A, Enari M, Talanian RV, Wong WW, Nagata S. 1998. Fas-induced DNA fragmentation and proteolysis of nuclear proteins. *Genes to cells : devoted to molecular & cellular mechanisms* 3:297-306
143. Orth K, Chinnaiyan AM, Garg M, Froelich CJ, Dixit VM. 1996. The CED-3/ICE-like protease Mch2 is activated during apoptosis and cleaves the death substrate lamin A. *The Journal of biological chemistry* 271:16443-6
144. Araki T, Shinoda S, Schindler CK, Quan-Lan J, Meller R, et al. 2004. Expression, interaction, and proteolysis of death-associated protein kinase and p53 within vulnerable and resistant hippocampal subfields following seizures. *Hippocampus* 14:326-36
145. Chang ZF, Lee HH. 2006. RhoA signaling in phorbol ester-induced apoptosis. *J Biomed Sci* 13:173-80
146. Sebbagh M, Renvoize C, Hamelin J, Riche N, Bertoglio J, Breard J. 2001. Caspase-3-mediated cleavage of ROCK I induces MLC phosphorylation and apoptotic membrane blebbing. *Nature cell biology* 3:346-52
147. Mills JC, Stone NL, Erhardt J, Pittman RN. 1998. Apoptotic membrane blebbing is regulated by myosin light chain phosphorylation. *The Journal of cell biology* 140:627-36
148. Croft DR, Coleman ML, Li S, Robertson D, Sullivan T, et al. 2005. Actin-myosin-based contraction is responsible for apoptotic nuclear disintegration. *The Journal of cell biology* 168:245-55
149. Markiewicz E, Dechat T, Foisner R, Quinlan RA, Hutchison CJ. 2002. Lamin A/C binding protein LAP2alpha is required for nuclear anchorage of retinoblastoma protein. *Mol Biol Cell* 13:4401-13

150. Sylvius N, Bonne G, Straatman K, Reddy T, Gant TW, Shackleton S. 2011. MicroRNA expression profiling in patients with lamin A/C-associated muscular dystrophy. *FASEB journal : official publication of the Federation of American Societies for Experimental Biology* 25:3966-78
151. Dubinska-Magiera M, Zaremba-Czogalla M, Rzepecki R. 2013. Muscle development, regeneration and laminopathies: how lamins or lamina-associated proteins can contribute to muscle development, regeneration and disease. *Cellular and molecular life sciences : CMLS* 70:2713-41
152. Castets M, Coissieux MM, Delloye-Bourgeois C, Bernard L, Delcros JG, et al. 2009. Inhibition of endothelial cell apoptosis by netrin-1 during angiogenesis. *Dev Cell* 16:614-20
153. Lammerding J, Schulze PC, Takahashi T, Kozlov S, Sullivan T, et al. 2004. Lamin A/C deficiency causes defective nuclear mechanics and mechanotransduction. *The Journal of clinical investigation* 113:370-8
154. Deguchi S, Maeda K, Ohashi T, Sato M. 2005. Flow-induced hardening of endothelial nucleus as an intracellular stress-bearing organelle. *Journal of biomechanics* 38:1751-9
155. Dittmer TA, Misteli T. 2011. The lamin protein family. *Genome biology* 12:222
156. Harada T, Swift J, Irianto J, Shin JW, Spinler KR, et al. 2014. Nuclear lamin stiffness is a barrier to 3D migration, but softness can limit survival. *The Journal of cell biology* 204:669-82

VITA

## VITA

**Keith R. Rennie**  
krennier@purdue.edu

EDUCATION

**Purdue University, West Lafayette, IN** May 2015  
Doctorate of Science in Biomedical Engineering

**Indiana University Purdue University (IUPUI), Indianapolis, IN** May 2010  
Masters of Science in Biomedical Engineering

**Purdue University, West Lafayette, IN** December 2007  
Bachelors of Science in Biomedical Engineering

EXPERIENCE

**Graduate Research Assistant, Ph.D. Candidate** (Indianapolis, IN) August 2011 – May 2015  
*Purdue University, Weldon School of Biomedical Engineering*

- Utilized a versatile parallel plate flow chamber for fluid shear stress experiments on aortic endothelial, fibroblast and endothelial/epithelial cancer cell lines.
- Examined proteomic and genomic cell expression changes using molecular biology techniques. Used western blotting techniques to analyze the phosphorylated and overall Death-associated protein kinase (DAPK) protein expression.
- Developed a novel target-specific DAPK primer used to quantify overall mRNA expression and gene modification using real time RT-PCR.
- Proficiency in flow cytometry procedures (FACSCalibur/FACScan) and CellQuest software to quantify apoptosis and cell cycle analysis.

- Confirmed the protective effect of fluid shear stress in attenuating cytokine, oxidative stress and serum starvation induced apoptosis.
- Developed shRNA (bacterial transformation) and transfected siRNA cell lines to study the mechanistic roles of both DAPK and lamin A/C. Effectively knocked down DAPK and lamin A/C expression for cell response studies to shear stress and environmental stimulants.
- Applied immunohistochemistry protocols and live cell imaging microscopy to map out target gene location, and successfully identified that DAPK sub-compartmentalizes in the actin-cytoskeletal network, as well as the effect of shear and apoptosis induction.
- Quantified cell caspase activity using ELISA and Luciferase assays, confirming previous apoptosis results in parallel experiments.

**Research Assistant, MSBME** (Indianapolis, IN) January 2009 – August 2011  
*IUPUI, Purdue School of Engineering and Technology*

- Published thesis titled “The Role of DAP-Kinase in Modulating Vascular Endothelial Cell Function Under Fluid Shear Stress”
- Effectively addressed various flow chamber design and hardware issues such as material degradation and failure, sterilization complications and cell environment contamination.
- Examined biomolecular cell response, such as mRNA/protein expression, cell structure, and cell turnover with molecular biology techniques.
- Conducted laminar shear stress flow experiments using a custom parallel plate flow chamber. Investigated the effect of fluid shear stress on bovine aortic endothelial cells.
- Analyzed both phosphorylated and overall DAPK cell expression with western blotting.

**Graduate Teaching Assistant** (Indianapolis, IN) January 2010 – May 2012  
*IUPUI, Purdue School of Engineering and Technology*

- BME 241. Biomechanics lab instructor for undergraduate biomedical engineering students.
- Successfully introduced laboratory concepts, protocols, and procedures for students to gain a hands-on understanding of biomechanics applications.

- Mentored undergraduate students in general biomedical engineering topics and relevant research areas.

## PUBLICATIONS

1. Rennie K, Ji JY. 2013. **The role of death-associated protein kinase (DAPK) in endothelial apoptosis under fluid shear stress.** *Life Sciences* 93:194-200.
2. Rennie K, Ji JY. 2013. **Effect of shear stress and substrate on endothelial DAPK expression, caspase activity, and apoptosis.** *BMC Research Notes* 6:10.
3. Rennie K, Ji JY. 2012. **Shear stress regulates expression of death-associated protein kinase in suppressing TNF $\alpha$ -induced endothelial apoptosis.** *Journal of cellular physiology* 227:2398-2411.
4. Rennie K, Ji JY. 2015. **Shear stress attenuates apoptosis due to TNF $\alpha$ , oxidative stress, and serum depletion via death-associated protein kinase (DAPK) expression.** *BMC Research Notes*.

## PRESENTATIONS

**Shear stress attenuates multiple apoptosis pathways by modulating endothelial DAPK expression.** Keith Rennie and Julie Y. Ji. Purdue University, Weldon School of Biomedical Engineering

- Poster at the 2013 Biomedical Engineering Society Annual Meeting in Seattle, WA from September 25<sup>th</sup> – 28<sup>th</sup>.

**Effect of shear stress and substrate on endothelial DAPK expression, caspase activity, and apoptosis.** Keith Rennie and Julie Y. Ji. Purdue University, Weldon School of Biomedical Engineering

- Poster at the 2012 Biomedical Engineering Society Annual Meeting in Atlanta, GA from October 24<sup>th</sup> – 27<sup>th</sup>.

**Shear stress attenuates apoptosis due to TNF $\alpha$ , oxidative stress, and serum depletion via DAPK.** Keith Rennie and Julie Y. Ji. Purdue University, Weldon School of Biomedical Engineering

- Poster at the 2012 Biomedical Engineering Society Annual Meeting in Atlanta, GA from October 24<sup>th</sup> – 27<sup>th</sup>.

**The Role of DAP-Kinase in Modulating Vascular Endothelial Cell Functions under Fluid Shear Stress.** Keith Rennie and Julie Y. Ji. IUPUI, Purdue School of Engineering and Technology

- Poster for the 2011 Biomedical Engineering Society Annual Meeting in Pittsburgh, PA from October 7<sup>th</sup> – 10<sup>th</sup>.

**Shear Stress Suppresses TNF- $\alpha$  Induced Apoptosis; In Part by Modulating DAPK Expression and Activity.**

Keith Rennie and Julie Y. Ji. IUPUI, Purdue School of Engineering and Technology

- Platform talk for the 2010 Biomedical Engineering Society Annual Meeting in Austin, TX from October 6<sup>th</sup> – 9<sup>th</sup>.

AWARDS AND MEMBERSHIPS

- Bilsland Dissertation Fellow 2014
- R. M. Spark – Men of Purdue Fellow 2007
- United Association of Journeyman Scholar 2006
- Biomedical Engineering Society (BMES) 2005 - 2015
- Biomedical Engineering Graduate Student Association (BMEGSA) 2009 – 2015

RESEARCH SKILLS AND BACKGROUND

- Flow cytometry
- Real-time RT-PCR
- Protein, DNA, and RNA analysis
- Immunohistochemistry
- Immunoprecipitation
- Luciferase assay
- PCR primer design
- Mammalian cell culture
- Fluorescence microscopy
- Bioengineering
- Biomedical engineering
- Apoptosis
- TUNEL assay
- Annexin V/PI assay
- Cellular mechanotransduction
- Fluid mechanics
- Atherosclerosis
- Cancer cell biology
- Molecular & cellular biology
- Cardiovascular biology
- Cancer research
- Protein-protein Interactions
- Genetic engineering
- Gene expression profiling
- siRNA transient gene silencing
- shRNA stable gene silencing
- Bacterial transformation
- Protein engineering
- Drug delivery
- Technical presentations
- Mathematical modeling
- Statistical analysis